Welding Research

SPONSORED BY THE WELDING RESEARCH COUNCIL
OF THE ENGINEERING FOUNDATION

W. SPRARAGEN, DIRECTOR

SUPPLEMENT TO THE WELDING JOURNAL, NOVEMBER, 1956

MEASUREMENT AND CALCULATION OF FERRITE IN STAINLESS-STEEL WELD METAL

Magne Gage found to be a useful and reliable instrument for the measurement of ferrite if properly used on as-welded specimens. Also, new constitution diagram for stainless-steel weld metal is proposed by authors

BY W. T. DELONG, G. A. OSTROM AND E. R. SZUMACHOWSKI

ABSTRACT. Because close control of the ferrite content of austenitic stainless weld deposits is needed in many applications, the accuracy of ferrite measurement and calculation is important. The ferrite content of over 600 weld pads of a wide range of sizes, types and coatings was studied. The use of a Magne Gage for measuring ferrite was studied, and the instrument was recommended for this purpose when used with the specific procedures outlined.

Measured ferrite was compared with ferrite as calculated from the Schaeffler diagram. A new diagram was proposed which used all of the Schaeffler equivalents plus a nickel equivalent of 30 for nitrogen. Measured ferrite was compared with ferrite as calculated from this diagram. This new diagram reduced the spread of values between measured and calculated ferrite for the 308 and 347 types, and improved the accuracy of calculation for the 316, 317 and 309 types.

Introduction

A crack-free deposit is one of the most important requirements of a good arc-welding electrode. One of the most effective ways of controlling the crack sensitivity of stainless weld deposits normally containing some ferrite is to control the ferrite level.

Recognition of the importance of ferrite in controlling cracking has developed over the past fifteen years. World War II produced a tremendous demand for austenitic armor welding electrodes capable of depositing crack-free root passes in highly restrained joints on heavy armor plate. During this period, it was found that Type 308 weld metal compositions having a high chromium to nickel ratio were more crack resistant than those which had a lower ratio of chromium to nickel. Proceeding from this fact, it was natural to add increased amounts of chromium, and eventually molybdenum, to increase the ferrite content and the crack resistance of the modified Type 308 welds. The logical relationship between the structure of the weld metal and the balance of those elements which promote austenite formation and those which promote ferrite formation was recognized. This knowledge was carried over to other stainless electrode types.

Schaeffler,[1] in his 1947 study of the use of austenitic electrodes for the welding of dissimilar metals, reviewed the previous literature. Included in this review were references to German papers[2, 3] on early constitution diagrams for chromium nickel steels and to the work of Field, Bloom and Linnert[4]

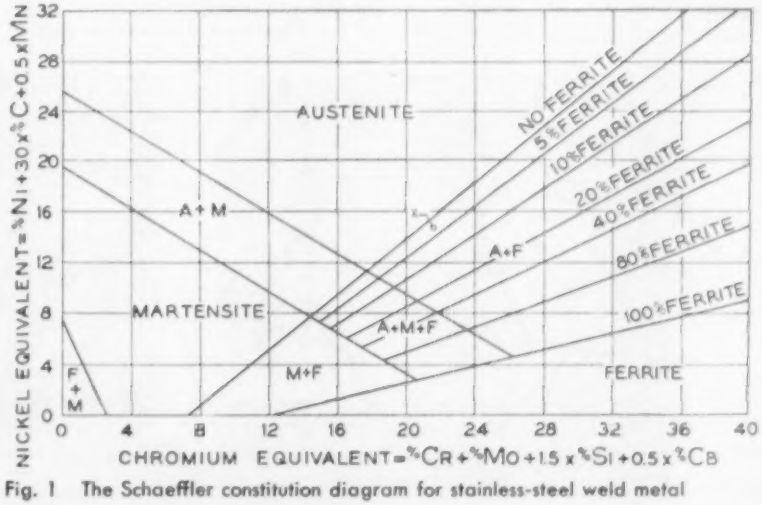

Fig. 1 The Schaeffler constitution diagram for stainless-steel weld metal

W. T. DeLong, G. A. Ostrom and E. R. Szumachowski are associated with the McKay Co., York, Pa.

Presented at the 1956 AWS National Spring Meeting held May 7–11, Buffalo, N. Y.

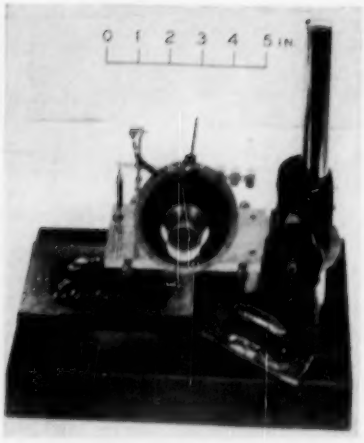

Fig. 2 Magne Gage with typical weld pads produced from 3/16 in. and 3/32-in. electrodes

on the effect of the chromium-nickel ratio and molybdenum content of the properties of armor welding electrodes.

This knowledge was carried over to stainless electrodes and led to the development of the widely accepted and very useful Schaeffler diagram[3] (Fig. 1) which was stated to be accurate for types 308, 309, 309 Cb, 310, 312, 316, 317, 318 and 347 within ±4% ferrite.

Simpkinson[4, 7] proposed the use of an Aminco-Brenner Magne Gage to measure ferrite in austenitic steels, and discussed the effect of size, shape and orientation of magnetic particles on the gage readings. The results showed that these factors all have an effect on the readings obtained and must be considered when the Magne Gage is used to determine ferrite.

Fleischmann[5] studied Magne Gage ferrite measurements and the standard magnetic properties of maximum permeability and saturation induction as determined on low and high magnetizing force permeameters. This work was done on four different Type 347 deposits. Compacts of bakelite-carbonyl iron were used as standards. He showed that if the ferrite had been spherodized by annealing, the Magne Gage readings were not as accurate an indication of ferrite quantity as the intrinsic induction at saturation. This work did not conflict with Simpkinson's. Both established that the size, shape and distribution of the magnetic particles affect the readings of instruments with low magnetic field strengths, such as the Magne Gage or the type of permeameter used to determine maximum permeability.

If high ferrite were desirable in all respects, crude measurements would suffice. Unfortunately, ferrite is undesirable if the temperature and time cycles encountered during manufacturing or service allow the formation of sigma phase. Curran and Rankin[8] illustrated this for Type 347 weld metal. For many high-temperature applications, some ferrite is desired for crack resistance, but a maximum limit is included in the requirements. Ferrite is also detrimental in some molybdenum-bearing types in many corrosion environments. Thus the major problem is to control the ferrite level of many types of weld deposits rather than to indiscriminately aim for a high ferrite level.

Purpose and Scope of This Study

The original data were collected to evaluate the use of the Magne Gage together with a simple pad preparation procedure to measure the ferrite level of a weld. A second purpose was to check the quality-control procedures used to control the ferrite level of the deposit. As the information was developed, it became apparent that it would be of practical interest to those concerned with specifying and measuring ferrite in weld metal.

There are three particular areas of interest:

1. The use of the Magne Gage for measuring ferrite. It is felt that the data should stimulate further interest in this instrument for this use.
2. The spread of data to be expected when measuring or calculating ferrite.
3. An improved constitution diagram for the calculation of ferrite.

The present Schaeffler chromium and nickel equivalents for the various elements were not studied. A study of these equivalents would require that the experiments be designed to minimize variations from other factors, and this investigation is primarily a study of the variations caused by these other factors.

Experimental Work

Magne Gage

The ferrite in the weld pads was measured with an Aminco-Brenner Magne Gage. This instrument has been described in detail in papers referred to previously,[6, 7] and will only be described briefly here. It is relatively simple and inexpensive, consisting of a permanent bar magnet on a pivoted arm, with a calibrated knob connected to the pivot bar through a spiral spring. The magnet is quite small and has a hemispherical point. To use the instrument, the calibrated knob is turned counterclockwise until the magnet remains in contact with the specimen. The knob is then turned clockwise to apply an increasing torque at the pivot. When the torque becomes sufficiently high, the magnet breaks free from the specimen. The

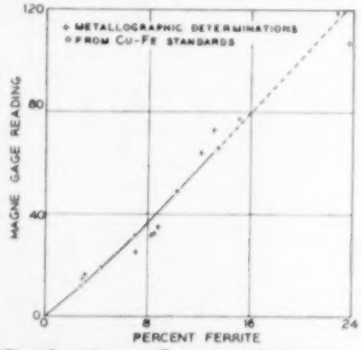

Fig. 3 Magne Gage readings versus ferrite content

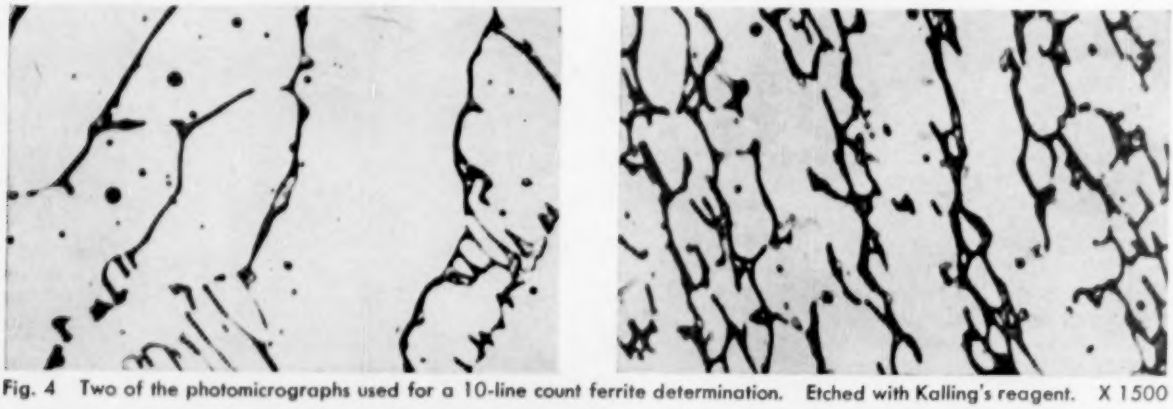

Fig. 4 Two of the photomicrographs used for a 10-line count ferrite determination. Etched with Kalling's reagent. X 1500

(*Left*) Sample 2—6.9% ferrite by 10-line count. (*Right*) Sample 5—12.7% ferrite by 10-line count.

Table 1—Magne Gage Reading Versus the Percent Ferrite as Determined by Metallographic Examination of a Number of Weld-Metal Pads

No.	*Size*	*Type*	*MG reading*	*Ferrite, %*
1	5/32	19-9 WMo	120	23.0
2	1/8	308 LC	25	7.1
3	3/16	19-9 WMo	64	12.1
4	3/16	19-9 WMo	73	13.1
5	5/32	347	66	13.4
6	....	....	35	8.4
7	1/8	19-9 WMo	108	23.6
8	1/8	317 LC	32	8.3
9	1/8	317 LC	32	8.5
10	1/8	308 LC	17	3.0
11	1/8	316 LC	16	3.1

dial reading taken can be used directly or can be converted to a zero base, as was done for data in this paper. The gage can be used with magnets of different strengths. All data were obtained with magnet number three which is usable from 0% to approximately 22% ferrite in the weld metal.

The Magne Gage is shown in Fig. 2. In order to show some of the details of the bar magnet, a plastic housing which normally covers the working mechanism has been removed.

Weld-Metal Pads

Over 600 weld pads were studied, representing all sizes of electrodes from 1/16 to 1/4 in.; three types of coatings, one lime (AWS-15) and two titania (AWS-16 and a special titania); and weld metal of types 308, 308 low carbon, 309, 309 Cb, 316, 316 low carbon, 317, 317 low carbon, 318 (316 Cb), 347 and a 308 molybdenum modified type.

The weld-metal pads were prepared in the simplest possible way. The base material was mild steel. Welding procedures were as recommended for stainless electrodes, i.e., a very short arc and relatively low current. The weld pads were only one bead wide to minimize welding time. Relatively thin beads were deposited to keep the metal from running. The beads were quenched from a red heat to minimize the time required to prepare the pads. The pads were made at least one inch high because experimental checks indicated that the mild-steel base plate has no effect on the Magne Gage reading when the pad height was over 3/4 in. The direction of welding was reversed for each pass to keep the top of the pad parallel to the base plate.

Typical weld pads made with 3/32- and 3/16-in. electrodes are shown in Fig. 2. Pads of this size and shape can be made in approximately 10 to 25 min., with the number of electrodes required varying from six for the 3/16-in. size to about twenty for the 3/32-in. and smaller sizes. Thus the pad was economical in both time and materials.

Magne Gage Readings on Pads. Readings were made only in the center section of a pad. The ends of the pads showed variations due to the conditions associated with starting and breaking an arc. Readings were made on the as-welded pad, with no surface preparation except a wire brushing sufficient to assure a clean surface suitable for chemical analysis. Five to ten readings were taken and averaged to get the ferrite of the pad. Only one pad and one set of readings were made from each lot of electrodes, with the exception of some experimental test series which were made to answer specific questions.

Calibration of the Magne Gage

There are a number of ways of correlating the ferrite content of a deposit with its Magne Gage reading. One is the use of absolute standards of magnetic iron particles in a nonmagnetic matrix. A second is to determine the ferrite content of pads by metallographic means. Both of these approaches were used.

The curve given in Fig. 3 was based on absolute standards of lightly sintered iron and copper powder compacts. The source of these standards is given in our acknowledgments. These standards were not used directly. In-

Table 2—Reproducibility of Magne Gage Ferrite Measurements from Pads Made by Various Welders (Average of Readings from Three Weld Beads)

Welder and description	*—Ferrite, %— 5/32 in. 309, pad 3408, DC lime*	*5/16 in. 309, pad 3409, DC titania*
Test Welder 1	7.6	5.1
Repeat several days later	7.0	4.6
Repeat several days later	....	4.0
Test Welder 2	6.8	4.4
Test Welder 3	6.6	4.4
Engineer 1	6.8	3.6
Engineer 2	6.2	2.2
Repeat after watching Welder 2	6.2	4.4
Engineer 3	5.6	2.0

Table 3—Ferrite Measurements on One-Bead Wide Pads Versus Four-Bead Wide Pads. Welder No. 1 (Average of Readings from One Weld Bead)

Type	*Size, in.*	*Coating*	*Pad No.*	*—Ferrite in pad, %— 4 beads wide*	*1 bead wide*
316 LC	5/32	Titania	3390	6.2	6.0
316 LC	5/32	Lime	3392	4.0	4.0
347	5/32	Titania	3393	9.0	9.2
347	5/32	Lime	3391	11.5	14.3, 11.1*
316 LC	1/8	Lime	3394	3.6	4.9, 4.2*
347	5/32	Titania	3395	10.4	8.4, 9.2*
347	5/32	Titania	3396	9.6	9.0
347	3/16	Lime	3397	7.6	8.0
309	5/32	Lime	3408	7.6	7.4
309	5/16	Titania	3409	5.1	5.3

* Repeat tests.

Table 4—Effect of Current on Measured Ferrite, Pad No. 3446, Type 309, 5/32-In., DC Titania Electrodes, Welder No. 1 (Average of Readings from Three Weld Beads)

Current, amp	*Ferrite, %*
110	4.6
130	5.3
150	5.3
170	5.1

Table 5—Base Material Type 304 Stainless Plate, Pad No. 3446, Type 309, 5/32-In., DC Titania Electrodes, Welder No. 1 (Average of Readings from One Weld Bead)

Layer	*Height above plate, in.*	*Ferrite, %*
Base plate	0.00	0.0
1	0.12	5.8
2	0.18	5.3
3	0.25	4.6
4	0.36	5.1
5	0.43	5.1
6	0.53	5.3
7	0.63	5.1

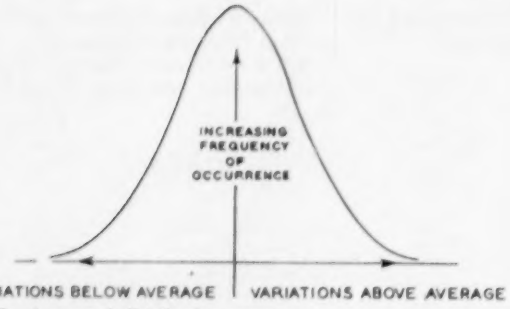

Fig. 5 A normal distribution curve

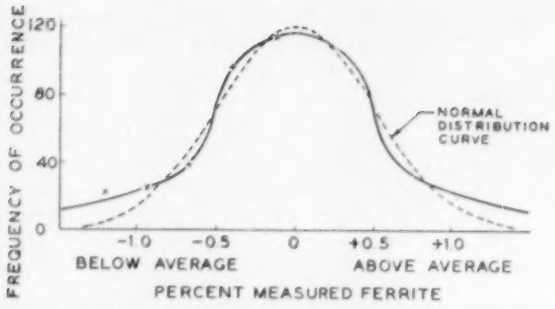

Fig. 6 Variation of individual Magne Gage ferrite measurements from the average for the same heat, size and coating

stead, the "ferrite values" of a number of specimens were determined with a Magne Gage whose calibration curve had been established with the iron copper compacts. The readings on our own instrument were then determined for these specimens, and the curve was drawn.

To determine whether the curve in Fig. 3 correctly represented a ferrite curve for weld metal, a metallographic study was made of a number of pads included in this study. The pads were sectioned perpendicularly to the axis of the beads, polished, etched, photographed and examined. Two of the samples are shown in Fig. 4. The ferrite was extremely fine because of the pad geometry and welding procedures, and a point count procedure of determining the ferrite level was judged too difficult. Therefore, a ten-line count method was used on the photographs. This consisted of drawing ten parallel and equally spaced lines on each photograph, and accurately totaling the length of ferrite intercepts on these lines with a draftsman's dividers. The total length of the ferrite intercepts divided by the total length of the lines gave the percent ferrite. Preliminary studies had shown that the average of the ferrite values of individual pictures at the top, middle and bottom of the bead in the center gave a reasonably good over-all value for ferrite; therefore, three pictures per pad were used. The average Magne Gage readings versus the metallographic ferrite determinations from these pads are given in Table 1 and included in Fig. 3. The metallographic checks established that the curve drawn from the copper iron standards was reasonable.

As pointed out by Fleischmann,[5] different permeability of the ferrite in different types of weld metal could affect the Magne Gage readings because of the low magnetic field strengths. To determine if this factor influenced the types of weld metal included in this study, four observers examined metallographically weld metal containing from 4.2 to 8.4% measured ferrite by Magne Gage. Sizes $^1/_8$ and $^5/_{32}$ in. were included, and one pad each of three types of coating and of weld metal types 308, 308 LC, 347, 309 and a molybdenum bearing 18-8 type. None of the sizes, coating types or weld metal types showed an abnormally higher or lower percentage of ferrite metallographically than would be expected from the Magne Gage reading. The results from the various observers showed a relationship between ferrite and Magne Gage reading, but a random distribution with regard to all the other variables. Of the 15 pads studied, the average ferrite estimated by the observers differed from the ferrite as measured by the Magne Gage by more than ±1% on only three pads. The three that were not within this tolerance, a 308, a 308 LC and a 347, were within ±2% of the measured ferrite. This data agreed with the data given in Table 1 in indicating that the variation in permeability of the ferrite in the alloys included in this study did not seem to have sufficient effect to warrant its consideration.

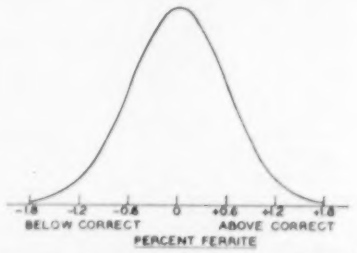

Fig. 7 The variations in calculated percent ferrite due to chemistry variations shown in Table 9 for Type 308 weld metal

Procedure Used for Analysing the Data

It was impractical and would not have been particularly useful to have included in this paper the data on each of the individual weld pads. Instead, the data were summarized in various ways. The study was made on a statistical basis because of the large number of pads and the variables involved. However, statistical terminology was avoided and only one major statistical tool was used—the frequency distribution curve. A typical normal distribution representing the theoretical normal curve of error and data due to chance inaccuracies is illustrated in Fig. 5. This had the advantage of

Table 6—Effect of Cooling Rate, Interpass Temperatures and Welder on Measured Ferrite. Average of Readings from One Weld Bead. Type 347, DC Titania, $^5/_{32}$-In.

Description	*Pad No.*	*Welder*	*Ferrite, %*
Original test, standard procedure	2956	1	6.6
Original test, standard procedure	3164	1	8.4
40 F quench and interpass	3165	1	8.6
Air cool, 150 F interpass	3166	1	6.4
40 F quench and interpass, 1 day later	3167	1	8.0
Air cool, 150 F interpass, 1 day later	3168	1	8.6
Standard procedure	3169	2	7.4
Standard procedure	3170	3	7.2
Standard procedure, 1 day later	3171	2	6.6
Standard procedure, 1 day later	3172	3	6.8

Table 7—Effect of Bead Thickness on Measured Ferrite. Average of Readings from One Layer. Type 309, DC Titania, $^3/_{16}$ In., Pads 3409-9-10-11, Welder No. 1 (Average of Readings from One Weld Bead)

Average bead thickness, in.	*Ferrite, %*
0.06	4.0
0.08	4.2
0.12	3.6

presenting the results graphically in an easily understood form.

Influence of Welding Procedure on Measured Ferrite

Several series of tests were run to determine the reproducibility of the measured ferrite as a number of conditions were varied. The results of these tests are given in Tables 2 to 7. Table 2 shows the results obtained by various welders, including three engineers whose poorer control of arc length tended to produce low ferrite. Table 3 shows the results with pads only 1 bead wide versus pads made 4 beads wide. The readings on the 4-bead pads were taken only on the center two beads. Table 4 gives the effects of various currents. Table 5 lists the results on various layers of a pad made on a nonmagnetic Type 304 plate. Table 6 shows the results with various cooling rates, interpass temperatures and welders. Table 7 shows the effect of bead thickness. On all tests, the spread of individual Magne Gage measurements on one weld layer was quite reasonable. Of 90 tests in this group for which individual readings were available, better than half showed a total spread between the highest and lowest reading of 0.8 to 1.2% ferrite. Over one-quarter of the remaining tests showed less variation than this and under one-quarter showed a total spread of from 1.4 to 2.6% ferrite. The spread of the values in the 4-bead wide pad, Table 3, was somewhat greater than on the single-bead wide pads. The data in this series of tests indicates that ferrite in an as-welded pad can be rather easily and reproducibly measured by means of a Magne Gage, and that differences in technique have relatively little effect on the measured percent ferrite.

To get a good average value for ferrite content of a weld in minimum time, the authors recommend that the pads be welded as described here, 1/2 inch high if on stainless plate, 1 inch high if on mild, and measurements made on the center portion of the pad. Two more layers should be added and the process repeated. If the readings do not agree within 1% ferrite, a third set of readings should be taken after two more layers have been added. This procedure should be repeated by a second welder and perhaps a third, to insure that standard welding techniques have been used.

The first experimental distribution curve presented shows the variations in Magne Gage readings. More than one batch of electrodes of a given type, size and coating were frequently made from a given heat of wire. These successive batches were sometimes made on the same day, sometimes weeks or even months later. Table 8 shows how

Table 8—Variations Between Magne Gage Readings Due to Experimental and Human Error

Variation from average MG reading	*Approximate ferrite variation, %*	*Frequency of occurrence*	*Frequency per 1.24 MG points*	*Cumulative % of total readings*
0/1.24	0.00/0.27	114	114	33.55
1.25/2.49	0.27/0.53	95	95	61.46
2.50/3.75	0.53/0.80	38	38	72.64
3.75/4.99	0.80/1.06	26	26	80.29
5.00/6.24	1.06/1.33	21	21	86.47
6.25/8.74	1.33/1.86	19	9.5	92.06
8.75/12.49	1.86/2.65	16	5.3	96.77
12.50/16.24	2.65/3.46	8	2.7	99.12
16.50/19.99	3.46/4.23	3	1.0	100.00
20.00 and over		0		
TOTAL		340		

Table 9—Variations in Ferrite Due to Errors in Chemistry

Ferritizers

Element	*Assumed variation from actual, %*	*Cr equivalent of element*	*Variation in Cr equivalent, %*	*Variation in calculated ferrite, %**
Silicon	±0.03	1.5	±0.045	±0.11
Chromium	±0.15	1.0	±0.15	±0.38
Molybdenum	±0.05	1.0	±0.05	±0.13
Columbium	±0.06	0.5	±0.03	±0.08

Austenitizers

Element	*Assumed variation from actual, %*	*Ni equivalent of element*	*Variation in Ni equivalent, %*	*Variation in calculated ferrite, %†*
Carbon	±0.004	30	±0.12	±0.24
Manganese	±0.02	0.5	±0.01	±0.02
Nickel	±0.10	1	±0.10	±0.20
Nitrogen	±0.005	30	±0.15	±0.30

* Based on 1% ferrite being equal to 0.4% chromium equivalent.
† Based on 1% ferrite being equal to 0.5% nickel equivalent.

Table 10—Summary of All Pads, Ferrite as Calculated from the Schaeffler Diagram Versus Measured Ferrite

No. (see Fig.)	*Weld metal type*	*Total No. of pads*	*Average equivalent Cr*	*Average equivalent Ni*	*Average difference between measured and calculated ferrite, %*
1	308 LC	103	19.9	12.0	−1.6
2	347	223	20.7	12.2	−1.0
3	308	94	20.4	12.5	−1.2
4	308 MO	38	22.1	13.7	−0.1
5	316	22	21.9	15.9	+5.1
	317	...	...	...	...
	318	...	...	...	...
6	316 LC	101	21.9	15.1	+3.1
	317 LC	...	...	...	...
7	309	74	24.6	17.2	+2.8
	309 CB	...	...	...	...
TOTAL		655			

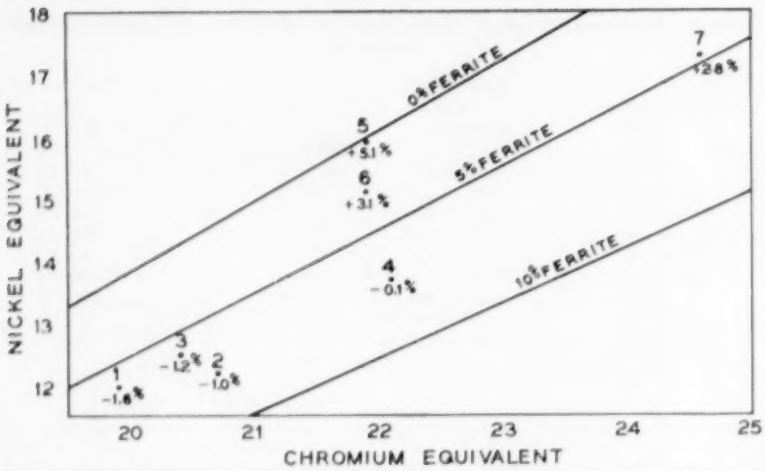

Fig. 8 Data from Table 10 plotted on an enlarged section of the Schaeffler diagram

The number above the point refers to the weld metal type as given in Table 10, the percentage below the point refers to the amount of measured ferrite above (+) or below (—) the calculated ferrite.

individual readings varied from the average of their group. Figure 6 is the distribution curve for this data, and includes a normal distribution curve for comparison. The shape of the curve was not changed if the data were plotted on a positive and negative basis. Therefore, the sign was ignored in collecting and plotting the variations. These data were of use in evaluating the spread of values between the calculated ferrite and the measured ferrite.

The over-all data from the tests given in Tables 2 to 7, and the distribution curve described in Table 8 and Fig. 6, led to two conclusions:

1. Ferrite in an as-welded deposit of the type described can be reproducibly measured with a Magne Gage. It is possible that the fine ferrite dispersion and the preferred vertical orientation of the stringers within the weld beads contribute to this uniformity.

2. It should not be difficult for laboratories with common standards, using the procedures recommended previously, to duplicate each other. Therefore, the measurement of ferrite with a Magne Gage is potentially useful in specifications.

Chemistry Variations

Since the calibration of ferrite from any constitution diagram is based upon the chemistry of the deposit, it is subject to variations between the true chemistry and the analyzed chemistry. The effect of these variations on the calculation of ferrite was considered on a theoretical basis.

Table 9 gives estimated analytical accuracies which may be expected about two-thirds of the time, not from a research laboratory but from a well-managed quality control laboratory which normally handles many such analyses. The analytical variations were converted to nickel and chromium equivalents and to the corresponding ferrite variations. The individual variations were squared, added together and the square root of the sum then represented the combined effect of all the variations. Making the assumption that the variations which occur follow a normal distribution curve as described earlier, the over-all effect on calculated ferrite level was represented by the curve for Type 308 shown in Fig. 7. This included only the elements carbon, manganese, silicon, chromium, nickel and nitrogen. If molybdenum and columbium variations had been included, the curve would be somewhat broader.

Putting the curve into words, about 68% of the laboratory determined analyses will give a ferrite result within 0.45% of the ferrite as calculated from the true chemistry, about 27% will be from 0.45 to 0.90% away, about 4% of the results will be from 0.90 to 1.35% away, and a small fraction of a percent will be more than 1.35% away from the ferrite calculated from the true chemistry.

Schaeffler Diagram

The Schaeffler constitution diagram for stainless steel weld metal[5] has been successfully and widely used to judge the ferrite content of weld metal. The first step in studying the weld pads available for this work was to compare the ferrite content as calculated from the chemistry with the ferrite content as measured.

Most of the deposit chemistry was estimated from the known chemistry of the core wire, using procedures which had been developed over a period of years and which are continually being checked.

Based on previous experience, these estimations were between one and one-half times the limits outlined in Table 9, and were judged reasonable and acceptable for the intended purpose. The actual deposit chemistry was used where available.

The ferrite level of each deposit was calculated from the chemistry using an enlarged Schaeffler diagram. The difference between the calculated and the measured ferrite was recorded for each pad. A positive value for this difference indicated that the measured was higher than the calculated ferrite, and a negative value that the measured was lower

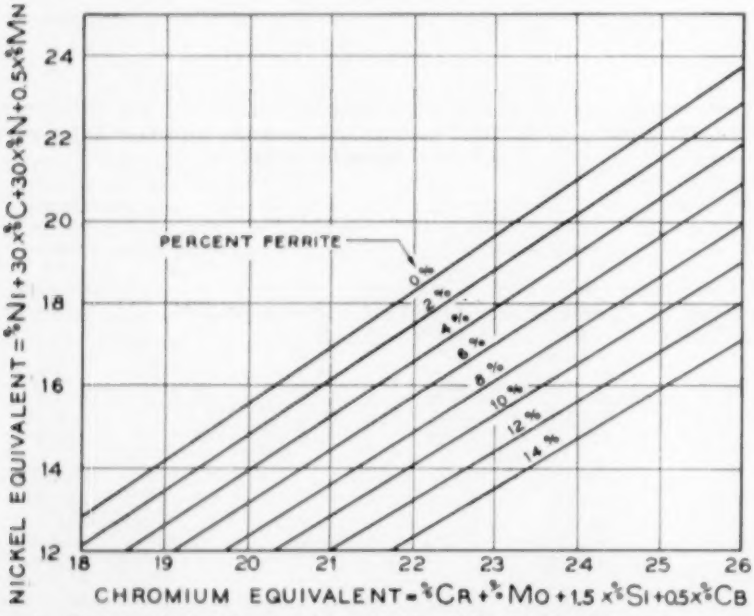

Fig. 9 New constitution diagram for austenitic stainless-steel weld metal

than the calculated ferrite. These data for specific types of weld pads were expressed in terms of averages in Table 10, and graphically on an enlarged section of the Schaeffler diagram in Fig. 8.

A study of Fig. 8 and the data used to derive it led to several conclusions. The first was predictable, a factor for nitrogen should be introduced into the calculations. It was apparent from a study of the individual pads that there were some which showed much less ferrite than expected. It was learned very early in the study that these pads were made from relatively high nitrogen heats, and the low ferrite levels explain why the types 308, 347 and 308 LC averaged 1.0 to 1.6% less ferrite than calculated. The remaining heats with normal nitrogen showed good agreement between calculated and measured ferrite, far better in fact than the ±4% claimed by Schaeffler. This observation has been confirmed by others who have been using the Schaeffler diagram to calculate ferrite in types 347 and 308 LC, and is a tribute to Schaeffler's excellent work in this field.

The second conclusion was that types 316, 309, and related types which have higher Cr and Ni equivalents than the 308 and 347 types, averaged appreciably higher in ferrite content than the Schaeffler diagram predicted, and that a new diagram should correct this discrepancy.

However, before modifying the diagram, it was desirable to establish an equivalent for nitrogen.

The Nickel Equivalent for Nitrogen. Nitrogen is known to be a strong austenitizer. Scherer[10] stated in 1940 that in highly alloyed chrome-nickel steels 0.10% nitrogen could replace 3 to 4% nickel. To establish a nitrogen factor to be used in a new constitution diagram, a study was made of 27 type 308, 347 and 308 low-carbon weld pads in which the nitrogen was very high, being over 0.115%. In each case, the percent ferrite below typical and the percent nitrogen above typical were determined for the particular size, coating and analysis. By dividing the decrease in the expected ferrite level by the excess percentage of nitrogen, the ferrite equivalent to 0.01% nitrogen was found. For 24 of the pads, this factor ranged from 0.4 to 0.8% ferrite, with an average of 0.6%. On the new diagram which will be described later, 0.6% ferrite is equivalent to 0.3% nickel, and therefore the nickel equivalent of nitrogen was set at 30 for the new diagram.

The New Diagram

Nitrogen analyses were run on a number of the weld pads and core wires. With the information developed, the nitrogen contents of over half of the pads included in the study were established. This group included all the high nitrogen heats, because all pads were included in which the measured ferrite was well below the calculated ferrite. Thus the pads considered in the balance of the paper contain an abnormally high proportion of high nitrogen pads.

New nickel equivalents were calculated for each pad for which a nitrogen value had been secured and the resulting data plotted. To bridge the gaps between the 308, 309 and 316 areas, pads were run on a series of laboratory-made electrodes. Two heats of 308 and 309 and one heat of 316 LC were included. On these core wires, a series of coatings were extruded with additions to decrease the chromium and nickel in one set, and to increase the chromium and nickel in another. With these tests to supplement the available data from the quality control pads, Fig. 9 was drawn. This diagram covers the chemical composition range of the weld metal types studied. The chromium equivalent is the same as for the Schaeffler diagram, but the nickel equivalent has been modified by the addition of a nitrogen factor, making the new nickel equivalent equal to % Ni plus 30 × % C plus 30 × % N plus 0.5 × % Mn.

The new diagram differs from the Schaeffler diagram for the same area in a number of ways. First, of course, the nitrogen equivalent has been added and has affected the location of all the lines, since all commercial stainless steels contain some nitrogen. Second, the slope of the constant ferrite lines has been increased to correct the discrepancies found between the calculated and measured ferrite on types 316, 309 and related types that were described earlier. A third difference is that the spacing between constant ferrite lines is relatively constant, while on the Schaeffler diagram the spacing between constant ferrite lines varies, being noticeably greater at the 10% ferrite area than in the zero to five or the 15 to 20% area. The data now available does not allow the extension of the new diagram to higher percentages of ferrite, but it is obvious that the spacing between ferrite

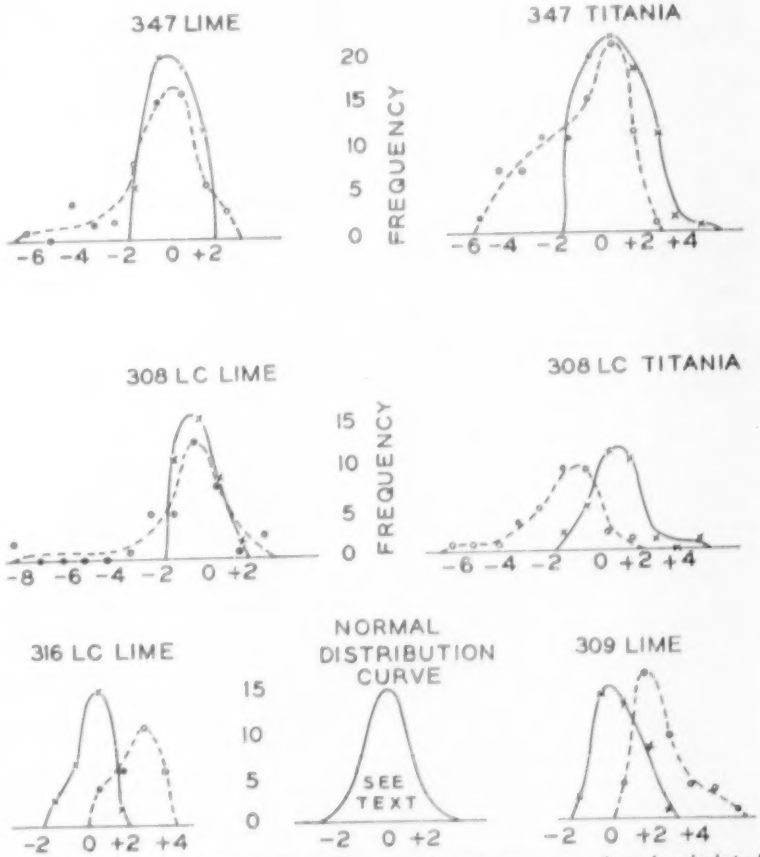

Fig. 10 Distribution curves for differences between measured and calculated ferrite for the Schaeffler diagram (0 and dotted lines) and the new constitution diagram (X and solid lines)

The values given are for the percent ferrite, with positive values indicating that measured ferrite exceeded the calculated, and negative that measured ferrite was less than calculated.

lines must decrease as the ferrite level increases.

Comparisons Between Calculated and Measured Ferrite

It was then possible to compare the spread between measured and calculated ferrite for the pads available, making this comparison first for the Schaeffler diagram, and then for the new diagram. These comparisons are shown graphically in Fig. 10, which includes 278 pads out of the 359 for which nitrogen values were available. The remaining weld metal type groups were too small to give reasonable distribution curves. Figure 10 also includes, for reference and comparison, a normal distribution curve based upon one and one-half times the chemistry variations given in Table 9, and the variations in measured ferrite as given in Fig. 4 increased by 50%. This increase was made because the curve given in Fig. 4 was based upon a comparison of individual values with the average of the set. Thus, the variation was not sufficiently large to cover this situation, where practically all of the values were single determinations. The curve showing deviations in measured ferrite is particularly applicable to these data, since it was drawn directly from the data. These assumptions gave standard deviations of 0.67% ferrite for the chemistry variations and approximately 0.75% ferrite for deviations in Magne Gage readings, for a combined standard deviation of 1.0% ferrite.

The distribution curves in Fig. 10 demonstrated two major points. First, the introduction of nitrogen in the nickel equivalent effectively brought the high-nitrogen, low-ferrite pads which show up on the left side of the Schaeffler based curves into agreement with the normal nitrogen pads. When the distribution curves were compared with the normal distribution curve included in Fig. 10, the results were in reasonable agreement both in shape and spread of values. The better shape was obtained largely by the addition of the nitrogen equivalent. The spread of values in most instances did not exceed ±2% ferrite, a figure which could be predicted from the known variations in Magne Gage readings and in chemistry. Second, the discrepancies found between measured and calculated ferrite in the Schaeffler diagram at higher chromium and nickel equivalents, as found in 316, 317 and 309 types, were corrected.

Those few deviations which exceeded ±2% ferrite on the new diagram distribution curves in Fig. 10 were on the positive side, i.e., the measured ferrite exceeded the calculated value by more than two percent. In general, these were found to be high nitrogen heats, where the nitrogen factor of 30 evidently overcompensated for the effect of the high nitrogen contents.

The factors of electrode size and coating type were found to have little practical effect on the ferrite content of the deposit. The averages of the variations studied did not differ from each other by more than one percent ferrite. We could, however, draw some tentative conclusions on the minor effects due to these variables. The two major groups of 347 and 308 low carbon were judged to have sufficient pads of relatively uniform chemistry and ferrite to allow us to draw these conclusions, which should be regarded as tentative because of the over-all wide spread of data. A rather unusual and unexpected feature of the data was that the titania-type coatings tended to average approximately one percent higher in ferrite for a given chemistry than the lime-type coating. This is not a particular advantage, or disadvantage, because ferrite at a desirable level is obtainable with either coating by proper control of chemistry. Variations between sizes were smaller than the variations between coatings. In general, the smaller sizes showed more negative variations, i.e., measured ferrite lower than calculated, than the larger sizes. This trend was appreciably more pronounced in the lime coatings than in the titania coatings.

Summary and Conclusions

A ferrite study was made on a large number of routine quality control pads. The study covered the measurement of ferrite by means of a Magne Gage and compared the measured ferrite with the ferrite as calculated from the Schaeffler diagram. The same comparison was made with ferrite calculated from a new diagram which included a nickel equivalent for nitrogen. A study of the Schaeffler equivalents for various elements was outside the scope of this paper.

The conclusions were as follows:

1. The Magne Gage, properly used on as-welded specimens, is a useful and reliable instrument for the measurement of ferrite. One laboratory should be able to check another within one percent ferrite in most cases. In addition, the tests are simple and inexpensive. The results indicate that further study of the Magne Gage using the procedures outlined would be worth while and could lead to a standard procedure for measuring and specifying ferrite content of weld metal.

2. Variation in calculated ferrite due to variations in chemistry is a factor which has not been given sufficient thought. Although this factor was studied on a theoretical basis, the results led us to believe that potential variations under good conditions are of the same order of magnitude as those involved in measuring ferrite with the procedures recommended.

3. A nickel equivalent of 30 was established for nitrogen.

4. A new constitution diagram for austenitic stainless-steel weld metal was proposed which included nitrogen in the nickel equivalent. This diagram was modified in shape and slope to improve the accuracy of ferrite calculation on types 309, 309 Cb, 316, 316 LC, 316 Cb, 317 and 317 LC over that obtained with the Schaeffler diagram. Ferrite calculation for the 308 and 347 types is improved on those samples which contain either high or low nitrogen.

Acknowledgment

The authors thank the officers of the McKay Co. for permission to publish this information, which was developed through the efforts of many members of the Research and Quality Control Laboratory at York, Pa.

In addition, they thank Allegheny Ludlum Steel Corp., Armco Steel Corp. and Universal Cyclops Steel Corp. for making many of the nitrogen determinations which were needed for this investigation.

The copper-powder iron-powder compacts on which the curve in Fig. 5 is based were prepared by the Materials Engineering Department, Westinghouse Electric Corp., Pittsburgh.

Bibliography

1. Schaeffler, A. L., "Selection of Austenitic Electrodes for Welding Dissimilar Metals," THE WELDING JOURNAL, **20** (10), Research Suppl., 601-s to 620-s (1947).

2. Strauss, B., and Maurer, E., "Die Hochlegierten Chrom-Nickel Staehle als Nichtrostende Stahle," *Krupp. Monatsh.*, **1**, 129–146 (August 1920).

3. Scherer, R., Riedrich, G., and Hoch, G., "Einfluss eines Gehaltes an Ferrit in austenitischen Chrom-Nickel-Stahlen auf den Kornzerfall," *Arch. Eisenhuttenw.*, **13**, 53–57 (July 1939), as available in Translation No. 891 of H. Brutcher, Altadena, Calif.

4. Field, A. L., Bloom, F. K., and Linnert, G. E., "Development of Armour Welding Electrodes: The Effect of Variation in Chromium-Nickel Ratio and Molybdenum Content of Austenitic (20 Cr–10 Ni) Electrodes on Properties of Armour Weldments," OSRD Report No. 3034, Dec. 14, 1943.

5. Schaeffler, A. L., "Constitution Diagram for Stainless Steel Weld Metal," *Metal Progress*, **56**, 680 and 680-B (November 1949).

6. Simpkinson, T. V., and Lavigne, M. J., "Detection of Ferrite by Its Magnetism," *Ibid.*, **55**, 164–167 (February 1949).

7. Simpkinson, T. V., "Ferrite in Austenitic Steels Estimated Accurately," *Iron Age*, **170**, 166–169 (Dec. 11, 1952).

8. Fleischmann, W. L., "Determination of Ferrite in Type 347 Stainless Steel Weld Deposits," THE WELDING JOURNAL, **33** (9), Research Suppl., 459-s to 468-s (1954).

9. Curran, R. M., and Rankin, A. W., "Welding Type 347 Stainless Steel for 1100 F Turbine Operation," *Ibid.*, **34** (3), 205–213 (1955).

10. Scherer, R., Riedrich, G., and Kessner, H. H., *Stahl u. Eisen*, as available in a translation by C. M. Cosman, *Iron Age*, **155**, 56–60 (Mar. 29, 1945).

DEVELOPMENT OF A FERRITIC-AUSTENITIC WELD JOINT FOR STEAM PLANT APPLICATION

Apparent solution to the cracking of ferritic-austenitic welded joints found in certain protective weld features and in the use of the proper type of austenitic electrodes

BY J. T. TUCKER, JR., AND F. EBERLE

ABSTRACT. Factors involved in the cracking of ferritic-austenitic weld joints subjected to temperature and pressure cycling were evaluated by thermal-cycling tension tests. An apparent solution to this cracking problem was found in certain protective weld features and in the use of austenitic electrode depositing weld metal of a coefficient of expansion approaching that of the ferritic steels.

Introduction

The economics of boiler design usually dictate that materials for a given application be selected on the basis of minimum cost for the necessary high-temperature properties. This practice has led to the combined use of austenitic stainless steels and low-alloy ferritic steels in superheaters, reheaters and main steam lines where high pressures and high temperatures above 1000° F prevail. The resulting weld junction between these dissimilar metals presents a complex-stress picture due to differences in thermal expansion and thermal conductivity of the two types of alloys. The austenitic alloys possess approximately a 30% higher coefficient of thermal expansion and a 40% lower thermal conductivity than the ferritic steels. When such dissimilar weldments are subjected to repeated heating and cooling cycles, the high thermal-expansion stresses combined with metallurgical changes occurring at elevated temperatures may lead to an unsatisfactory service life.

This possibility has been anticipated and studied in the authors' laboratory in 1947 by means of a thermal-cycling test on a full-size steam pipe, 10¾-in. OD x 1.1-in. wall, containing two dissimilar welds made with 19Cr9Ni – Cb electrodes which joined a section of 2¼-Cr1Mo steel to sections of 18Cr8Ni – Cb steel and 16Cr13Ni2Mo – Cb steel.

J. T. Tucker, Jr., is Supervisor, Stress Analysis Group, and F. Eberle is Chief Metallurgical Engineer, Research Center, Babcock & Wilcox Co., Alliance, Ohio.

Paper presented at ASME Metals Engineering Division Conference held in conjunction with 1956 AWS National Spring Meeting, May 7–11, Buffalo, N. Y.

This investigation very closely duplicated the actual operating conditions in the main steam line of a central station boiler. Briefly, the test consisted of bringing the piping up to a metal temperature of 1100° F and to an internal steam pressure of 1500 psi, maintaining these conditions for 109 hr, that is, long enough to allow for some plastic stress readjustment and to provide time for elevated temperature effects to occur, and then removing the pressure and cooling the system down to room temperature.

After 47 pressure and temperature cycles and 4631 hr at 1100° F, circumferential cracks were found at the dissimilar junctions between the 2¼ Cr1Mo base metal and the 19Cr9Ni – Cb weld metal. Subsequent examination revealed that the cracks occurred in the 2¼ Cr1Mo steel in the zone immediately adjacent to the fusion interface with the austenitic weld metal. The cracks, which were intergranular in nature, had propagated inwardly parallel to the highly stressed weld junction and had branched out in all directions for a short distance along the inward path, as shown in Fig. 1. The principal factors which contributed to the failure of the dissimilar welds in the full-size pipe test were believed to have been:

1. The cyclic differential thermal expansion stresses superimposed on the residual welding stresses, the pressure stresses and the thermal conductivity stresses.
2. The relatively low oxidation resistance of the low-alloy ferritic steel which permitted accelerated stress oxidation.
3. The weakening of the critical zone in the ferritic steel by carbon migration into the adjacent austenitic weld metal.
4. Sufficient time at elevated temperature for metallurgical deteriorations to occur.

After the anticipated difficulty had become a reality, a paper describing this work was presented in June 1950[1] to acquaint the industry with the potential hazard of this type of construction. However, results of other investigators working concurrently on the same problem[2, 3] did not corroborate the authors' findings, as their tests did not produce defects of a serious nature at the dissimilar weld junctions. These contradictory results obtained with the same types of materials pointed out the need for additional work to increase the understanding of the various factors affecting the life of a dissimilar weld.

Development of a Suitable Testing Method

Investigating the variables which influence the behavior of ferritic-austenitic welds by means of full-size pipe specimens was obviously impractical from the standpoint of manpower and expense. Therefore, it became necessary to devise a simpler and more economical specimen which, with the exception of the possible influence of size and weld geometry, would contain the essential features contributing to the cracking in the full-size pipe test. For this purpose, three types of specimens, which contained a ferritic-austenitic weld junction prepared by joining 2¼ Cr1Mo steel to 18Cr8Ni – Cb steel with 19Cr9Ni – Cb electrodes, were tested with thermal cycles to determine which was best suited to study the dissimilar weld problem.

The first type of specimen investigated was a standard 0.505-in.-diam tensile coupon containing a ferritic-austenitic weldment at the center of its gage length. This specimen was held for about 20 hr at 1100° F under a tension stress of 2600 psi corresponding to the longitudinal stress prevailing in the tested full-size pipe. The load was then removed and the specimen was allowed to cool down to room temperature. These temperature-stress cycles were repeated until inspection at the weld junctions revealed cracking whereupon

Table 1—Study of Factors Affecting Dissimilar Weld Life

Spec. No.	Specimen type	Specimen size, in.	Rate of cycling	Test temperature, °F	Stress, psi	Total cycles	Time at temperature, hr	Condition of dissimilar junction	Fig. No.
	2¼Cr1Mo/19Cr9NiCb/18Cr8NiCb	10¾/4 OD, 1.1 thick	1/week	1100	2600	47	4631	Cracked	1
	2¼Cr1Mo/19Cr9NiCb/16Cr13Ni2Mo	10¾/4 OD, 1.1 thick	1/week	1100	2600	47	4631	Cracked	
			Stressed tensile specimens						
1	2¼Cr1Mo/19Cr9NiCb/18Cr8NiCb	0.505	1/day	1100	2600	55	1395	Cracked	2
2	2¼Cr1Mo/19Cr9NiCb/18Cr8NiCb	0.505	1/4 hr	1100	2600	472	100	Cracked	2
3	2¼Cr1Mo/19Cr9NiCb/18Cr8NiCb Helium Atmosphere	0.505		1100	2600	1	1436	No defects	3
4	2¼Cr1Mo/19Cr9NiCb/18Cr8NiCb	0.505	1/4 hr	1100	2600	471	100	Cracked	4
5	Lead bath, 2¼Cr1Mo/19Cr9NiCb/18Cr8NiCb	0.505	1/4 hr	1100	2600	243	280	Cracked	
6	2¼Cr1Mo/19Cr9NiCb/18Cr8NiCb	0.505	1/day	1050	2600	68	1426	No defects	5
7	2¼Cr1Mo/19Cr9NiCb/18Cr8NiCb	0.505	1/day	1050	2600	253	4705	Cracked	5
8	2¼Cr1Mo/19Cr9NiCb/18Cr8NiCb	0.505	1/day	1200	2600	68	1314	Fractured	
9	Postheat treated at 1350 F, 2¼Cr1Mo/19Cr9NiCb/18Cr8NiCb	0.505	1/day	1100	2600	137	2541	Fractured	6
10	2¼Cr1Mo, circular notch	0.505	1/day	1100	2600	266	5038	No defects	
11	2¼Cr1Mo, notch one side	0.505	1/day	1100	2600	78	1271	Discontinued	
			Unstressed bar specimens						
1U	2¼Cr1Mo/19Cr9NiCb/18Cr8NiCb	0.750	1/day	1100	0	263	5623	Cracked	
2U	2¼Cr1Mo/19Cr9NiCb/18Cr8NiCb	0.750	1/day	1100	0	263	5623	Cracked	
3U	Water-quenched, 2¼Cr1Mo/19Cr9NiCb/18Cr8NiCb	0.750	1/day	1100	0	253	4841	Fractured	
4U	2¼Cr1Mo/19Cr9NiCb/18Cr8NiCb	0.750	1/4 hr	1100	0	1717	1756	Cracked	
5U	2¼Cr1Mo/19Cr9NiCb/18Cr8NiCb	0.750	1/4 hr	1100	0	1965	1869	Cracked	
6U	2¼Cr1Mo/19Cr9NiCb/18Cr8NiCb	0.750	1/day	1050	0	248	5484	No defects	

Table 2—Externally Unstressed Specimens

Spec. No.	Specimen type	Specimen size in.	Rate of cycling	Test temperature, °F	Stress, psi	Total cycles	Time at temperature, hr	Condition of dissimilar junction
1U	2¼Cr1Mo/19Cr9NiCb/18Cr8NiCb	0.750	1/day	1100	0	263	5623	Cracked
2U	2¼Cr1Mo/19Cr9NiCb/18Cr8NiCb	0.750	1/day	1100	0	263	5623	Cracked
3U	Water-quenched, 2¼Cr1Mo/19Cr9NiCb/18Cr8NiCb	0.750	1/day	1100	0	253	4841	Fractured
4U	2¼Cr1Mo/19Cr9NiCb/18Cr8NiCb	0.750	1/4 hr	1100	0	1717	1756	Cracked
5U	2¼Cr1Mo/19Cr9NiCb/18Cr8NiCb	0.750	1/4 hr	1100	0	1965	1869	Cracked
6U	2¼Cr1Mo/19Cr9NiCb/18Cr8NiCb	0.750	1/day	1050	0	248	5484	No defects
7U	Calorized, 2¼Cr1Mo/19Cr9NiCb/18Cr8NiCb	0.750	1/day	1100	0	248	5196	No defects
8U	Gas-chromized, 2¼Cr1Mo/19Cr9NiCb/18Cr8NiCb	0.750	1/day	1100	0	244	4890	Cracked
9U	12Cr overlay, 2¼Cr1Mo/19Cr9NiCb/18Cr8NiCb	0.750	1/day	1100	0	76	1487	Discontinued
10U	80Ni20Cr overlay, 2¼Cr1Mo/19Cr9NiCb/18Cr8NiCb	0.750	1/day	1100	0	76	1487	Discontinued
11U	Stab. ferritic base matl., 2¼Cr1MoTi/19Cr9NiCb/18Cr8NiCb	0.750	1/day	1100	0	76	1487	Discontinued
12U	Stab. ferritic base matl., 2¼Cr1MoTi/19Cr9NiCb/18Cr8NiCb	0.750	1/4 hr	1100	0	596	405	Discontinued
13U	Ferritic weld metal, 2¼Cr1Mo/low-C 2¼Cr1Mo/18Cr8NiCb	0.750	1/day	1100	0	246	5156	Discontinued
14U	Ferritic weld metal, 2¼Cr1Mo/low-C 2¼Cr1Mo/18Cr8NiCb	0.750	1/4 hr	1100	0	1799	1791	Cracked
15U	Tubular specimen, 2¼Cr1Mo/19Cr9NiCb/18Cr8NiCb	2½ OD, 0.471 thick	1/day	1100	0	63	1280	Cracked
16U	Tubular specimen, 2¼Cr1Mo/19Cr9NiCb/18Cr8NiCb	2½ OD, 0.471 thick	1/day	1100	0	294	5120	Cracked
17U	Tubular specimen, 2¼Cr1Mo/19Cr9NiCb/18Cr8NiCb	6½ OD, 1.00 thick	1/day	1100	0	109	1878	Cracked
18U	Tubular specimen, 2¼Cr1Mo/19Cr9NiCb/18Cr8NiCb	6½ OD, 1.00 thick	1/day	1100	0	294	5120	Cracked

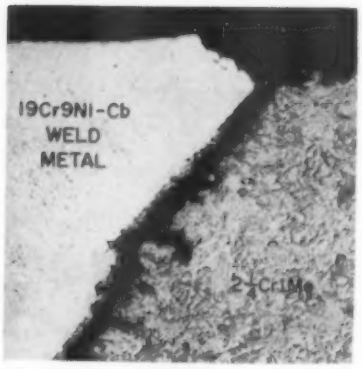

47 cycles 1100° F 4631 hr

Fig. 1 Dissimilar weld crack in 10³/₄-in. OD x 1.1-in.-wall test pipe after pressure and temperature cycles (1100°F–room temp.) X 100. (Reduced by ½ upon reproduction)

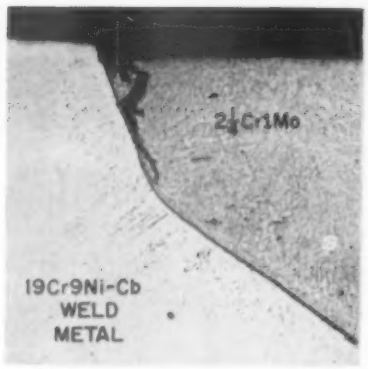

1100° F 1395 hr
55 slow cycles

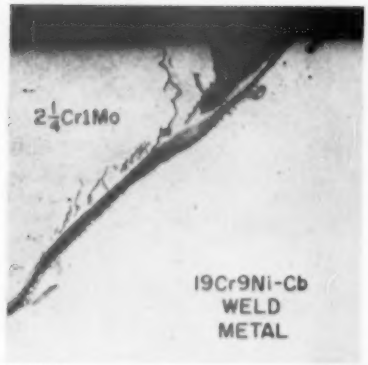

1100° F 100 hr
472 fast cycles

Fig. 2 Dissimilar weld crack in slow- and fast-cycled 0.505 tensile specimens. X 100. (Reduced by ⅓ upon reproduction)

the specimen was sectioned for metallurgical examination. The holding time at elevated temperature was reduced from 109 hr in the pipe test to 20 hr in an effort to reduce testing time, anticipating that the shorter dwell at temperature would still be adequate to permit significant elevated temperature effects to occur. The results with the first tensile-type specimen (Specimen 1, Table 1) confirmed this assumption in that dissimilar weld cracking of the same type as in the full-size pipe test occurred after 55 temperature-stress cycles with a total time of 1395 hr at 1100° F, as compared to 47 cycles and 4631 hr at 1100° F in the latter. The cracking was less extensive but this was attributed to the less severe stress condition and the fact that the total time at temperature was only about one-third that of the full-size pipe test.

A second type of specimen investigated was an externally-unstressed ³/₈-in.-diam bar 6 in. long containing a dissimilar weld in the center of its length. This specimen, which had a zero longitudinal stress, was thermally cycled from an electric muffle furnace where it was held at 1100° F for 20 hr before cooling to room temperature. This method had the advantage of not requiring a special furnace for each individual specimen, but permitted a number of specimens supported in a test rack to be cycled at the same time in a single furnace. However, this advantage was overshadowed by the greater number of cycles required to produce cracking as was demonstrated by Specimen 1U in Table 1. This specimen required 263 cycles and a total time of 5623 hr at 1100° F to produce cracking as compared to 55 cycles and 1395 hr for the thermal-cycling tension test. The important fact brought out by this test method was that dissimilar welds cycled without externally applied stress will suffer the same type of deterioration and cracking as externally-stressed welds, but that the time for failure was notably longer.

The third type of specimen explored was an externally-unstressed tubular specimen containing a dissimilar weld in the center of its length. Two specimen sizes were investigated, 2½-in. OD x 0.471-in.-wall tubing and 6½-in. OD x 1.00-in.-wall piping. These specimens were tried because they contain the weld geometry effects and stress complexities of the full-size pipe test. The tubular specimens were cycled in the same manner as the unstressed ³/₈-in.-diam bar specimens and produced typical dissimilar weld cracking with 63 cycles and 1280 hr at 1100° F (Specimen 15U, Table 2), indicating that the test was more severe than the externally-unstressed ³/₈-in.-diam bar test. Specimen size and cost made this method of testing unattractive as compared to the thermal-cycling tension test, and it was therefore discontinued after two check specimens had also developed cracks. These externally-unstressed tubular data appear in Table 2.

In summary, characteristic dissimilar weld cracking was produced by thermal cycling from 1100° F with the following four specimen types:

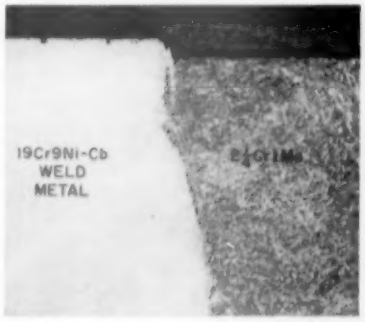

1100° F 1436 hr

Fig. 3 Dissimilar weld interface of tensile specimen held continuously under stress at temperature without cycling. X 100. (Reduced by ½ upon reproduction)

for studying the factors causing ferritic-austenitic weld junction failure and for evaluating preventative measures. A description of the apparatus and the final testing procedure employed are discussed later.

A Study of Factors Affecting Dissimilar Weld Life

Holding Time at Temperature

The appreciable difference in holding

	Number of cycles to produce cracks	*Holding time at 1100° F, hr*
1. 10³/₄-in. OD x 1.1-in.-wall, full-size steam piping, axial stress 2600 psi	47	4631
2. Standard 0.505 tensile specimen under 2600 psi stress	55	1395
3. ³/₈-in. diam bars externally unstressed	263	5623
4. 2½-in. OD x 0.471-in.-wall tube, 6½-in. OD x 1.00-in.-wall pipe externally unstressed	63 109	1280 1878

Of these four testing methods described, the thermal-cycling tension test which developed characteristic dissimilar weld cracking with about the same number of thermal cycles as the full-size pipe test, appeared to be best suited

time between the first tensile specimen and the full-size pipe test indicated that, perhaps, the dwell at temperature, during which plastic stress readjustment and elevated temperature effects occur, was not really as important as it seemed

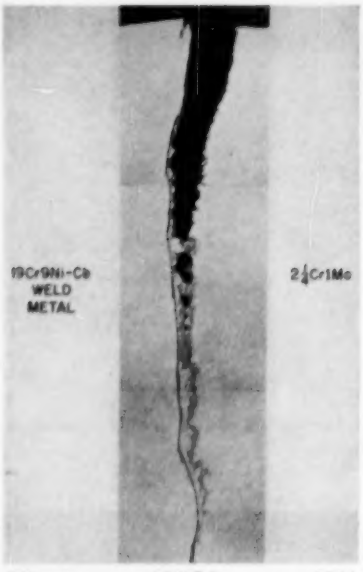

471 cycles 1100° F 100 hr

Fig. 4 Dissimilar weld crack in tensile specimen cycled in helium containing trace of oxygen. (Reduced to X 30)

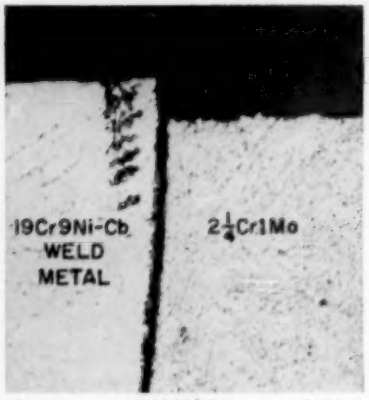

68 cycles 1100° F 1426 hr
(X 100)

327 cycles 1100° F 6228 hr
(X 7)

Fig. 5 Dissimilar weld sections of tensile specimens cycled at 1050° F. (Reduced by 1/3 upon reproduction)

to be according to the observed progressive stress-oxidation type of failure, but that the failure was predominantly caused by the seesaw action of the differential expansion stress caused by cycling. To check this, a duplicate 0.505-in.-diam tensile specimen (Specimen 2, Table 1) containing a 19Cr9Ni – Cb weld between 2¼ Cr1Mo and 18Cr8Ni – Cb was tested in an identical manner, but it was held under stress at temperature (1100° F) for only 10 min to attain temperature uniformity, and then cooled to room temperature. It required 472, or 9 times as many, such fast cycles with a total time at 1100° F of 100 hr to produce the characteristic stress-oxidation crack in the 2¼ Cr1Mo steel, thus indicating that holding time at elevated temperature does have a significant influence upon the weld failure and is necessary to make dissimilar weld testing representative of actual service conditions. The cracks formed in the slow- and in the fast-cycled tensile specimens are shown in Fig. 2.

Stress-Oxidation at Constant Temperature

Since it was evident that the combined action of cyclic stress and holding time at temperature was necessary to produce dissimilar weld cracking in the same number of cycles as the big pipe test, the question was raised as to whether stress-oxidation at the highly stressed weld interface would be sufficient to produce cracking without repeated thermal cycling. Accordingly, a third 0.505-in.-diam tensile specimen (Specimen 3, Table 1) containing a 19Cr9Ni – Cb weld between 2¼ Cr1Mo and 18Cr8Ni – Cb was held continuously (without cycling) at 1100° F under a stress of 2600 psi for 1436 hr. Microscopic examination showed that the dissimilar weld junction had not cracked but that preferential oxidation had uniformly reduced the diameter of the 2¼ Cr1Mo section of the specimen, as shown in Fig. 3. This test pointed out that stress-oxidation and the preferential oxidation step formed at the highly stressed weld interface would not cause cracking and that cycling the highly stressed material along the weld interface was necessary to produce the characteristic dissimilar weld failure. This test also indicated that maintaining a dissimilar weld in a steam pipe continuously at operating temperature would significantly extend its life.

Cyclic Stressing in the Absence of Oxygen

Since cracking was not produced in the presence of oxygen without cycling, a study was then made to determine if cracking could be produced with cyclic stresses alone, in the absence of oxygen. One 0.505-in.- diam tensile specimen containing a 19Cr9Ni – Cb weld between 2¼ Cr1Mo and 18Cr8Ni – Cb was fast-cycled in a helium atmosphere, and a second specimen in a lead bath. After the tests were completed, it was found that both specimens had cracked (see Table 1, Specimens 4 and 5). Unfortunately, there had been a small amount of oxygen in the helium and also in the lead bath

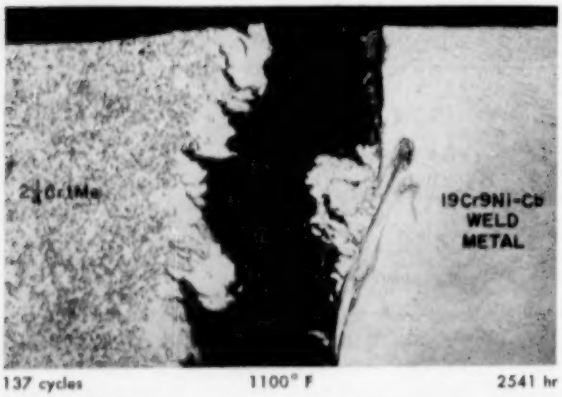

137 cycles 1100° F 2541 hr

Fig. 6 Dissimilar weld fracture in tensile specimen post-weld treated at 1350° F and thermal-stress cycled at 1100° F. X 100. (Reduced by 1/2 upon reproduction)

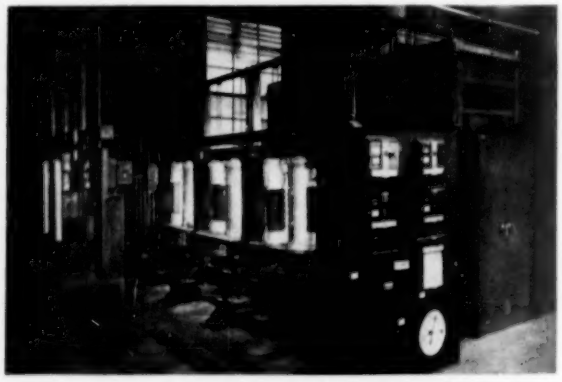

Fig. 7 Test apparatus for thermal-cycling tension tests

which allowed some oxidation to occur, although to a considerably smaller degree. Therefore, the attempt to determine the effect of thermal cycling on a dissimilar weld in the complete absence of oxygen was unsuccessful, but it did show that cracking would occur under cyclic stresses with a very limited oxygen supply, as is illustrated in Fig. 4. These tests have not been repeated because of the more urgent need of finding a practical solution to the cracking problem.

Thermal Cycling from a Lower Temperature 1050° F

The transition from the ferritic chromium-molybdenum steels to the austenitic 18Cr8Ni-type alloys in superheaters generally is made at about 1100° F, which represents the limit of satisfactory oxidation resistance combined with adequate creep-rupture strength for these low-alloy steels. However, since there were main lines with dissimilar weldments in service at 1050° F, the practical question was raised as to whether the lower operating temperature, with corresponding decrease in the differential thermal expansion stresses and in the rate of oxidation, might significantly increase the number of thermal stress cycles which these dissimilar weld joints could withstand. Accordingly, two 0.505-in.-diam tensile specimens containing 19Cr9Ni – Cb welds between $2^1/_4$Cr1Mo and 18Cr8Ni – Cb were subjected to the thermal-cycling tension test at 1050° F. The first specimen (Specimen 6, Table 1) was examined metallurgically after 68 cycles and 1426 hr at 1050° F, and no defects were found at the weld interface (see Fig. 5). Its companion specimen (Specimen 7, Table 1) was continued under test until visual inspection revealed the presence of a stress-oxidation notch at the dissimilar weld junction after 253 cycles and 4705 hr at 1050° F. Additional cycling led to crack propagation extending through the entire specimen cross section in a total of 327 cycles and 6228 hr at 1050° F, as shown in Fig. 5. These results, therefore, indicate that at 1050° F cycle life may be considerably longer than at 1100° F.

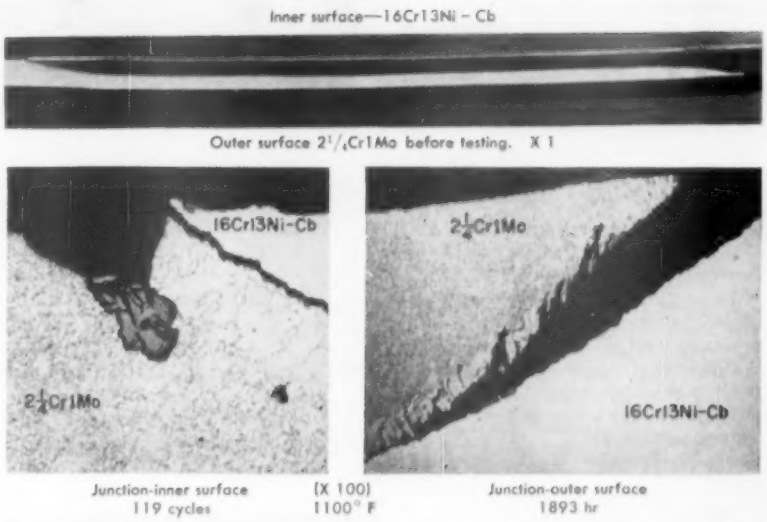

Fig. 8 Cracked composite tube connection after thermal-stress cycling. (Reduced by $^1/_2$ upon reproduction)

Thermal Cycling from a Higher Temperature, 1200° F

A further effort to reduce testing time and to demonstrate the effects of a higher metal temperature was made on a 0.505-in.-diam tensile specimen (Specimen 8, Table 1) containing a 19Cr9Ni – Cb weld between $2^1/_4$Cr1Mo and 18Cr8Ni – Cb by employing a cycling temperature of 1200° F which would accelerate stress-oxidation attack and increase thermal expansion stresses and carbon migration. Under these conditions, complete fracture of the dissimilar weld occurred at 68 cycles whereas at 1100° F with about the same

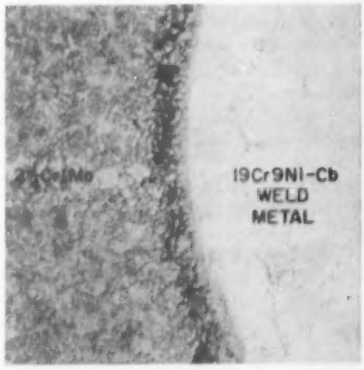

Fig. 9 Cracking of dissimilar weld junction protected with 12Cr overlay. X 100. (Reduced by $^1/_2$ upon reproduction)

Table 3—Oxygen Barriers and Ferritic Welds

Spec. No.	Specimen type	Specimen size, in.	Rate of cycling	Test temperature, ° F	Stress, psi	Total cycles	Time at temperature, hr	Condition of dissimilar junction	Fig. No.
12	Calorized, $2^1/_4$Cr1Mo/19Cr9NiCb/18Cr8NiCb	0.505	1/day	1100	2600	198	3699	Cracked	
13	Chrome-plated (0.003 in.), $2^1/_4$Cr1Mo/19Cr9NiCb/18Cr8NiCb	0.505	1/day	1100	2600	268	4376	Fractured	
14	Chrome-plated (0.010 in.), $2^1/_4$Cr1Mo/0.6 Mo/18Cr8NiCb	0.505	1/day	1100	2600	278	5050	Fractured	
15	12Cr overlay, $2^1/_4$Cr1Mo/19Cr9NiCb/18Cr8NiCb	0.505	1/day	1100	2600	345	5416	Cracked	9
16	80Ni20Cr overlay, $2^1/_4$Cr1Mo/19Cr9NiCb/18Cr8NiCb	0.505	1/day	1100	2600	308	5315	No defects	10
17	$2^1/_4$Cr1Mo/low-C $2^1/_4$Cr1Mo/18Cr8NiCb	0.505	1/day	1100	2600	277	5067	Cracked	
18	$2^1/_4$Cr1Mo/low-C $2^1/_4$Cr1Mo/18Cr8NiCb	0.505	1/day	1100	5200	50	841	Discontinued	
19	$2^1/_4$Cr1Mo/low-C $2^1/_4$Cr1Mo/18Cr8NiCb	0.505	1/day	1100	2600	168	3256	Cracked	
20	$2^1/_4$Cr1Mo/0.6 Mo/18Cr8NiCb	0.505	1/day	1100	2600	268	5024	Cracked	11
21	$2^1/_4$Cr1Mo/0.6 Mo/18Cr8NiTi	0.353	1/day	1100	2600	58	1190	Fractured	
22	$2^1/_4$Cr1Mo/0.6 Mo/18Cr8NiTi	0.372	1/day	1100	2600	249	5000	Cracked	
23	9Cr1Mo/flash weld/18Cr8NiCb	0.338	1/day	1100	2600	218	4089	Fractured	

number of cycles only a small crack had formed. This test pointed out that the metal temperature has a considerable effect on the number of temperature-stress cycles a dissimilar weld can withstand without cracking. However, excessive scaling of the 2¼-Cr1Mo steel raised doubts as to the applicability of the results, and future testing was, therefore, generally confined to 1100° F.

Postweld Heat Treatment

To investigate the possible beneficial effect of postweld heat treatment on a dissimilar weld, a specimen containing a 19Cr9Ni – Cb weld was heated to 1350° F for 1 hr and furnace cooled immediately after welding prior to testing. This treatment should minimize the air-hardening effect resulting from martensite formation during welding and should also reduce the magnitude of residual welding stresses. This specimen, shown in Fig. 6, fractured after 137 temperature-stress cycles and 2541 hr at 1100° F, whereas unstress-relieved specimens under similar conditions displayed only crack formation, showing that post weld heat treatment did not give an improvement (compare Specimens 1 and 9 in Table 1). The lack of carbides in the fracture zone reveals that considerable carbon migration has occurred from the 2¼ Cr1Mo material adjacent to the weld interface because of the high annealing temperature.

The test results obtained in the study of the factors affecting dissimilar weld cracking are summarized in Table 1.

The Thermal-Cycling Tension Test

It is evident from the results obtained from these tensile specimens containing 19Cr9Ni – Cb welds that dissimilar weld failures are caused by cyclic differential thermal expansion stresses combined with sufficient time at elevated temperature for oxidation, stress relaxation and metallurgical deterioration to occur and that both conditions are necessary to duplicate the cracking produced by the simulated service test with a full-size steam pipe. It is also evident that any variation in temperature, number of cycles or holding time between cycles can have a very appreciable effect on the life of a dissimilar weld. Since these factors could be controlled, the thermal-cycling tension test on tensile specimens containing dissimilar welds appeared to be a suitable and relatively inexpensive method of evaluating dissimilar weld behavior. Moreover, this method of testing gave results which, with some measure of confidence, could be translated into actual service conditions. The specimen preparation and the test apparatus employed in the subsequently described evaluation of protective weld features were as follows.

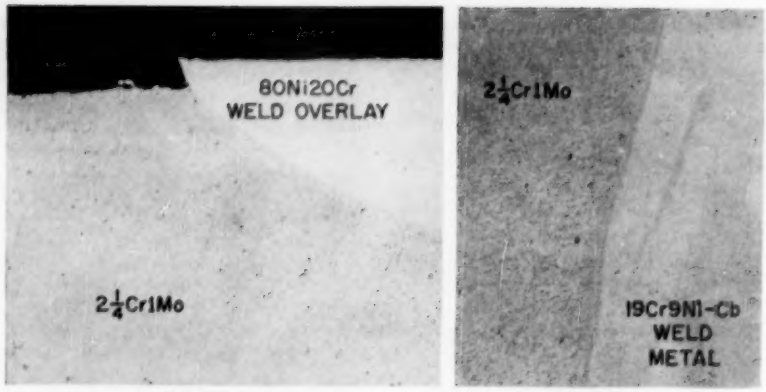

Fig. 10 Dissimilar weld junction protected with 80Ni20Cr weld overlay after thermal cycling. X 100. (Reduced by ½ upon reproduction)

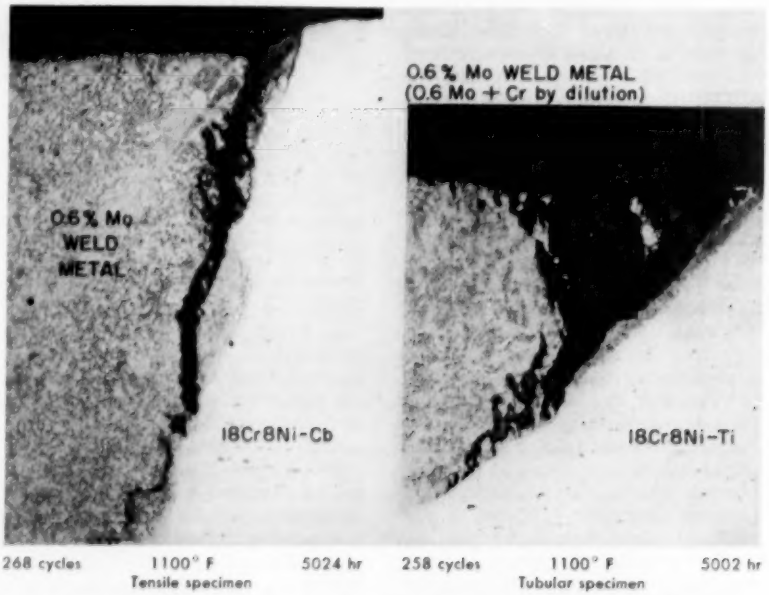

Fig. 11 Dissimilar weld junction made with 0.6 Mo electrodes after thermal-stress cycling. X 100. (Reduced by ½ upon reproduction)

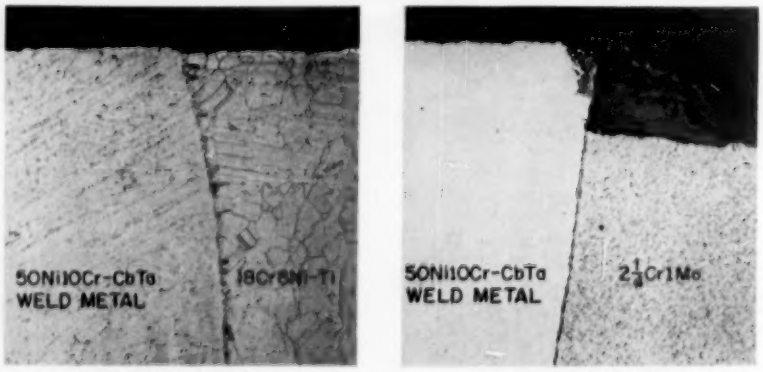

Fig. 12 Dissimilar weld junction made with 50Ni10Cr–CbTa electrodes after thermal-stress cycling. (Reduced by ½ upon reproduction)

Table 4—Welds with Intermediate Coefficient of Expansion

Spec. No.	Specimen type	Specimen size, in.	Rate of cycling	Test temperature, °F	Stress, psi	Total cycles	Time at temperature, hr	Condition of dissimilar junction	Fig. No.
24	2¼Cr1Mo/50Ni10CrCbTa/18Cr8NiTi	0.505	1/day	1100	2600	255	5013	No defects	12
25	2¼Cr1Mo/50Ni10CrCbTa/18Cr8NiTi	0.505	1/day	1200	2600	362	6228	Fractured	
26	2¼Cr1Mo/50Ni10CrCbTa/18Cr8NiTi	0.505	1/day	1200	2600	263	5004	No defects	
27	2¼Cr1Mo/50Ni10CrCbTa/18Cr8NiTi	0.505	1/day	1100	2600	291	5748	Under test	
28	Heavy weld, 2¼Cr1Mo/50Ni10CrCbTa/18Cr8NiCb	0.505	1/day	1100	2600	247	5000	No defects	
29	Heavy weld, 2¼Cr1Mo/50Ni10CrCbTa/18Cr8NiCb	0.505	1/day	1100	2600	539	10000	No defects	
30	Heavy weld, 2¼Cr1Mo/50Ni10CrCbTa/18Cr8NiCb	0.505	1/day	1200	2600	388	7056	Fractured	
31	Machined from heavy wall tube, 2¼Cr1Mo/50Ni10CrCbTa/18Cr8NiTi	0.505	1/day	1100	2600	150	3068	Under test	
32	2¼Cr1Mo/50Ni10CrCbTa/18Cr8NiCb	0.320	1/day	1100	11000	375	2992	Fractured	
33	2¼Cr1Mo/50Ni10CrCbTa/18Cr8NiCb	0.320	1/day	1100	13500	232	1856	Fractured	
34	Overlay, 2¼Cr1MoTi/R-48 Inconel/18Cr8NiCb	0.505	1/day	1100	2600	264	5101	No defects	
35	2¼Cr1MoTi/R-48 Inconel/18Cr8NiCb	0.505	1/day	1100	2600	302	5133	No defects	13
36	2¼Cr1MoTi/R-48 Inconel/18Cr8NiCb	0.505	1/day	1100	2600	279	5007	No defects	
37	Heavy weld, 2¼Cr1Mo/BP-65 Inconel/18Cr8NiCb	0.505	1/day	1100	2600	254	5003	No defects	
38	Heavy weld, 2¼Cr1Mo/BP-65 Inconel/18Cr8NiCb	0.505	1/day	1200	2600	288	5330	Fractured	
39	Heavy weld, 2¼Cr1Mo/BP-65 Inconel/18Cr8NiCb	0.505	1/day	1100	2600	302	6125	Under test	
40	Machined from heavy-wall tube, 2¼Cr1Mo/BP-65 Inconel/18Cr8NiTi	0.505	1/day	1100	2600	101	2074	Under test	
41	2¼Cr1Mo/BP-65 Inconel/18Cr8NiCb	0.320	1/day	1100	11000	300	2400	Fractured	
42	2¼Cr1Mo/BP-65 Inconel/18Cr8NiCb	0.320	1/day	1100	13500	145	1160	Fractured	

The tensile specimens were machined from fully-restrained flat test plates containing ferritic-austenitic welds which were examined radiographically and microscopically after welding. The machined specimens were examined with the fluorescent-penetrant method and were tested in the as-welded condition, with several specified exceptions. The various combinations of base metals, weld metals and the special protective features tested are described in the text of the paper or are listed in the Summary Tables 1 to 5 with the test results.

Each specimen was dead-weight loaded through a lever system to a longitudinal stress of 2600 psi in the apparatus shown in Fig. 7 and was heated to test temperature in an electric furnace in approximately 2 hr. These conditions of stress and temperature were maintained for 20 hr, whereupon the stress was removed and the specimen raised above the furnace and cooled in air to room temperature in approximately 2 hr. The specimen was then again lowered into the furnace, and the cycle was repeated daily until the specimen had accumulated 5000 hr at test temperature corresponding to the total exposure time in the full-size pipe test and involving approximately 260 temperature-stress cycles or, until daily visual inspection or monthly examination under a magnification of 30 × supplemented with fluorescent - penetrant inspection revealed the formation of a notch or crack at a weld junction. When there was sufficient indication that an oxide notch or crack was present, the specimen was sectioned longitudinally at 90-deg intervals and examined microscopically.

Difficulty of Detecting Crack Initiation

In the earlier part of the investigation, the various specimens were evaluated on the basis of their cycles to failure. However, subsequent experience with this test revealed that it was difficult, if not impossible, to determine, without destroying the specimen, whether or when a notch or crack had begun to form at a weld interface. Many times the crack or notch at the weld interface was so tightly filled with oxide or scale that neither fluorescent nor visual inspection under a magnification of 30 × could detect it; and the failure became evident only on complete rupture of the specimen during testing or by metallurgical examination after the specimen had completed the specified test duration of 5000 hr at temperature. When notches or cracks were detected by visual inspection, they were found in various stages of propagation from a very small notch to a crack covering 80% of the weld interface; and it was not possible to determine after which number of thermal cycles the crack had been initiated. Thus, it was evident that a comparison of specimens on the cycles-to-failure basis sometimes gave only a very general indication of an improved condition and that a better method of comparing and evaluating dissimilar welds was needed. This new basis for comparison was given by subsequently developed welds which withstood 250 to 270 temperature-stress cycles at a total exposure time of 5000 hr at test temperature without any defects at the weld junction other than preferential oxidation at the low-alloy surface. Therefore, the cycles-to-failure basis of comparison was discontinued and only those specimens completing the thermal-cycling tension tests for 5000 hr at test temperature without defect were considered satisfactory.

Thermal Cycling Externally Unstressed Specimens

Although externally-unstressed ¼-in.-diam bar specimens require a longer testing time, as was previously discussed, a series of thermal-cycling tests with such specimens was performed because this method allowed more specimens to be tested simultaneously and thereby widened the scope of study. Some specimens contained 19Cr9Ni–Cb welds between 2¼Cr1Mo and 18Cr8Ni–Cb while others contained this same weld protected with features such as pack calorizing, gas chromizing, carbide-stabilizing ferritic base metal and oxygen-barrier weld overlays. Specimens containing dissimilar welds made with low-carbon 2¼Cr1Mo electrodes

Table 5—Tubular Specimens Under Pressure

Spec. No.	Specimen type	Specimen size, in.	Rate of cycling	Test temperature, °F	Longitudinal stress, psi	Total cycles	Time at temperature, hr	Condition of dissimilar junction	Fig. No.
1T	2¼Cr1Mo/composite weld junction/16Cr13NiCb	2¼ OD, 0.26 thick	1/day	1100	2600	114	1767	Cracked	8
2T	2¼Cr1Mo/composite weld junction/16Cr13NiCb	2¼ OD, 0.26 thick	1/day	1100	2600	306	6000	Cracked	..
3T	2¼Cr1Mo/composite weld junction/16Cr13NiCb	2¼ OD, 0.26 thick	1/day	1100	2600	201	3948	Under test	..
4T	2¼Cr1Mo/0.6 Mo/18Cr8NiTi	2½ OD, 0.25 thick	1/day	1100	2600	274	5000	Cracked	
5T	2¼Cr1Mo/0.6Mo/18Cr8NiTi	2½ OD, 0.25 thick	1/day	1100	2600	258	5002	Cracked	11
6T	2¼Cr1Mo/50Ni10Cr–CbTa/18Cr8NiTi	2½ OD, 0.28 thick	1/day	1100	2600	252	4996	No defects	14
7T	2¼Cr1Mo/50Ni10Cr–CbTa/18Cr8NiTi	2½ OD, 0.28 thick	1/day	1100	2600	205	4064	Under test	..
8T	2¼Cr1Mo/BP-65/18Cr8NiTi	2½ OD, 0.28 thick	1/day	1100	2600	273	5403	No defects	15
9T	2¼Cr1Mo/BP-65/18Cr8NiTi	2½ OD, 0.28 thick	1/day	1100	2600	209	4091	Under test	..

were also tested. The results of these tests are summarized in Table 2. Briefly, they indicate that typical dissimilar weld cracking will occur without externally applied stresses if the specimens are given sufficient cycles. However, the number of cycles required to crack specimens containing some of the protective features became prohibitive and the specimens were discontinued. This type of test points out clearly that the external stresses applied in the thermal-cycling tension test has a definite accelerating effect in producing dissimilar weld cracking.

Evaluation of a Composite Dissimilar-Metals Connection

Several composite tube connections joining austenitic and ferritic steels were obtained during the course of the present investigation. These connections had been developed abroad and were believed to resist thermal cycling because of the geometry of the dissimilar weld interface. This joint reportedly was made by forge welding two disks of 2¼Cr1Mo and 16Cr13Ni–Cb steels together and flowing the joint into tubular form by a sinking operation. The weld junction was thereby elongated over a distance of about 7 to 8 in. in the center of the wall of the resulting tubing, as shown in Fig. 8. This long weld junction parallel to the tube wall and the compressive action at the weld interface produced by the more highly expanded austenitic metal on the inner tube surface had been thought to be able to accommodate the high thermal-expansion stresses without disintegration of the weld interface.

Two tubular specimens of this type (Specimens 1T and 2T in Table 5) were stressed longitudinally to 2600 psi with internal pressure and were thermally cycled in an electric furnace from 1100° F to room temperature at a rate of one cycle per day. The first specimen developed cracks at the dissimilar interface in 114 cycles and 1767 hr at 1100° F. In the second specimen cracking was found at the dissimilar interface by metallurgical examination after the specimen had received 306 cycles and a total of 6000 hr at 1100° F. This cracking is illustrated in Fig. 8.

In view of the present results, this composite joint does not appear to be significantly more resistant to thermal cycling than standard dissimilar welds made with 18–8 type electrodes. Another version of the first two specimens, containing a thin dissimilar weld interface layer of nickel, is now undergoing test.

Protective Weld Features

The foregoing study of the various factors thought to be principally responsible for dissimilar weld failures guided the test program for developing a satisfactory weld along three main channels, namely:

1. The prevention of oxygen attack at the weld interface by covering this highly stressed zone with an oxygen barrier.
2. The use of low-carbon ferritic weld metal which lessens carbon migration and has been used successfully in attaching austenitic alloy hanger lugs to ferritic superheater tubing.
3. A reduction of the differential expansion stresses at the dissimilar junction by utilizing a weld metal with a coefficient of thermal expansion approaching that of the ferritic base metal.

Oxygen Barriers

The observation that dissimilar weld cracking was usually initiated by a stress-oxidation notch and occurred always in the less-oxidation-resistant ferritic steel adjacent to the weld interface suggested the possibility that covering the surface at the dissimilar weld interface with an oxidation-resistant material (oxygen barrier) would retard or prevent oxygen attack at the highly stressed dissimilar weld interface and thereby increase its service life. Accordingly, 0.505-in.-diam tensile specimens containing a 19Cr9Ni–Cb weld between 2¼Cr1Mo and 18Cr8Ni–Cb and protected by pack calorizing, dense chrome plating and oxidation-resistant weld overlays with a coefficient of thermal expansion similar to that of the ferritic base metal (12Cr, 80Ni20Cr) were tested with the thermal-cycling tension test.

The results of these tests, summarized in Table 3, show that calorizing and chrome plating protect the dissimilar weld junction as long as the coatings adhere and are intact, but that the cyclic nature of the test and the variations in thermal expansion eventually cause the coatings to crack, after which failure occurs in the usual manner.

The specimen protected by a 12Cr weld overlay (Specimen 15, Table 3) was examined after 5416-hr exposure at 1100° F, involving 345 temperature-stress cycles, and was found to contain many small cracks in the 2¼Cr1Mo base metal at the overlay junction as well as in the 12Cr weld deposit at the junction with the 19Cr9Ni–Cb weld metal. The weld interface between the 2¼Cr1Mo base metal and the 19Cr9Ni–Cb weld metal had completely disintegrated, as shown in Fig. 9.

The weld overlay deposited with 80Ni20Cr electrodes (Specimen 16, Table 3) withstood over 5000 hr at 1100° F, involving 308 temperature-stress cycles without notch or crack formation at the weld overlay-base metal junction or at the protected junction (see Fig. 10). Since this weld

overlay completely protected the weld junction during the test, it could probably be used as a method of emergency repair. The fact that this overlay is a high chrome-nickel austenitic alloy with high oxidation resistance, and the further fact that its coefficient of expansion is intermediate between the ferritic and austenitic base metals, probably accounts for the favorable thermal-fatigue behavior. Other austenitic alloys with similar characteristics would probably also be successful as oxygen barriers.

Ferritic Welds

During the early part of this investigation, the Manufacturing Division of our Company demonstrated[4] that sound welds can be made between low-carbon austenitic alloys and ferritic steels with low-carbon ferritic electrodes covered with a lime-ferritic-type coating. Their tests with a thermal-cycling apparatus showed that low-carbon $2^1/_4$-Cr1Mo (0.03% carbon) electrodes were superior to austenitic 25Cr20Ni electrodes in welding austenitic hanger lugs to ferritic superheater tubes. Other tests on an elevated-temperature rotating-beam fatigue machine indicated that tubular specimens containing dissimilar welds made with a low-carbon, 0.6% molybdenum weld electrode had a much higher fatigue life than similar specimens welded with 19Cr9Ni – Cb weld metal. As a result of these tests 0.6 Mo electrodes were subsequently used for dissimilar welds in superheater construction.

Later in the test program, after the thermal-cycling tension test had pointed out that holding time at temperature between cycles was an important factor in producing dissimilar-weld cracking, several specimens containing ferritically welded joints were prepared to determine their resistance to cracking at 1100° F in the thermal-cycling tension test. The results of these tests, summarized in Table 3 and illustrated by Fig. 11, demonstrated that these ferritically welded joints suffered characteristic dissimilar-weld cracking in the low-alloy weld metal adjacent to junction with the austenitic base metal. Due to the previously mentioned difficulty of determining crack initiation, the depth of the observed cracks and the associated thermal cycles varied within wide limits, but none of the ferritically welded joints reached a cyclic test duration of 5000 hr at 1100° F without cracking.

In parallel with these cycling tensile tests, two ferritically-welded 0.6 Mo tubular specimens made from $2^1/_2$-in. OD x 0.25-in.-wall tubing of $2^1/_4$Cr1Mo and 18Cr8Ni – Ti were cycled to 1100° F under internal pressure in the tubular stress-rupture apparatus.[5] Both specimens completed the 5000 hr at test temperature without apparent difficulty; however, metallurgical examination again revealed that both welds had developed characteristic dissimilar weld cracks during the test, as shown in Fig. 11. These results are summarized in Table 5.

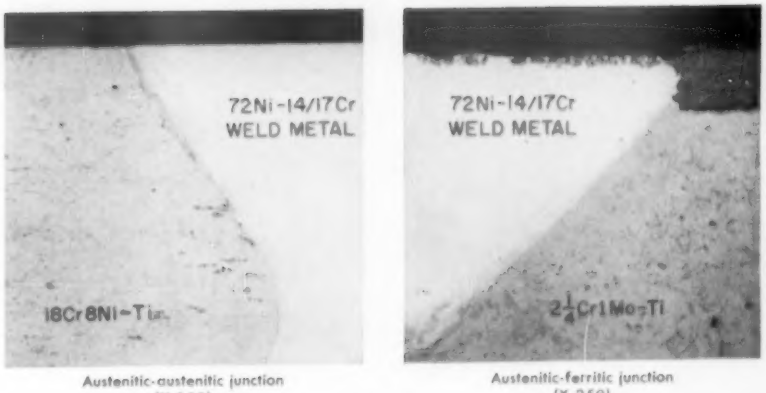

Austenitic-austenitic junction (X 100) 302 cycles 1100° F — Austenitic-ferritic junction (X 250) 5133 hr

Fig. 13 Dissimilar weld junction made with R-48 Inconel (72Ni – 14/17Cr) electrodes after thermal-stress cycling. (Reduced by $^1/_3$ upon reproduction)

The test results indicate that some of the ferritic welds in superheaters operating under cyclic conditions at metal temperatures of 1100° F may eventually develop cracks; however, those welds operating under less severe conditions should attain a reasonable service life as variations in the various factors producing dissimilar-weld cracking have a very significant effect on the life of a dissimilar weld.

Also investigated was a flash (butt) weld of 9Cr1Mo to 18Cr8Ni – Cb with the thought in mind that the broader fusion zone and greater oxidation resistance of the higher chromium steel might improve the thermal-cycling life. This specimen (Specimen 23, Table 3) ruptured completely after 218 temperature-stress cycles and 4089 hr at 1100° F, with the crack propagating through the ferritic material (9Cr1-Mo) adjacent to the wide transition zone, even though this material was more oxidation resistant than the $2^1/_4$-Cr1Mo material used in previous specimens. Thus, a flash weld of 9Cr1Mo to 18Cr8Ni – Cb was not satisfactory for this type of service.

Welds with Coefficient of Expansion Similar to That of Ferritic Steels

Since the cyclic differential thermal expansion stress is the predominant factor in producing the propagating dissimilar-weld cracking in the low-oxidation-resistant ferritic base metal, consideration was given early in this investigation to lowering or entirely removing the differential expansion stresses from the ferritic-austenitic weld interface. This could be accomplished by joining the austenitic and ferritic base metals with an austenitic weld metal having high oxidation resistance and a coefficient of expansion similar

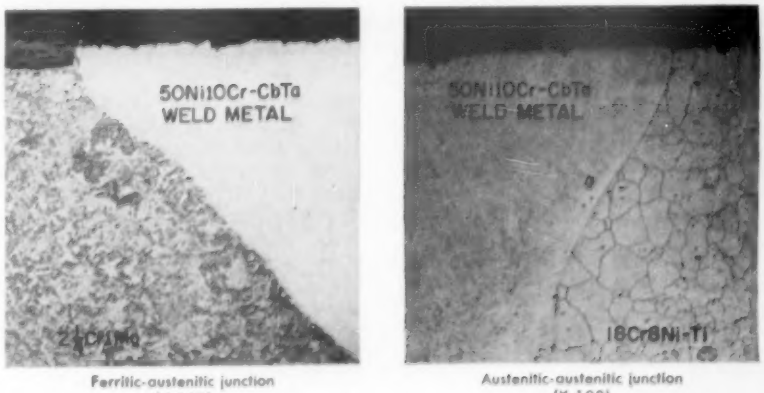

Ferritic-austenitic junction (X 100) 252 cycles 1100° F — Austenitic-austenitic junction (X 100) 4996 hr

Fig. 14 Dissimilar weld from tubular specimen made with 50Ni10Cr – CbTa electrodes after pressure and temperature cycling. (Reduced by $^1/_3$ upon reproduction)

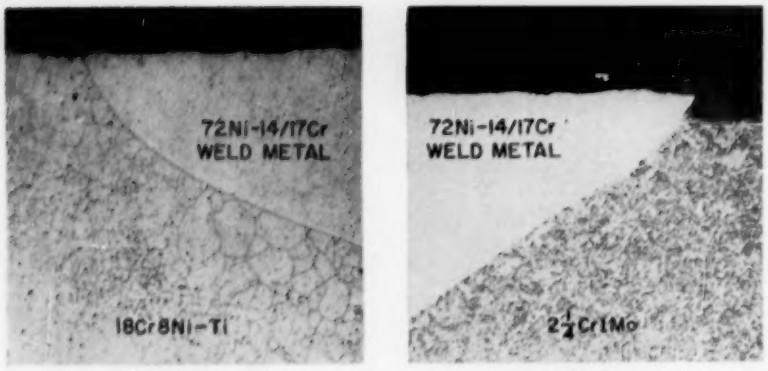

Austenitic-austenitic junction (X 100) 273 cycles — 1100° F — Austenitic-ferritic junction (X 100) 5003 hr

Fig. 15 Dissimilar weld from tubular specimen made with BP-65 Inconel (72Ni – 14/17Cr) electrodes after pressure and temperature cycling. (Reduced by 1/3 upon reproduction)

Creep strength, psi, for 0.1%/1000 hr at 1100° F		Stress for rupture, psi, in 10,000 hr at 1100° F	
20Cr80Ni (3)	8,000	2¼Cr1Mo (1)	10,000
2¼Cr1Mo (1)	9,200	25Cr20Ni Weld M. (4)	14,500
Inconel (72Ni – 14/17Cr) (2)	12,000	Inconel (72Ni – 14/17Cr) (2)	15,200
18Cr12Ni – Cb (1)	23,000	19Cr9Ni – Cb Weld M. (4)	23,700
25Cr20Ni (1)	23,000	50Ni10Cr – CbTa (4)	28,000
		18Cr12Ni – Cb (1)	28,340

(1) Tubing stock, annealed (Babcock & Wilcox Co. data).
(2) Hot rolled, annealed (Inco Tech. Bull. T-7).
(3) Hydrogen-annealed at 1740° F (Natl. Bur. of Standards Circular C447, p. 363, and *Jnl. Iron & Steel Inst.*, 137, 177P (1938).
(4) Babcock & Wilcox Co. data.

Fig. 16 Creep and stress-rupture properties of some pertinent materials

Table 6—Thermal Expansion Data for Pertinent Alloys, Room Temperature to 1100°F*

Material	*Mean coefficient of linear expansion in./in./° F × 10⁻⁶*
2¼Cr1Mo tubing (1700° F/F. C.)	7.67
2¼Cr1Mo – Ti wrought (1700° F/slow F. C.)	7.46
Low-C 2¼Cr1Mo weld metal (2 hr 1350° F/F. C.)	7.06
12Cr-weld metal (as-welded)	6.4
18Cr12Ni – Cb tubing (2000° F/W)	10.18–10.35
18Cr12Ni – Ti tubing (2000° F/W)	10.26–10.31
19Cr9Ni – Cb weld metal (as-welded)	9.77–10.06
25Cr20Ni weld metal (as-welded)	9.51–9.84
80Ni20Cr weld metal (as-welded)	8.6
Inconel 132 weld metal (as-welded)	8.08–8.33
50Ni10Cr wrought (2000° F/W)	7.43
50Ni10Cr weld metal (as-welded)	7.95
50Ni10Cr – CbTa weld metal (as-welded)	8.22–8.30
34Ni21Cr	9.8

* From tests made in the authors' laboratory.

to that of the ferritic base metal or intermediate between those of the austenitic and ferritic base metals involved. A weld of this type would not completely eliminate the high differential expansion stresses but would transpose them from the low-oxidation-resistant ferritic-austenitic junction to the austenitic-austenitic junction where the high oxidation resistance and the high creep-rupture strengths of the austenitic steels are better able to withstand temperature and stress cycles.

A survey of the commercially available electrodes revealed that there were only three which possessed the desired characteristics—an 80Ni20Cr type, an Inconel 132(75Ni15Cr) type and a 25Cr20Ni type electrode. The latter was eliminated from consideration because of the inadequate service behavior of dissimilar welds made with this electrode. Shop experience and laboratory tests on welds made with 80Ni20Cr and Inconel 132 type electrodes revealed that these electrodes did not deposit sound weld metal free from gas porosity and fissuring. They were therefore not considered satisfactory for welding pressure parts in boilers. At this time, the manufacturers of these types of electrodes were contacted for their latest developments, but they were not able to supply an electrode meeting the requirements for weld metal soundness.

It was then decided to investigate the possibility of developing an austenitic electrode with a lower nickel content which would deposit sound weld metal having an expansion coefficient similar to that of the 2¼Cr1Mo base metal. For this purpose, a systematic series of Cr-Ni-Fe alloys at fixed chromium and varying nickel levels were prepared and their expansion characteristics determined. One of these experimental alloys, a 50Ni10Cr40Fe composition, displayed a coefficient of expansion between room temperature and 1100° F close to that of the 2¼Cr1Mo steel. This 50Ni10Cr alloy was subsequently modified with a CbTa addition and developed into a covered welding electrode which displayed very satisfactory welding characteristics and deposited sound weld metal free from defects. The CbTa addition raised the expansion characteristics of the weld metal somewhat, but as subsequent experience showed, not significantly, and it also improved the creep-rupture strength at 1100° F so that it became equal to that of the 18Cr8Ni – Cb (Type 348) tubing material (see Table 6 and Fig. 16).

The thermal-cycling behavior of welds between 2¼Cr1Mo and 18Cr8Ni – Cb or 18Cr8Ni – Ti made with this electrode was then thoroughly explored with the thermal-cycling tension test, using 0.505 tensile specimens. When, in the

course of this investigation, improved versions of the Inconel 132 electrode became available, (Inconel R – 48 and Inconel BP – 65), they were also included in the test program.

In the initial cyclic tests, conducted at 1100° F under a stress of 2600 psi for 5000 hr, involving approximately 260 cycles, the weldments made with the 50Ni10Cr – CbTa and the R – 48 Inconel electrodes (Specimens 24 and 35, Table 4) were found free of defects at both the ferritic-austenitic and the austenitic-austenitic weld junction, as shown in Fig. 12 and Fig. 13. It was therefore decided to make the test severer by raising the test temperature from 1100 to 1200° F to obtain a comparison of the two types of electrodes. Four weldments were tested at this higher temperature, i.e. three weldments made with 50Ni10Cr-CbTa electrodes (Specimens 25, 26, and 30, Table 4) and one with a further improved Inconel electrode (Specimen 38, Table 4), designated as Inconel BP – 65. The R – 48 Inconel electrode was not tested further because of weld metal porosity observed in the preceding welds, notwithstanding the fact that it had successfully withstood the 5000-hr test at 1100° F. In these tests at 1200° F, one of the 50Ni10Cr-CbTa weld specimens was examined after 5000 hours; and when it was found to contain only a shallow, broad, V-shaped oxide notch at the ferritic-austenitic weld junction, the tests at 1200° F on the other two 50Ni10Cr-CbTa weldments and on the Inconel BP-65 weldment were continued beyond 5000 hr. Under these conditions, the Inconel BP-65 weld specimen fractured after 5330 hr and 288 cycles; and of the two remaining 50Ni10Cr – CbTa weld specimens, one fractured after 7056 hr and 388 cycles and the other after 6228 hr and 362 cycles. This showed that both 50Ni10Cr – CbTa specimens withstood approximately 30% more cycles than the second improved Inconel BP-65 weldment. The failure in the Inconel BP-65 specimen was located in the ferritic-austenitic fusion zone, whereas the fracture of the two 50Ni10Cr – CbTa weldments had occurred about $^1/_{16}$ in. away from the ferritic-austenitic interface in the $2^1/_4$Cr1Mo base metal.

In a further effort to determine the relative merits of the 50Ni10Cr – CbTa and the Inconel BP-65 electrodes, dissimilar weld 0.505 tensile specimens prepared with them were again subjected to the cycling tension test at 1100° F, but under much higher stresses, i.e., 11,000 and 13,500 psi, respectively. Under these conditions, both types of weldments fractured on the ferritic-austenitic junction side, the 50Ni10Cr – CbTa weldment again showing a better cycle life than the Inconel BP-65 weldment at both 11,000 and 13,500 psi stress, as indicated by the following test data:

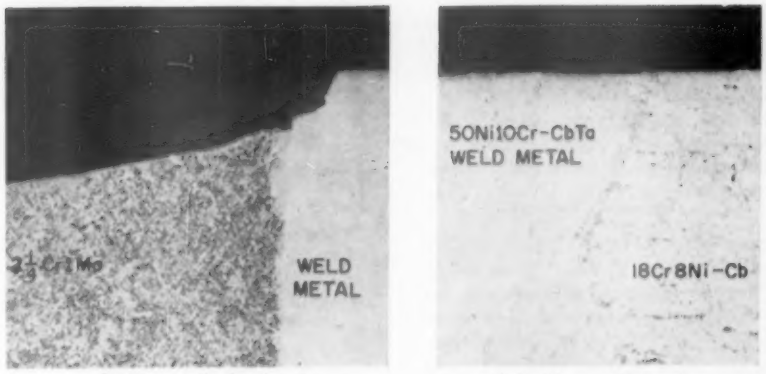

Ferritic-austenitic junction (X 100) 539 cycles — 1100° F — Austenitic-austenitic junction (X 100) 10,000 hr

Fig. 17 Dissimilar weld junction made with 50Ni10Cr – CbTa electrodes after 539 temperature-stress cycles with 10,000 hr at 1100° F. (Reduced by $^1/_3$ upon reproduction)

Weld metal	*Temperature, ° F*	*Stress, psi*	*Cycles to failure*	*Time at temperature, hr*
50Ni10Cr – CbTa	1100	11,000	375	2992
BP-65 Inconel	1100	11,000	300	2400
50Ni10Cr – CbTa	1100	13,500	232	1856
BP-65 Inconel	1100	13,500	145	1160

In parallel with these tests, another pair of dissimilar weldments made with the 50Ni10Cr – CbTa and Inconel BP-65 electrodes (Specimens 29 and 39, Table 4) were, again in form of 0.505 tensile specimens, subjected to daily thermal cycling from 1100° F under 2600 psi for a total duration of 10,000 hr. At this time, only the 50Ni10Cr – CbTa weld specimen has completed its 10,000 hr involving 539 temperature-stress cycles and upon examination has been found free of defects at both weld junctions as shown in Fig. 17. The weldment made with the Inconel BP-65 electrode has passed 6000 hr and is still under test. These data are summarized in Table 4.

As a final evaluation of these electrodes, two pairs of dissimilar weldments prepared with them were tested in tubular form, using $2^1/_2$-in. OD x 0.28-in.-wall commercial superheater tubing of $2^1/_4$Cr1Mo and 18Cr8Ni – Ti, respectively (see Table 5). The specimens were daily cycled from 1100° F to room temperature in the tubular stress-rupture apparatus to give the welds a test under simulated superheater service conditions. One pair of specimens (Specimens 6T and 8T, Table 5) was examined after 5000 hr, involving 252 and 273 cycles, respectively. Both types of weldments were found to be free of defects, as shown in Figs. 14 and 15. The tests on the second pair will be continued to 10,000 hr.

Conclusions

The present results permit the following conclusions:

1. The thermal-cycling tension test gives a realistic indication of dissimilar weld behavior in tubing and piping under cyclic conditions of temperature and stress in steam plant service.

2. Satisfactory welds between $2^1/_4$-Cr1Mo and 18Cr8Ni – Cb, capable of withstanding cyclic conditions of temperature and stress, can be made by eliminating the high thermal-expansion stresses at the ferritic-austenitic junction with an austenitic weld metal which is highly oxidation resistant and which has a coefficient of thermal expansion similar to that of the ferritic material.

3. Two electrodes, a 50Ni10Cr – CbTa and an Inconel BP-65 electrode have produced equally satisfactory results at 1100° F. However the newly developed 50Ni10Cr – CbTa electrode has several advantages over the Inconel electrode, namely, a much lower nickel content, a notably higher creep-rupture strength at 1100° F, and a higher resistance to thermal cycling at temperatures above 1100° F. The 50Ni10Cr – CbTa electrodes are not presently available because of the severely restricted nickel allocation.

4. The relatively low thermal expansion austenitic weld metal transfers the high thermal-expansion stresses

from the ferritic-austenitic to the austenitic-austenitic junction, where the two austenitic steels with their high oxidation resistance and high creep-rupture strength are better able to withstand the cyclic conditions of stress and temperature without deterioration.

5. All of the oxygen barriers were unsatisfactory in preventing dissimilar-weld cracking at the ferritic-austenitic junction, except austenitic-weld overlays with a coefficient of expansion similar to that of the ferritic steels. These weld overlays protected the dissimilar junction during thermal-cycling tests and could possibly be used for emergency repairs.

6. Detection of dissimilar-weld cracking by the usual nondestructive inspection methods is very difficult and the inspection results are very erratic because of the tendency of the crack to be very tightly packed with oxide and thus escape detection. Therefore, the only positive way of detecting these failures early is by microscopic examination of samples removed from the dissimilar weld junction.

Acknowledgment

Acknowledgment is herewith made to M. Christensen, of Babcock & Wilcox Co. Research Center, who has developed the coating for the 50Ni10Cr – CbTa electrode.

Bibliography

1. Blaser, R. U., Eberle, F., and Tucker, J. T., Jr., "Welds Between Dissimilar Alloys in Full-Size Steam Piping," *Proc. ASTM*, **50**, 789–808 (1950).

2. Weisberg, H., "Cyclic Heating Test of Main Steam Piping Joints Between Ferritic and Austenitic Steels—Sewaren Generating Station," *Trans. ASME*, **71**, 643–664 (1949).

3. Stewart, W. C., and Schreitz, W. G., "Thermal Shock and Other Comparison Tests of Austenitic and Ferritic Steels for Main Steam Piping," *Ibid.*, **72**, 1043–1060 (1950).

4. Carpenter, O. R., Jessen, N. C., Oberg, J. L., and Wylie, R. D., "Some Considerations in the Joining of Dissimilar Metals for High-Temperature, High-Pressure Service," *Proc. ASTM*, **50**, 809–860 (1950).

5. Kooistra, L. F., Blaser, R. U., and Tucker, J. T., Jr., "High-Temperature Stress-Rupture Testing of Tubular Specimens," *Trans. ASME*, **74**, 783–791 (1952).

BULLETIN SERIES

Requests for single copies should be sent to the

AMERICAN WELDING SOCIETY, *29 W. 39th St., New York 18, N. Y.*

Requests for bulk lots ten or more, should be sent to the

WELDING RESEARCH COUNCIL, *29 W. 39th St., New York 18, N. Y.*

No. 20 **High-Strength, Low-Alloy Steels; Analytical Chemistry Fosters Progress in Steelmaking; Steel Quality;** *by Charles M. Parker, January 1955. $1.00.*

No. 21 **Coating Moisture Investigations of Austenitic Electrodes of the Modified 18–8 Type,** *by K. P. Johannes, D. C. Smith and W. G. Rinehart, February 1955. $1.00.*

No. 22 **Welded Tee Connections,** *by A. G. Barkow and R. A. Huseby, May 1955. $1.00.*

No. 23 **Cracking of Simple Structural Geometries,** *by S. T. Carpenter and R. F. Linsenmeyer, July 1955. $1.00.*

No. 24 **Nickel and High-Nickel Alloys for Pressure Vessels,** *by R. M. Wilson, Jr., and W. F. Burchfield, January 1956. $1.00.*

No. 25 **Bibliography on The Welding of Stainless Steels, 1926–1955 with Author Index,** *by Katherine Janis, March 1956. $1.00.*

No. 26 **Investigation of the Influence of Deoxidation and Chemical Composition on Notched-Bar Properties of Ship Plate Steels,** *by F. W. Boulger, R. H. Frazier and C. H. Lorig, April 1956. $1.00.*

No. 27 **Mechanical Properties and Weldability of Six High-Strength Steels,** *by R. D. Stout and J. H. Gross; Economic but Safe Pressure-Vessel Construction, by J. J. Murphy, C. R. Soderberg, Jr., and D. B. Rossheim, May 1956. $1.00.*

No. 28 **Aluminum and Aluminum Alloys for Pressure Vessels,** *by Marshall Holt, June 1956. $1.00.*

No. 29 **Development of Brazing Alloys for Joining Heat Resistant Alloys,** *by Forbes M. Miller, Homer S. Gonser and Robert L. Peaslee, July 1956. $1.00.*

No. 30 **Oxidation-Resistant Brazing Alloys,** *by George H. Sistare, Jr. and Allen S. McDonald, September, 1956. $1.00.*

ISOTHERMAL STUDIES ON THE WELD-METAL MICROCRACKING OF ARC WELDS IN MILD STEEL

Temperature-dependence of time required to achieve isothermal immunization against weld-metal microcracking and reasonableness of the hydrogen-retained austenite hypothesis are studied through laboratory investigation

BY A. E. FLANIGAN AND Z. P. SAPERSTEIN

ABSTRACT. In the case of E6010 welds on A285-C plate, an attempt was made to determine the temperature-dependence of the time required for isothermal immunization against weld-metal microcracking. Immediately after welding, small specimens were subjected to isothermal treatments at temperatures from 1700 to 212° F. They were then quenched in room-temperature water to evaluate their resistance to cracking.

The time required for immunization was found to have a maximum value in the case of specimens treated at 875° F. In the range from 750 to 212° F the immunization times were surprisingly short and appeared to be nearly independent of temperature. The latter observation is in agreement with indications that in practice it is the cooling rate at rather low temperatures which is ordinarily decisive in determining whether or not cracking will occur.

Few, if any, cracks were found in specimens which were quenched in water immediately following welding. This finding, together with some of the isothermal data, suggests that susceptibility was absent initially but tended to develop in a temperature range somewhat below A_1 if cooling in that range was sufficiently slow.

The experimental data were used to test the reasonableness of the hydrogen-retained austenite hypothesis concerning the mechanism of weld-metal microcracking. Qualitatively, the hypothesis appeared to be compatible with the data. A quantitative check did not seem feasible, however, and was not attempted.

1. Introduction

Recently attention has been devoted to the phenomenon of weld-metal microcracking in the arc welding of mild steel and a number of observations have been described in the literature.[1–11] In addition, at least three reviews of the subject have been published.[12–14]

The phenomenon is concerned with the occurrence of fine-scale fissuring in the weld metal. The term "microcracking" has sometimes been employed since the fissures are ordinarily so small that their detection requires careful microscopic examination. There is reason to suspect that this type of defect occurs rather commonly in welding practice,[6] especially when heavy work is welded without preheating. Since the presence of cracks in weld metal is generally undesirable, the subject would seem to be one of some practical importance.

It has been shown that weld-metal microcracking occurs in practice when the cooling weld is allowed to pass too rapidly through the low-temperature range following deposition, i.e., when it is allowed to cool too rapidly through the range extending from several hundred degrees Fahrenheit to atmospheric temperature. It has been shown also that microcracking can be prevented by means which insure that passage through the low-temperature range is not too rapid. (Preheating is effective in this regard.) It has been shown, moreover, that prevention is favored by the use of low-hydrogen electrodes.

All who have studied the phenomenon seem to agree that a leading role is played by hydrogen which is dissolved by the molten weld during deposition. It has also been suggested that dissolved nitrogen may be a factor of importance.[5] Because of obvious similarities in behavior, it has appeared to many that weld-metal microcracking may be rather closely related to the better-known underbead cracking of welds and to the "flaking" of forgings, rails and other hot-worked products.

As has been stated above, it appears that the cooling rate following welding is ordinarily decisive in determining whether or not weld-metal microcracking will occur. Presumably, sufficiently slow cooling permits the occurrence of some favorable (but as yet incompletely understood) process which renders the weld immune to cracking if this process is fulfilled before attainment of the low temperature at which cracking can occur. One might suspect that, whatever the nature of the postulated favorable process (say, the escape of hydrogen), it would occur more readily the higher the temperature. Why is it, then, that in practice it is the weld's cooling rate in the *low-temperature* range which is ordinarily found to be so critical? An obvious possibility is that, under ordinary conditions, the cooling weld traverses the higher temperatures so rapidly that there is not sufficient time to permit the fulfillment of the favorable process at these temperatures. The cooling of the weld ordinarily becomes much slower during passage through the lower temperatures.[4] Thus, if the process is to occur at all, it may be forced to do so in the latter range. It is, of course, necessary that the process be fulfilled before the temperature of cracking is reached.

If one accepts the above picture, he is inclined to wonder if immunity to subsequent cracking might not be attainable at any temperature whatsoever during cooling if only sufficient time were available. One wonders, also, how the required immunization time might vary with temperature. This paper is concerned with an investigation which was designed primarily to supply answers to these questions.* It describes the behaviors of welds which were subjected to isothermal treatments

Alan E. Flanigan is Professor of Engineering and **Zalman P. Saperstein** is a graduate student at the University of California, Los Angeles.

Much of this material was presented orally at the 1954 AWS National Fall Meeting held in Chicago, November 1 to 5.

*The investigation, conducted in the Engineering Department of the University of California, Los Angeles, was supported by grants from the University's Committee on Research and from the Welding Research Council of the Engineering Foundation.

at 11 temperatures from 1700 to 212° F immediately after the completion of welding. As will be seen, it was found that immunity to subsequent cracking could be attained with sufficiently long exposure at most of the temperatures in this range. Moreover, a good deal was learned about the temperature-dependence of the time required for isothermal immunization and it became clear why in practice it is ordinarily the cooling rate in the low-temperature range which is critical.

It was hoped that, in addition to answering the above questions, the investigation might shed some new light on the mechanism of microcracking and on the nature of the above-mentioned "favorable process" which must occur during cooling if cracking is to be forestalled. Although some illumination was perhaps obtained, it must be admitted that important aspects of the mechanism remain obscure. In particular, it was hoped that the data could be used to test the merits of the "hydrogen-retained austenite" hypothesis which, in various forms, has been suggested by several writers as a likely explanation for weld-metal microcracking and which has been used also to account for the phenomena of underbead cracking and flaking. In general, it would appear that the data are consistent with this hypothesis. (Perhaps it would be safer to say that no fatal contradictions are as yet apparent.) By no means, however, can it be said that the hypothesis has been proved or that other explanations may not eventually prove superior.

Of the observations to be related perhaps the most interesting (and most surprising) are those which suggest the occurrence of a brief period of increasing susceptibility, instead of a monotonic trend toward immunization, during the early stages of cooling. Such observations include those concerned with the unexpectedly high resistance to microcracking exhibited by welds which were quenched to room temperature immediately after welding. To the authors' knowledge, similar observations have not been reported in the literature on weld-metal cracking or in that on flaking. These observations would seem to have interesting implications with regard to the mechanism of weld-metal microcracking. Perhaps the implications will prove to apply to the case of flaking as well.

2. The Specimen and Welding Conditions

Bead-on-plate welds were deposited manually with AWS-ASTM E6010 electrodes on ASTM A285-C plate of firebox quality. The plate was obtained from the same heat which had been used previously in this laboratory in studies of microcracking.[6,8] The

Fig. 1 The specimen

chemical analysis of the plate was as follows: 0.19% C, 0.33% Mn, 0.07% Si, 0.03% S, and 0.015% P. (No attempt was made to detect or measure other elements.)

For the following reasons it was considered desirable to employ a specimen of small size.

(*a*) It was desired that the mid-length portion of the weld (the region to be studied) be at a temperature no lower than A_1 upon the completion of welding. The basis for this desire lay in the hope that the decomposition of austenite could be delayed until isothermal treatment had been started.

(*b*) It was desired to minimize the time required for the specimen to attain the temperature of the isothermal bath into which it would be quenched after welding.

Figure 1 shows the 2- x 1- x $^3/_8$-in. specimen which was selected. The 2-in. length was considered to be the shortest consistent with the desire to retain a 1-in. length of weld metal after discarding the crater portion and the first $^1/_2$ in. of the weld. The 1-in. width was considered to be about the least consistent with the desire to produce a weld of normal contour. The $^3/_8$-in. thickness of the specimen was dictated by the thickness of the plate which was to be employed. It is, perhaps, of interest to note that the specimen dimensions are precisely those employed by Wooding in his study of the influence of isothermal treatment on the underbead cracking tendencies of a nickel-chromium-molybdenum steel.[15]

Before welding, the mill scale was ground away from the specimen along the path of the weld. A bead-on-plate weld was then deposited manually along the major centerline as shown in Fig. 1. A popular brand of $^5/_{16}$-in. E6010 electrode was employed at 25 volts with a current of 175 amp. The arc speed was 7.7 ipm, corresponding to a welding time of about 15 sec per specimen. Within $1^1/_2$ sec after the completion of welding, the specimen was quenched into an appropriate isothermal bath. Analysis of the weld metal at midlength disclosed the following composition: 0.08% C, 0.53% Mn, 0.09% Si, 0.030% S, 0.022% P, 0.04% Ni, 0.02% Cr, 0.005% V, 0.005% Mo, 0.11% Cu, 0.02% Co, 0.01% Sn, 0.02% Ti, 0.025% N.

Because of the small width of the specimen, the ratio of heat imput to volume was considerably greater than is ordinarily encountered in welding practice. Consequently, when allowed to cool in still air following welding, the specimen tended to cool more slowly than would usually be the case in practice. In a number of cases the actual cooling curves were determined by means of thermocouples which were placed in the molten weld metal at midlength during deposition. Individual curves for a set of 22 air-cooled specimens yielded mid-length temperatures ranging from 1750 to 1100° F at the instant of completion. The average value for these specimens was 1440° F. As stated earlier, it was desired that the mid-length temperature be at or above A_1 at the completion of welding. The considerable variation in the measured temperatures occurred in spite of all efforts to control the welding variables. Perhaps it is responsible, in part, for the scattering of results obtained in some of the tests.

3. The Detection of Microcracks

After welding, the specimens were subjected to a variety of treatments and were then sectioned and examined for the occurrence of microcracking. Sectioning was done in the longitudinal plane of symmetry (see Fig. 2). After sawing, this plane was polished electrolytically in a solution of CrO_3 in acetic acid.* Electrolytic polishing is believed to be more effective than ordinary mechanical polishing as a method of revealing weld-metal microcracks.[6, 7, 16]

Following polishing (and without subsequent etching), the central 1-in. length of the weld metal from each specimen was subjected to a careful microscopic examination at × 200. The crack-like markings were counted carefully during this examination. In some cases (dependent on prior treatment), no such indications were found. At the other extreme, hundreds were observed in a single specimen. Figure 3, illustrating the latter case, shows a portion of a specimen in which an un-

* The usual polishing procedure consisted of several steps. First, the specimen was subjected to a low-grade mechanical polish followed by a nital etch. The etched surface was then removed by a second mechanical polish. This was followed by electrolytic polishing. It was thought originally that use of the intermediate etch might tend to accentuate the indications of cracking. (Perhaps the etchant would seep into cracks to a depth that would not be affected by the subsequent repolishing.) Experience indicated, however, that the final appearance of a specimen prepared in this manner differed little, if any, from the appearance of one not accorded the intermediate etch.

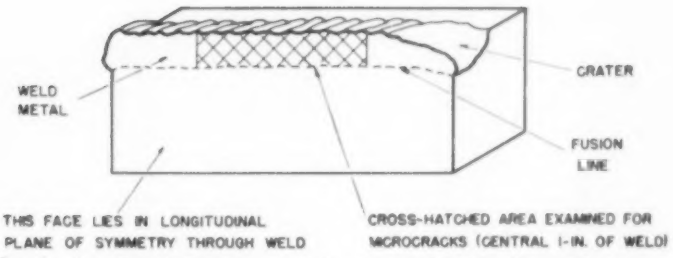
WELD METAL
CRATER
FUSION LINE
THIS FACE LIES IN LONGITUDINAL PLANE OF SYMMETRY THROUGH WELD
CROSS-HATCHED AREA EXAMINED FOR MICROCRACKS (CENTRAL 1-IN. OF WELD)
Fig. 2 Location of the area used in examination for microcracks

usually large number of crack-like markings was counted.

Counting was made difficult by the fact that after certain types of treatment some of the crack-like markings were exceedingly small. Because of an initial uncertainty concerning the significance of the smaller ones, it was decided to divide the marks into two groups as follows:

"Class A"—those having a length greater than about 0.0005 in. (0.013 mm).

"Class B"—those having a length less than about 0.0005 in.

While it was possible to recognize and count the markings of Class A rather easily, those of Class B presented difficulty because of their small size.

At first it was felt that there might be no significance to the marks of Class B since many of them were rather vague and it seemed possible that similar markings might be typical of even the soundest welds. It soon became apparent, however, that they were found only after particular types of treatment, while after other types they were systematically absent.

Figure 4 shows an assortment of Class A and Class B markings in a specimen which exhibited both types. The arbitrary nature of the distinction between the larger members of Class B and the smaller members of Class A is apparent in this figure. (Figure 3 also exhibits both types.)

In most cases, even the markings of Class A were considerably smaller than those which had been encountered in this laboratory in earlier work based on larger welds and other types of postwelding treatment.[6] In the earlier work the markings had exhibited lengths of the order of 0.01 in. and it had been shown that they actually represented cracks in the weld metal. It had been shown also that there was an adverse effect on the mechanical properties of the weld. In the present instance, however, it seemed possible that the much smaller markings which were so commonly encountered might not necessarily indicate the presence of cracks. Perhaps they could be explained in some other manner. In the hope of gaining clarification on this matter, an effort was made to investigate the possibility of a correlation between mechanical behavior and the incidence of the small markings. On the basis of this work (described in Section 19), it appeared either that the markings indeed represented cracks or that they denoted a predisposition to cracking under mechanical loading.

Some further remarks on the subject of crack lengths will be found in Section 20.

It should be mentioned, perhaps, that the duration of the storage period between the postwelding treatment and microscopic examination varied from specimen to specimen. In some cases it amounted to only a few hours. In others, it was a matter of many days. There seemed to be no indication, however, that the duration of this period was a matter of consequence.

4. Consequences of Air Cooling and Water Quenching

Before describing the behavior of the isothermally treated welds, it will be of interest to refer to some preliminary tests on two other groups of specimens. The first group consisted of welds which were allowed to cool in still air after welding. The second consisted of specimens which were quenched in water at room temperature immediately following the completion of welding.

The air-cooled group contained 9 specimens. Neither Class A nor Class B microcracks were found in any of these welds.

It had been anticipated that severe microcracking might occur in the quenched welds since such an effect had been observed in earlier work employing longer welds on more massive specimens. It was something of a surprise, therefore, to find that microcracking was much less frequent in the present smaller specimens. In the present work quenching was accomplished by plunging the specimens into a large volume of water at 66-85° F within $1\frac{1}{2}$ sec after the completion of welding. Table 1 describes the frequency of cracking in a group of 40 quenched specimens. The average number of Class A microcracks was only 1.4 per specimen. (No Class A cracks were noted in 21 cases.) None of the 40 specimens exhibited Class B cracks. Thus it appeared that, under the conditions of the study, severe cooling immediately following the completion of welding did not favor the formation of weld-metal microcracks. As will be seen in Section 6, this indication later proved to be consistent with evidence obtained in the isothermal studies. It is believed that this behavior of the quenched specimens may have important implications concerning the mechanism of cracking, a point which is discussed in Section 13.

At this stage it should be mentioned, perhaps, that the conditions employed

Table 1—Frequency of Microcracking in 40 Specimens* Quenched in Water at 66-85° F Immediately after Welding

No. of Class A microcracks observed in a given specimen	0	1	2	3	4	5	12
No. of specimens exhibiting the above-specified no. of microcracks	21	8	2	3	3	2	1

* No Class B microcracks were found in any of these specimens.

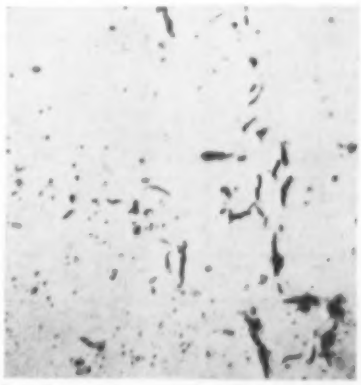
Fig. 3 A portion of a specimen containing an unusually large number of microcracks. X 275, not etched

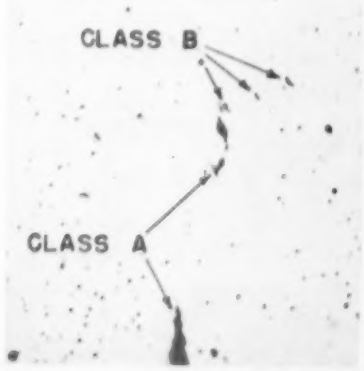

Fig. 4 A group of microcracks illustrating the distinction between Class A and Class B. X 200, not etched

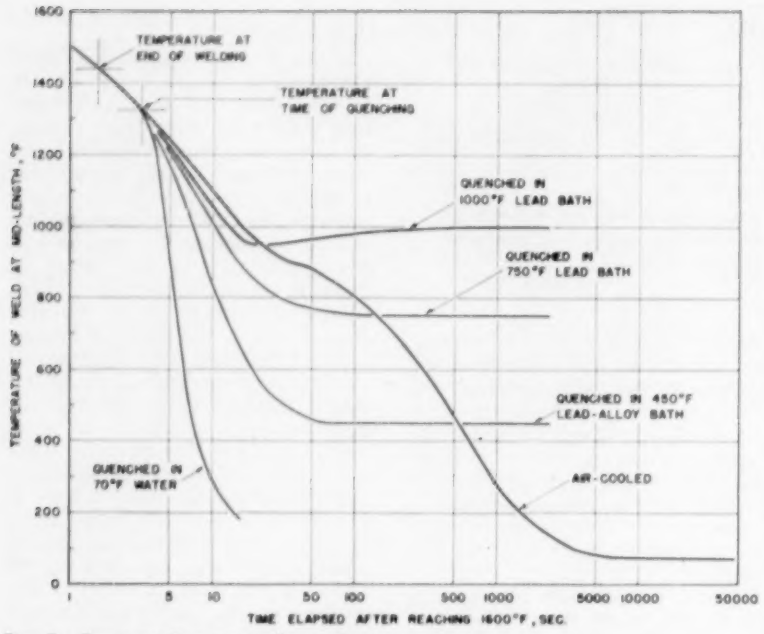
TEMPERATURE AT END OF WELDING
TEMPERATURE AT TIME OF QUENCHING
QUENCHED IN 1000°F LEAD BATH
QUENCHED IN 750°F LEAD BATH
QUENCHED IN 450°F LEAD-ALLOY BATH
AIR-COOLED
QUENCHED IN 70°F WATER
TEMPERATURE OF WELD AT MID-LENGTH, °F
TIME ELAPSED AFTER REACHING 1600°F, SEC.

Fig. 5 Some cooling curves for various treatments

in the present work (i.e., the combination of materials, geometry, and procedure) may have constituted something of a borderline condition with regard to the near-immunity to microcracking exhibited by directly quenched welds. At one stage in the work, a few welds were deposited with another brand of E6010 electrodes under otherwise standardized conditions and cracking was found to be somewhat more prevalent with the new brand. On another occasion, some welds were made employing higher welding currents with the standard electrodes and there was an indication (though an uncertain one) that the higher current provoked a greater incidence of microcracking. Why an increase in current should have such an effect, if indeed it does, is not apparent.

5. Procedures in Isothermal Treatment

Isothermal treatments were performed at 11 temperatures ranging from 212 to 1700° F. A molten salt bath was employed at 1700° F while both molten salt and molten lead were used at 1600° F. Boiling water was used at 212° F. Treatments at the 8 intermediate temperatures were carried out in baths of molten lead or low-melting lead alloys.

The specimens were quenched into the isothermal baths within $1^1/_2$ sec after the completion of welding. The average value of the mid-length temperature is believed to have been about 1320° F at the instant of quenching (see Fig. 5). Ideally, of course, it was to be desired that the specimen assume the temperature of the bath instantaneously. Since the heat capacity of the specimen was by no means negligible, however, an appreciable period was required for attainment of the bath temperature, this in spite of the fact that the specimen was agitated. Figure 5 shows some actual cooling curves (in terms of the temperature at mid-length) for specimens treated at 1000, 750 and 450° F. Each of the curves represents the average behavior of several specimens. The thermal lags which attend quenching are apparent in the figure.

From Fig. 5, one may see that the term "isothermal treatment" is used loosely in this paper. Indeed, in the case of specimens held only briefly in an "isothermal" bath (say, 30 sec at 750° F) this figure indicates that the temperature of the bath was never attained. In the case of long-time specimens (say, 30 min at 750° F) the bulk of the treatment was isothermal in nature but during the early stages the specimen was inevitably at higher temperatures. As will be pointed out presently, this is a matter of some importance and must be taken into account when one attempts to interpret the results of the tests.

Figure 5 shows also an average cooling curve for specimens which were air cooled after welding and a curve for specimens which were quenched directly into water at 70° F.

Following isothermal treatment, specimens were removed from the baths and were immediately quenched in water at 66–85° F in an attempt to induce cracking. They were then subjected to microscopic examination.

6. Results of Isothermal Treatments at Temperatures Below A_1

Figures 6 through 13 describe the behavior of specimens which were subjected to isothermal treatments at eight temperatures in the range from 1290 to 212° F. They depict the

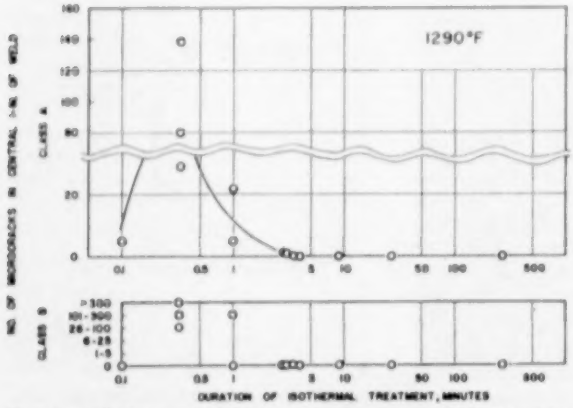

Fig. 6 Influence of isothermal treatment at 1290° F prior to quenching

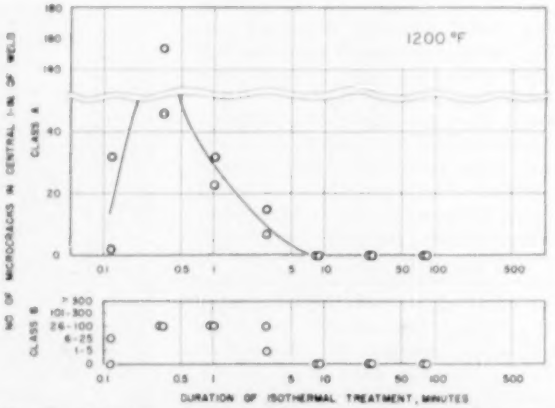

Fig. 7 Influence of isothermal treatment at 1200° F prior to quenching

manner in which the duration of isothermal treatment influences the response to subsequent quenching. The latter is shown both in terms of the incidence of Class A microcracks and the tendency toward the appearance of Class B microcracks as defined in Section 3. In the figures, each symbol represents the behavior of a single specimen. It should be explained, perhaps, that the quasi-logarithmic scale which has been used to describe the frequency of Class B microcracks (in the lower portion of each figure) was introduced only for the sake of convenience. It was intended to have no other significance. The same may be said for the split scales which have been used in the upper portions of some of the figures in connection with the frequency of Class A microcracks.

As may be seen in Figs. 6 through 10, both Class A and Class B microcracks were encountered in specimens treated at temperatures above 750° F. In the case of these temperatures it may be seen also that the data for the two classes of cracks tend to parallel each other. In the case of the lower temperatures (Figs. 11 through 13), however, Class B microcracks were seldom found. Ordinarily only those of Class A were encountered.

NOTE: *Throughout the remainder of this paper (except as otherwise noted) the discussions of the various experimental results will refer only to the data on Class A microcracks. Both types of data will be presented side by side in the various figures and tables but, for the sake of convenience, discussion of the data on Class B cracks will be deferred to Section 20. At that point attention will be called to the instances in which the behaviors in terms of the two classes of microcracks fail to parallel each other.*

Examination of the data on Class A microcracks in Figs. 6 through 13 discloses that the effect of isothermal treatment may be divided into two stages. In the first stage (involving short times) specimens are found to become increasingly susceptible to the microcracking induced by subsequent quenching. In the second stage (involving longer times) susceptibility is seen to wane and at most temperatures complete immunity would seem to be attained in the times employed. Some implications of these observations in terms of the mechanism involved will be discussed in Sections 12 through 14.

As stated in Section 4, susceptibility was found to be either slight or completely absent in specimens which were quenched immediately after the completion of welding. Presumably, then, the susceptibility associated with the first stage of isothermal treatment develops with great rapidity. According to Figs. 6 through 8, for instance, the required time is seen to amount to only a few seconds in the case of specimens treated at 1290, 1200 and 1000° F.

Recognizing the rapidity with which susceptibility develops at the higher temperatures, one wonders if it is not possible that susceptibility may develop, even in specimens treated at the lower temperatures, during passage through the high temperature range. Such a possibility would seem to be consistent with the time lag which, as pointed out in the preceding section, is known to attend the attainment of the temperatures of the isothermal baths. Consider, for instance, the case of a specimen treated at 450° F. Figure 5 indicates that, as late as 4 sec after quenching, the temperature of the weld at midlength is still in the region of 1000° F. In view of this possibility, one is inclined to wonder if any of the susceptibility exhibited by specimens treated at the lower temperatures (as 450° F) actually developed at the nominal temperatures of treatment. This matter will be discussed further in Section 10.

We now note that the performance of the isothermally treated specimens would appear to be consistent with the behavior of the air-cooled specimens and the directly quenched specimens of Section 4. The latter may now be interpreted as follows:

(*a*) It was found that specimens exhibited no microcracks if air-cooled to room temperature after welding. Presumably, cooling was slow enough not only to allow the development of susceptibility in the early stages of cooling but also to permit a subsequent recovery of immunity.

(*b*) It was observed in the present work that specimens quenched to room temperature immediately after welding exhibited few, if any, microcracks. Cooling rate determinations indicated that the mid-length portions of the welds were in the neighborhood of 1320° F at the time of quenching. Presumably, the welds were still immune to cracking at this time and subsequent cooling through the higher temperatures was so rapid that susceptibility did not develop. As mentioned in Section 4, it was found in earlier work with larger specimens (9-in. welds on 4 x 9 x $^{3}/_{4}$-in. plates) that the welds exhibited numerous microcracks at midlength when quenched immediately after the completion of welding. We are now in a position to explain this behavior also. The welding of these specimens required about 70 seconds and it is known that the midlength portions had cooled to about 400° F even before quenching.[4] During this period, presumably, there had been ample time to allow the development of susceptibility but not enough time to permit the recovery of immunity.

The evidence pointing to an initial period of increasing susceptibility is probably one of the most interesting features of the present work. Perhaps, however, such indications should not be regarded as altogether surprising. The literature contains several references to instances in which hydrogen-induced cracking has occurred under conditions which may be somewhat

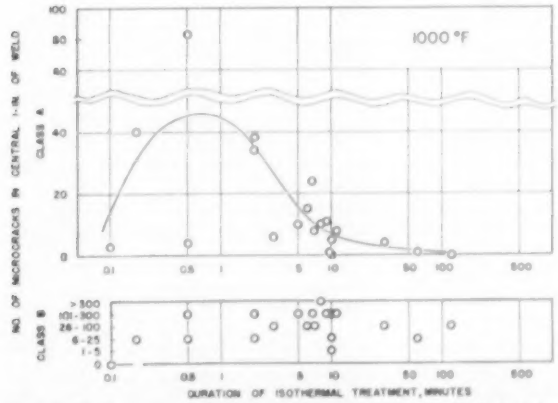

Fig. 8 Influence of isothermal treatment at 1000° F prior to quenching

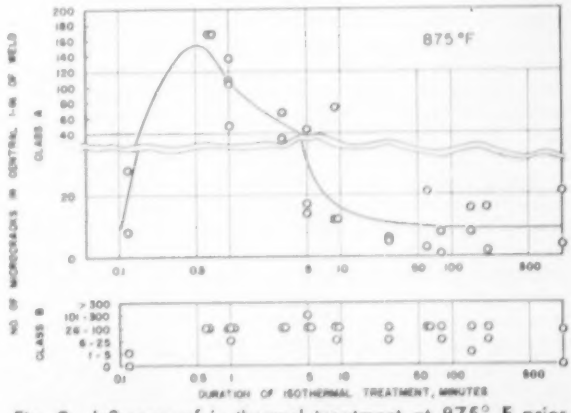

Fig. 9 Influence of isothermal treatment at 875° F prior to quenching

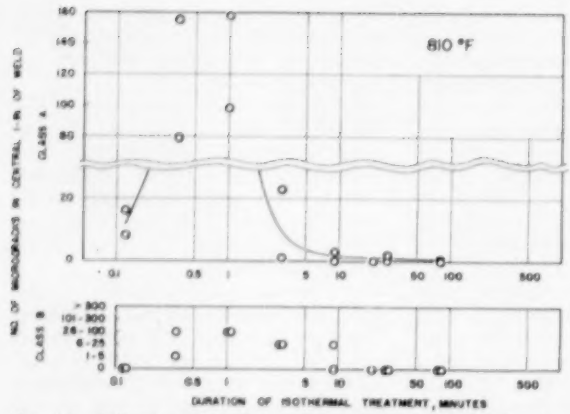

Fig. 10 Influence of isothermal treatment at 810° F prior to quenching

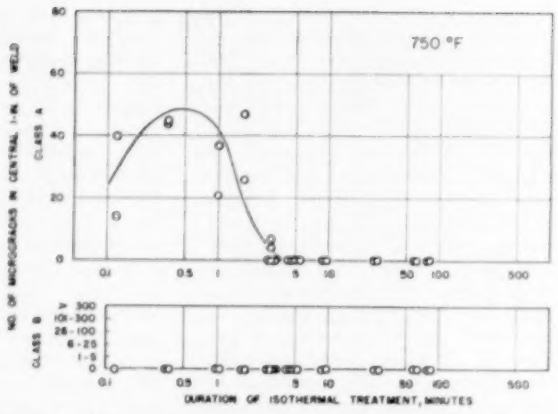

Fig. 11 Influence of isothermal treatment at 750° F prior to quenching

analogous. Lefevre[17] found that fisheye formation in welds was minimized by either very rapid or very slow cooling. Fisheyes were more frequent in welds which were cooled at intermediate rates. Andrew, Lee, Mallek and Quarrel[18] charged a ball-bearing steel with hydrogen at an austenitic temperature and found that specimens which were quenched from this temperature exhibited no flakes. Many flakes were present, however, after air cooling. Bennek, Schenk and Muller[19] (as cited in Reference 17) also observed that the incidence of flakes decreased with very fast cooling rates. It is also of interest to note the behavior of certain alloy steels which were subjected to end-quench tests after being charged with hydrogen.[16, 18] In some (but not all) cases it was observed that the quenched ends of such specimens were free from cracks while cracks occurred in distant regions which had cooled more slowly.

7. On the Permanency of the Immunity Achieved by Isothermal Treatment

As has been seen in Section 6, a condition of apparent immunity was achieved by sufficiently long isothermal treatment at most of the temperatures employed. One wonders what might happen if, after isothermal immunization at one temperature, specimens were treated at a second temperature before being quenched to room temperature. Would the immunity achieved at the first temperature prove permanent or would susceptibility develop at the second temperature? In an attempt to answer this question a group of four specimens was subjected to consecutive treatments at 750 and 875° F. The latter temperature was selected for the second stage of treatment in view of the high degree of susceptibility which had been exhibited earlier by specimens treated at that temperature.

The four specimens were quenched into molten lead at 750° F immediately after welding. Ninety minutes later they were transferred to an 875° F bath where they were held for various periods (1/4, 3, 9 and 27 min) before being quenched into water at room temperature. Subsequent examination disclosed no microcracks of either class in any of these specimens. It was concluded, therefore, that, at least in the case of this particular combination of temperatures, the immunity achieved in the first step of the treatment was indeed permanent.

8. Temperature-Dependence of the Time Required for Isothermal Immunization

Because the times required for specimens to approach the temperatures of the isothermal baths were by no means negligible, Figs. 6 through 13 furnish little information concerning the relation between temperature and the time required for isothermal attainment of susceptibility. These figures are more useful, however, for estimating the times required for isothermal immunization. This follows from the fact that the thermal lag is more or less confined to the period of increasing or fully-developed susceptibility. Subsequently, conditions are more nearly isothermal. As stated earlier, a primary aim of the investigation was the determination of this relation between temperature and the time required for isothermal immunization.

The desired relation may be obtained by drawing smooth curves to fit the data of Figs. 6 through 13 (as has been done in the figures) and by cross-plotting on the basis of these curves. Figure 14 was obtained in this manner. It shows the relation between the temperature of treatment and the time required to attain an arbitrary degree of immunity corresponding to a level of two Class A microcracks per specimen. The latter criterion was used as a matter of convenience. It would be more desirable to speak of the times required for complete immunity but the latter values are not as well defined. Strictly speaking, the times shown in Fig. 14 are not true immunization times. They are actually the total times during which specimens were exposed to the constant-temperature baths. They include the period of thermal lag and the stage in which susceptibility rather than immunity was fostered.

Figure 14 permits the following observations concerning the relation between temperature and the time required for isothermal immunization. The required time is seen to increase with decreasing temperature in the range from 1290 to 875° F. At 875° F the time is extremely long.* In the range from 875 to 750° F it decreases sharply with decreasing temperature. From 750 to 212° F the required time is rather short and would appear to be nearly independent of temperature. Since Fig. 14 is based on work at only eight temperatures, there is of course some uncertainty over the correctness of the shape of the smooth curve which has been drawn. This is especially so in the case of the rather large temperature gaps from 212 to 450° F, from 450 to 750° F, and from 1000 to 1200° F.

Before proceeding to a further discussion of Fig. 14, it may be of interest to refer at this time to the work of investigators who have studied a number of steels in an effort to determine the temperature-dependence of the time required to attain isothermal immunization against flaking. Andrew, Lee, Lloyd and Stevenson[20] austenitized a 0.6% carbon steel in an atmosphere of

* According to Fig. 14, the time required to attain immunity at 1000° F is also rather long, namely, 40 min. Moreover, there may be reason to question the validity of this value. As is apparent in Fig. 8, there is an unfortunate lack of data for the longer times at 1000° F. The 40-min value, based on the scanty Class A data which are shown in Fig. 8, is seemingly belied by the Class B data of the same figure. There is no indication that immunity in terms of Class B cracks was approached even in 120 min, the longest time employed at 1000° F.

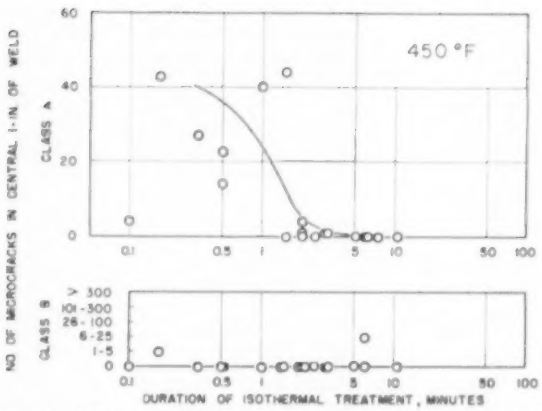

Fig. 12 Influence to isothermal treatment at 450° F prior to quenching

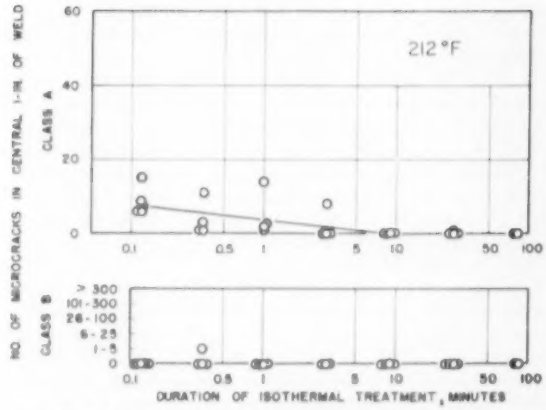

Fig. 13 Influence of isothermal treatment at 212° F prior to quenching

hydrogen. Their specimens were then quenched into isothermal baths held at a number of temperatures. Ten minutes later they were removed from the baths and were quenched in water. It appeared that the 10-min holding time was sufficient to achieve immunity in the temperature range from 1290 to 930° F and in that from 750 to 300° F. Immunity was not achieved in this time, however, at 840° F, the only temperature employed between 930 and 750° F. It is of interest to note that the behavior of this steel was qualitatively consistent with that observed in the present work both with respect to the existence of an intermediate range of sluggish immunization and with respect to the rather rapid immunization at lower temperatures.

There have also been a number of investigations on alloy steels which contained various amounts of nickel, chromium and molybdenum.[16,18,20,21] Particularly extensive were the studies of Dubovoi and those of Andrew *et al.* (see Figs. 63, 65, and 67 of Reference 21 and Figs. 55 and 56 of Reference 20). In their work it appeared that in most (but not all) cases the time required for the immunization of a given steel was shorter both in a temperature range somewhat below A_1 and in one far below A_1 than it was at the intermediate temperatures. Thus, with respect to the existence of an intermediate temperature range of most sluggish immunization, the behavior of these alloy steels often tended to parallel that of the weld metal studied in the present work.

Somewhat analogous results were derived in two studies on alloy steel welds. Wooding[15] and Steinberger and Stoop[7] attempted to determine the times required for isothermal immunization against underbead cracking and against weld-metal cracking, respectively. In each case, it was found that immunization was more rapid at relatively low temperatures than in a somewhat higher temperature range.

9. Some Practical Implications

In Fig. 14 it is worthy of note that the immunization times are so short at the lower temperatures, even at 212° F. On the basis of Fig. 14 alone, one might predict that in ordinary welding practice the cooling rate in the low-temperature range would be decisive with regard to microcracking. This follows from the fact that in practice a cooling weld would ordinarily dwell in the high-temperature range long enough to become susceptible but would not remain long enough to achieve immunity. If immunity is to be acquired, it would seem necessary in practice that this be accomplished during passage through the low-temperature range. According to Fig. 14, an exposure of somewhat more than 3 min in this range might be expected to suffice. Such an estimate is in rather satisfactory quantitative agreement with observations made under a variety of conditions in earlier studies in this laboratory and elsewhere. Some of these observations are summarized in the following paragraph.

In a study concerned with the effectiveness of preheating as a means of microcrack prevention it was found that, under the conditions employed, the critical preheating temperature caused the weld to dwell for a period of about 4 min at temperatures above 200° F.[5] In a study concerned with the effects of weld length and plate width as variables it was found that the critical conditions corresponded once again to a period of about 4 min at temperatures above 200° F.[4] In

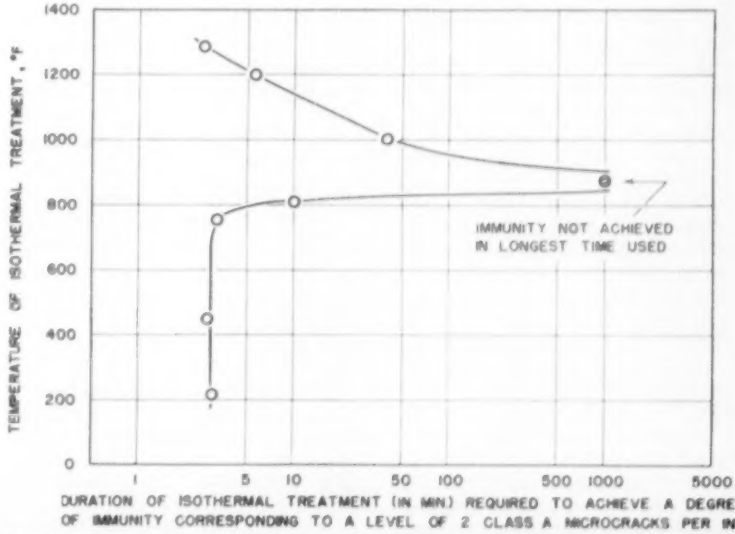

Fig. 14 Temperature-dependence of the time required for isothermal attainment of immunity

another study, concerned with the effects of water quenching after various periods of air cooling, it was found that a delay of from 4 to 8 min before quenching sufficed to prevent embrittlement.[4] At the end of this time, the weld had cooled to a temperature of about 300° F. Rather similar results were obtained in work by Harris, Matthiesen and Newmark.[10] In tests on both multipass and single-bead welds Bland found his "critical quenching time" to be about 3 min.[1] In his work the specimens were preheated to 212° F prior to welding and were quenched into boiling water after various periods of air cooling. It will be noted that in all of the above-cited cases the critical periods for low-temperature exposure were in the range from 3 to 8 min. In the work of Rollason and Roberts, however, it appeared that under certain conditions a shorter time sufficed.[3] Working with air-cooled welds, they found that microcracking was avoided when a weld cooled to 212° F in about 1 min. All of the references in this paragraph are concerned with the welding of mild steel with hydrogen-rich electrodes. With the exception of Bland's multipass welds, all specimens were of the single-bead variety.

It would seem fortunate that in welding practice conditions are often such that cooling welds pass through the lower temperatures sufficiently slowly. It seems fortunate also that, in cases where cooling might otherwise be too rapid, it is a simple matter to retard low-temperature cooling by means of preheating.

For the prevention of microcracking in mild steel welds, it would seem necessary only to insure that low-temperature cooling is sufficiently slow to permit the attainment of immunity before the weld reaches a temperature at which it is possible for cracking to occur. If this suggestion is correct, it would of course be desirable to know, at least approximately, the temperature at which cracks can be expected to form in the case of a susceptible weld. Perhaps, however, there is no single temperature which can be expected to serve as a critical value under all conditions. It may be that the temperature of crack formation is influenced by such factors as, for example, the prior history of the weld, the state of stress, and chemical composition. In Reference 8 it was found under the conditions employed that most of the microcracks formed at temperatures below 212° F in an air-cooled weld. A few may have formed at a somewhat higher temperature. In the present study it is clear that, in the case of the welds treated isothermally in boiling water, cracking must have occurred at temperatures below 212° F. In general, however, no effort was made to determine the temperatures of crack formation in the present work.

Numerous and extensive studies on the phenomena of flaking and underbead cracking in alloy steels would seem to indicate that these types of cracking also tend to occur at rather low temperatures. Such indications are of interest since they are consistent with the suspicion that the mechanisms of these phenomena are similar to that of weld-metal microcracking.

In certain weldability studies in the past much importance has been attached to the rate of cooling at elevated temperatures as, for example, at 1000° F. While such rates are undoubtedly important in some respects, they would seem to be of little practical interest in connection with weld-metal microcracking in mild steel.

10. Hardness Tests

After having been examined for microcracks, some of the isothermally treated welds were subjected to hardness tests. As indicated in Fig. 15, ten hardness indentations were made in the central 1 in. of each of these specimens. The measurements were made on the Rockwell 30T scale. Each of the hardness values cited in this section represents the average value of the ten determinations made on a single specimen.

Figure 16 describes the results of hardness determinations made on the entire group of welds treated isothermally at 810° F. It will be seen that in this case the duration of treatment had little, if any, effect on hardness. Thus by comparison of Figs. 16 and 10 there would seem to be no correlation between hardness (on a macroscopic scale, at least) and the frequency of microcracking. The short-time specimens containing large numbers of microcracks are perhaps no harder than the long-time specimens containing few microcracks or none at all. Moreover, it would seem that the decomposition of austenite must have been nearly complete even in the shortest times employed in the work at 810° F. Otherwise, the final hardness would be expected to vary with the duration of isothermal treatment prior to quenching. It, of course, cannot be concluded from Fig. 16 that the transformation of austenite was entirely complete prior to quenching even in the case of the longest holding time employed. It is conceivable that small amounts of austenite might have survived the isothermal treatment and that, because of the small amount involved, subsequent decomposition at lower temperatures might have had little effect on over-all hardness.

Less extensive hardness data were obtained in the case of several other temperatures, namely, 1200, 875, 450 and 212° F. In Fig. 17, which shows these data, each bar represents the behavior of a single specimen. The figure permits two observations of interest. In the first place, it is seen again that there is very little difference between the hardness values for a short holding time at a given temperature and those for much longer times. Thus, once again, there would appear to be no

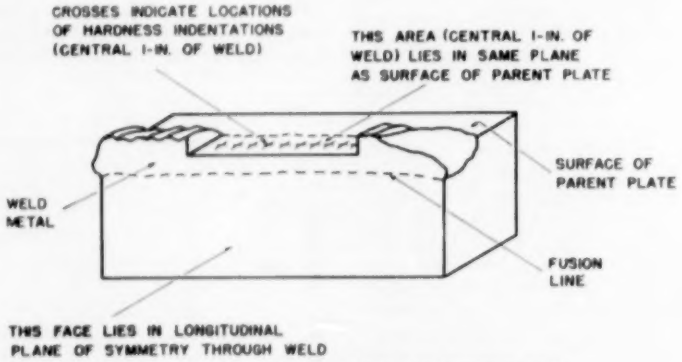
CROSSES INDICATE LOCATIONS OF HARDNESS INDENTATIONS (CENTRAL 1-IN. OF WELD)
THIS AREA (CENTRAL 1-IN. OF WELD) LIES IN SAME PLANE AS SURFACE OF PARENT PLATE
SURFACE OF PARENT PLATE
WELD METAL
FUSION LINE
THIS FACE LIES IN LONGITUDINAL PLANE OF SYMMETRY THROUGH WELD

Fig. 15 Location of indentations made in the hardness tests

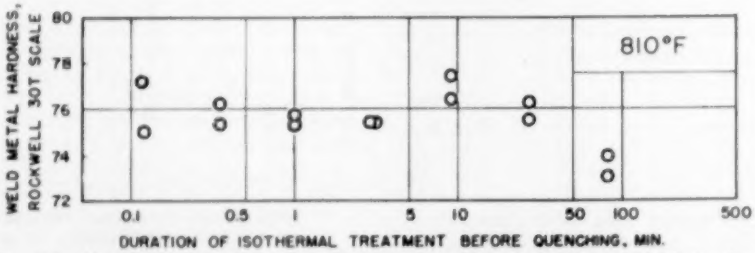

Fig. 16 Hardness data for the specimens treated isothermally at 810° F prior to quenching

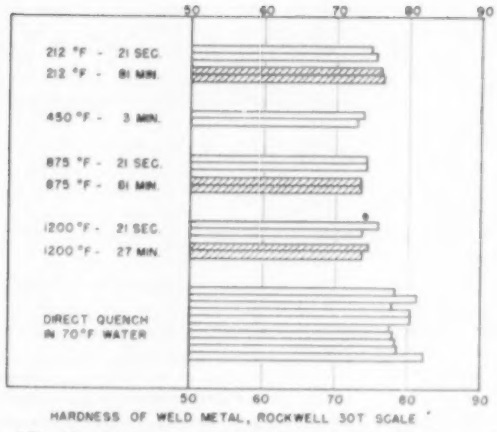
50 60 70 80 90
212 °F - 21 SEC.
212 °F - 61 MIN.
450 °F - 3 MIN.
875 °F - 21 SEC.
875 °F - 61 MIN.
1200 °F - 21 SEC.
1200 °F - 27 MIN.
DIRECT QUENCH IN 70°F WATER
50 60 70 80 90
HARDNESS OF WELD METAL, ROCKWELL 30T SCALE

Fig. 17 Hardness data for specimens subjected to various treatments

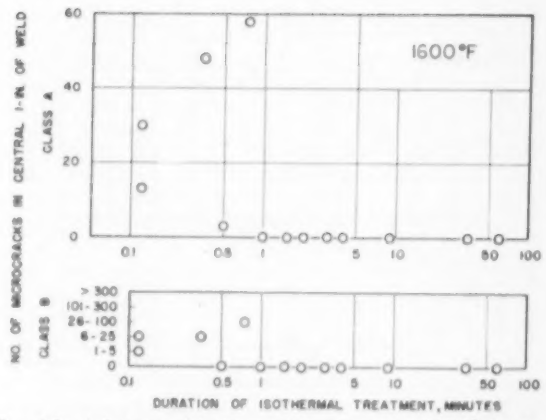

Fig. 18 Influence of isothermal treatment at 1600° F prior to quenching

correlation between hardness and the frequency of microcracking. A second observation is concerned with the relation between hardness and the temperature of treatment. According to Fig. 17, there would appear to be very little difference in the hardness values associated with the several temperatures. Welds treated at 212° F, for example, are not much harder than those treated at 1200° F. This suggests strongly that in all cases the bulk of the transformation must have occurred in essentially the same temperature range regardless of the temperature of "isothermal" treatment. This would imply that, in all cases, transformation must have been nearly complete within only a few seconds after the completion of welding and that it must have occurred at a rather high temperature. It appears probable that, as a result of the thermal lag, specimens achieved the temperatures of the isothermal baths only after the bulk of the austenite had already transformed.

Figure 17 also indicates the hardnesses of some of the welds which were quenched into room-temperature water immediately after welding. It may be seen that the hardness in the latter case is somewhat greater than that associated with any of the isothermal treatments. But, as has been noted in Section 4, the directly quenched welds were nearly immune to microcracking. Thus, it would appear once again that there is no correlation between weld-metal hardness and the incidence of cracking.

11. The Hydrogen-Retained Austenite Hypothesis

Up to this point various experimental results have been described and certain practical implications have been mentioned. At this stage it is in order, perhaps, to indulge in some speculation on the natures of the mechanisms which are involved. It is believed that the experimental results are not inconsistent with a version of what might be termed the "hydrogen-retained austenite" hypothesis. This section will be devoted to a description of the hypothesis. The three which follow will consider the compatibility of the hypothesis with the principal results of the present investigation. They will also refer to certain elaborations of the hypothesis which are suggested by the data.

The hydrogen-retained austenite hypothesis has frequently been suggested as an explanation for the underbead cracking of welds and for the flaking of forgings and other hot-worked products. In the extensive literature on these subjects several versions of the hypothesis have been suggested. (An excellent summary has been prepared recently by Sims.[22]) According to a version preferred by the authors, the following features are associated with the hypothesis.

(*a*) For cracking to occur it is necessary that a dangerously large quantity of hydrogen be contained in the steel. In the case of welds, the necessary hydrogen may be derived from the atmosphere of the welding arc. In the case of forgings and other hot-worked products, hydrogen may be introduced in the steel-making process or, less frequently, during subsequent processing.

(*b*) During the course of the austenite decomposition which attends cooling from high temperatures, there is probably a tendency for hydrogen to become segregated in the remaining austenite since its solubility in that phase is higher than in the products of decomposition. In this way it is possible that especially high concentrations of hydrogen are produced locally.

(*c*) In turn, an increased hydrogen content may tend to further stabilize the untransformed austenite thus permitting it to cool to lower transformation temperatures than would otherwise be the case.[23-26]

(*d*) The decomposition temperature of the last portions of hydrogen-laden austenite is critical. If decomposition occurs at a sufficiently high temperature, the plasticity of the product and the diffusivity of the hydrogen are sufficient to permit a favorable redistribution of the embrittling hydrogen before cracking can occur. If, on the other hand, decomposition occurs at a sufficiently low temperature, the lower diffusivity of hydrogen and the greater brittleness of the transformation product may lead to cracking. The details of the process by which the low-temperature transformation of hydrogen-rich austenite may produce cracking are not clear and need not concern us in this paper.

(*e*) The temperature at which the last austenite decomposes can be expected to depend on many factors. Among them are the cooling rate, the concentration of austenite-stabilizing elements, and perhaps the nature of the stress system.

(*f*) Needless to say, stress as well as brittleness, is required for the occurrence of cracking. It is visualized that the necessary stress may arise in a variety of ways among which the following may be mentioned.

1. The stresses induced by the volume changes which are associated with the transformation of austenite.
2. The aerostatic stresses which may arise from the accumulation of molecular hydrogen in "lattice rifts" and other discontinuities.
3. The thermal stresses which attend differential cooling.

It is to be emphasized that, according to the above scheme, the interaction of hydrogen and retained austenite is complex and insidious. On one hand,

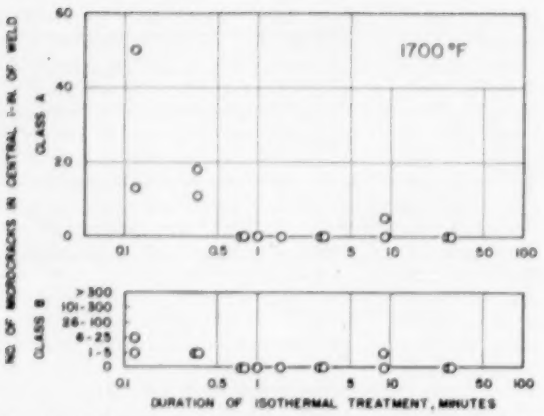

Fig. 19 Influence of isothermal treatment at 1700° F prior to quenching

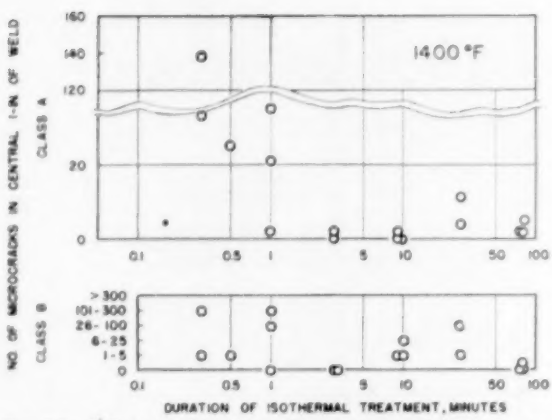

Fig. 20 Influence of isothermal treatment at 1400° F prior to quenching

it is the incompleteness of the austenite transformation at elevated temperatures which permits the dangerous concentration of hydrogen during cooling. On the other hand, the accumulation of hydrogen may tend to stabilize the austenite, thus permitting it to resist transformation until dangerously low temperatures are reached. Low-temperature transformation alone tends to produce a rather brittle transformation product. The presence of hydrogen makes for further embrittlement.

But in practice flaking and underbead cracking are not commonly encountered in mild steel. They are ordinarily found only in the more hardenable steels. Is it reasonable, then, to expect cracking to occur by a related mechanism in the case of mild-steel weld metal where both the carbon content and the alloy content are so low? In this connection the following peculiarities of weld metal are of interest.

(*a*) Certainly, the over-all hydrogen content of the weld metal is unusually high. (In the present work welds quenched to room temperature immediately after welding were found to exhibit hydrogen contents of at least 15 cc per 100 g.)

(*b*) The consequences of dendritic segregation might be expected to be especially severe in the case of weld metal since there is so little opportunity for segregation to be relieved by high-temperature diffusion following solidification. Such segregation (perhaps involving hydrogen, carbon and the various alloying elements) is of interest since the initiation of cracks is a localized phenomenon and can be expected to depend on local, rather than over-all, composition.

(*c*) Since some nitrogen is introduced in the welding process, the over-all nitrogen content of the weld metal may be higher than that found ordinarily in steel products. More important perhaps, the localized concentration of this element may be accentuated by segregation. Nitrogen is known to promote the stability of austenite and Rollason and Roberts have expressed the belief that nitrogen may be an important factor in weld metal microcracking.

The above considerations would seem to furnish a basis for believing that mild-steel weld metal might be susceptible to cracking by the hydrogen-retained austenite mechanism. Such a possibility has, of course, been suggested by others who have studied weld-metal cracking.

Before proceeding, it must be emphasized that the discussion which follows in the next three sections is not aimed at establishing the unique suitability of the hydrogen-retained austenite hypothesis as a means of explaining the experimental findings which are related in this paper. (Indeed, it would appear that for the present some of the observations, especially those of a quantitative nature, cannot be explained fully.) The discussion is intended to show only that the findings are probably not inconsistent with the hypothesis. There remains the possibility that other explanations may be equally successful or may even prove superior. No effort will be made in this paper, however, to explore other possibilities.

12. Concerning the Development of Susceptibility During Isothermal Treatment

Can the experimental results which have been related in this paper be reconciled with the hydrogen-retained austenite hypothesis? This section discusses the question in relation to the growth of susceptibility which was observed to occur during the early stages of isothermal treatment. The two sections which follow will deal with the near-immunity of specimens which were quenched directly after welding and with the eventual development of immunity during isothermal treatment.

It seems reasonable to presume that hydrogen is rather uniformly distributed throughout the austenite of the cooling weld as the latter approaches the neighborhood of A_1. As a consequence, the hydrogen content may not be sufficiently high in any location to be dangerous (according to the hypothesis outlined in the preceding section). With a further drop in temperature, decomposition of the austenite begins. For susceptibility to develop it is necessary, according to the hypothesis, that the hydrogen content of any untransformed austenite increase during the course of transformation and that it attain a critical value. We shall now consider in some detail the manner in which this may be accomplished.

Consider an island of austenite which is being invaded by an advancing transformation front. Consider in particular the fate of hydrogen which is dissolved in this austenite in the immediate vicinity of the interface. There is the possibility that, as the transformation front advances, some of this hydrogen may remain in the still-untransformed austenite by diffusing inward ahead of the front. If so, it will, of course, contribute to an increase in the hydrogen concentration in the shrinking island of austenite. There is also the possibility that some of the hydrogen will take up residence in the newly formed transformation product. It is of interest now to inquire into the factors which may be expected to determine the proportion of the hydrogen which follows each of these two courses.

At temperatures not too far below A_1, the transformation of austenite requires the diffusion of carbon and the rate is presumably limited by this consideration. (This would certainly seem to

be the case for temperatures at which the transformation product consists of ferrite and pearlite. It may also apply at somewhat lower temperatures.) But, at any given temperature, hydrogen is probably much more mobile than carbon. Hence, one might expect that the hydrogen in the path of the transformation front would be redistributed in a manner dictated by the equilibrium solubilities in the austenite and ferrite phases. Accordingly, since the solubility in austenite is known to be higher than that in ferrite, one might expect that the hydrogen concentration would increase steadily in an island of austenite as the latter undergoes transformation. The concentration might become large and a dangerous condition might be produced in this manner.*

It is worth noting that one would expect the last patches of untransformed austenite to occur in regions of high alloy content resulting from dendritic segregation. Any stabilizing influence exerted by the high hydrogen content would be reinforced here by the presence of alloying elements with the result that the last small patches of austenite might be unusually persistent. It is precisely such a condition which would be expected to make for microcracking during subsequent cooling. Upon the quenching of austenite stabilized in this manner, the completion of transformation might occur at unusually low temperatures.

It is believed that the above considerations satisfactorily account for the observation that a period of increasing susceptibility occurs during the early stages of isothermal treatment. (As noted in Section 6, it seems probable that in all cases the temperature lags which attended immersion of specimens in the "isothermal" baths were so great as to permit most of the transformation to occur at temperatures not far below A_1, regardless of the nominal temperature of treatment.)

13. Concerning the Near-Immunity of Directly Quenched Specimens

In a further attempt to test the hydrogen-retained austenite hypothesis, we refer now to the near-immunity which was exhibited by welds quenched in water immediately following welding. How can the behavior of these specimens be reconciled with the hypothesis and with the remarks of the preceding section? In an attempt to answer this question, we shall consider the probable influence of the transformation temperature on the tendency for hydrogen to concentrate in the remaining austenite during decomposition.

In the preceding section we have considered only the case of transformation at temperatures not too far below A_1, i.e., the case in which the advance of the transformation front is dependent on the diffusion of carbon. Under such conditions, it has been argued, it may be possible for some of the hydrogen to concentrate in the shrinking regions of austenite. Consider now the other extreme, namely, the case in which transformation occurs at temperatures so low that it need not await the diffusion of carbon (as, for instance, in the transformation to martensite). At such temperatures one might expect the transformation front to advance so rapidly that there would be little opportunity for hydrogen to accumulate by migrating ahead of the interface. Seemingly, this would tend to minimize the likelihood of attaining a critical hydrogen concentration in the last remnants of untransformed austenite.

According to such a picture, the near-immunity of the directly-quenched welds can be explained merely by recognizing that the quenched welds passed through the high-temperature range more rapidly than did the specimens which were subjected to isothermal treatment (see Fig. 5 in this regard). Even in the case of quenched welds, most of the transformation undoubtedly occurred in the high-temperature range but, presumably, the duration of exposure to such temperatures was not sufficiently great to permit a critical degree of hydrogen enrichment to occur. Additional transformation then occurred at lower temperatures which did not favor further enrichment. The assumption that a significant proportion of the transformation occurred at the lower temperatures in quenched welds is consistent with the hardness data of Fig. 17.

This attempt to account for the near-immunity of directly quenched welds would seem to be consistent with the observation that the degrees of susceptibility developed in specimens treated isothermally at 450 and 212° F (the two lowest temperatures employed) were apparently less than those developed in the specimens treated at higher temperatures. (Compare the numbers of microcracks shown in Figs. 12 and 13 with those indicated in Figs. 6 through 11.) It need only be recognized that the specimens treated at the lower temperatures spent the least time in the high-temperature range. Presumably, the times were sufficiently long to produce some susceptibility but not long enough to produce the greater degree which might have resulted from somewhat slower cooling.

Perhaps the occasional occurrence of microcracking in some of the directly quenched specimens can also be explained in a parallel fashion. On the average, the elevated-temperature cooling rates of the quenched specimens may have been only slightly greater than required for the development of a low degree of susceptibility. If such were the case, the borderline nature of the cooling rates might have allowed occasional development of susceptibility in certain regions.

In the foregoing portions of this section and in Section 12, the mechanism of hydrogen concentration in austenite has perhaps been oversimplified. Consideration has been given only to the possibility that some of the hydrogen which is dissolved in an austenite patch near the boundary might diffuse inward ahead of the shrinking boundary. There is, perhaps, another possibility which deserves consideration. Consider that portion of the hydrogen which, in the process of transformation, is forced to take up residence in the transformation product. It is conceivable that later, under certain conditions, some of it might find its way back to a nearby patch of as-yet-untransformed austenite. Such a tendency would be consistent with the belief that the hydrogen is more soluble in austenite than in the transformation products. But there is a competing tendency which favors the diffusion of this hydrogen toward internal voids and rifts and toward external surfaces. What then determines whether it diffuses into a nearby austenite patch or in the direction of a free surface? The direction of flow would be expected to depend on a number of factors, many of them strongly dependent on temperature. Certainly these factors would include the diffusivity and the solubility of hydrogen in each phase. It is conceivable that at some temperatures the combination of factors might favor a significant flow of hydrogen into nearby patches of untransformed austenite. At other temperatures this might not be the case. A quantitative treatment of the subject will not be attempted at this time. It need only be noted that such an explanation becomes consistent with the experimental data if one assumes that it is only the higher temperatures which favor the enrichment of austenite in this manner.

14. Concerning the Development of Immunity

After the foregoing speculation on the manner in which susceptibility is produced, it is natural to wonder about the mechanism which is responsible for the subsequent attainment of immunity. A satisfactory explanation must account for the following observations.

Observation "a." At all temperatures prolonged isothermal treatment induces a trend toward immunity.

Observation "b." The time required for the accomplishment of isothermal

* An alternative (and perhaps supplementary) process by which hydrogen might concentrate in regions of as-yet-untransformed austenite will be suggested at the end of the next section.

immunization varies with temperature in the manner shown in Fig. 14.

It would seem that the first observation can be explained readily enough. It has been suggested earlier that susceptibility may be associated with the existence of small patches of hydrogen-rich untransformed austenite. Consistent with this explanation, the subsequent development of immunity would seem to be favored by the following possibilities.

Possibility "a." With sufficiently prolonged treatment there is the possibility that complete transformation of the austenite might be accomplished isothermally. If only the transformation temperature were sufficiently high, the transformation product might possess properties which would render the hydrogen content harmless and thus prevent the formation of cracks during and after transformation.

Possibility "b." There is the possibility that the high concentration of hydrogen in the last vestiges of austenite might be relieved by outward diffusion across the austenite boundary before transformation. In the early stages of isothermal treatment such a process might, in some cases, be impeded by a high concentration of hydrogen just outside the boundary. In such cases the condition might be only temporary since, with the passage of time, the barrier would tend to be lowered through diffusion to regions of lower hydrogen content.

Possibility "c." There is the further possibility of an interaction between the escape of hydrogen and the stability of the austenite. The partial escape of hydrogen from a patch of untransformed austenite might spur transformation.[23]

These possibilities would seem adequate to account for observation "a" which requires only a qualitative explanation. Observation "b," however, presents a more difficult problem since it is quantitative in nature. Here it is necessary to account for the shape of the curve in Fig. 14. In particular, it is necessary to explain the sluggishness of immunization at 875° F and the remarkably short immunization times at all temperatures from 750 to 212° F.

At first glance, one might be tempted to attribute the sluggishness at 875° F to the dominance of possibility "a." In certain alloy steels, the time required for the completion of transformation (in the absence of hydrogen) exhibits a maximum value in the region of this temperature. (As has been suggested earlier, the last remnants of austenite in the present welds may occur in regions which as a result of dendritic segregation are rich in alloy content.) On the other hand, both at temperatures near A_1 and at those below 750° F, the shape of the curve in Fig. 14 would appear difficult to reconcile with the dominance of possibility "a." At temperatures near A_1, the time required for the attainment of immunity is seen to decrease with increasing temperature in Fig. 14, while the time required for the completion of the isothermal transformation of austenite (in the absence of hydrogen) generally increases with increasing temperature. At temperatures below 750° F, Fig. 14 shows that the time required for isothermal achievement of immunity is remarkably short and is nearly independent of temperature. Again, there would appear to be no satisfactory parallel between the observed behavior and the time which (in the absence of hydrogen) would presumably be required for the completion of isothermal transformation.

Thus, to account for the shape of the curve in Fig. 14 possibility "a" would seem to be insufficient. It would appear necessary to invoke possibilities "b" and "c" as well, i.e., to consider the temperature-dependence of the rate at which hydrogen can be expected to escape from untransformed austenite and perhaps to consider the interaction between its escape and the stability of the austenite. The picture then becomes complex and prediction becomes difficult. To make even semiquantitative predictions it becomes necessary to know with some precision the manner in which temperature affects the solubility and diffusivity of hydrogen both in austenite and in the various products of decomposition.* Moreover, it requires a knowledge of the manner in which these effects are modified by the segregation of various elements and perhaps by the influence of stress. Since there is a lack of the prerequisite knowledge, the authors prefer not to attempt an explanation for observation "b."

It does not follow, of course, that the hydrogen-retained austenite hypothesis must be rejected. Rather it would appear to be difficult to test the hypothesis in this case since pertinent data are lacking.

15. Further Observations on Isothermal Treatment at 875° F

As noted earlier, microcracks were found in specimens which had been held as long as 18 hr at 875° F, the longest time employed at that temperature. Does this mean merely that the achievement of immunity is unusually sluggish at 875° F or does it indicate perhaps that some of the microcracks formed during the isothermal treatment? In the latter case, of course, no amount of holding would be expected to produce a crack-free condition. In an attempt to answer this question, two groups of specimens were subjected to the tests which are related in the remainder of this section.

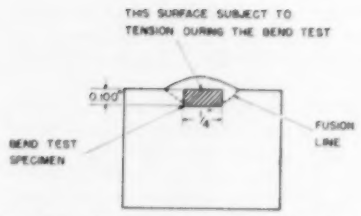

Fig. 21 Cross-sectional view showing location of material used for the bend-test specimen

The two specimens comprising the first group were placed in an isothermal bath at 875° F immediately following welding. Fifty seconds later they were transferred to a second bath at 1600° F where they were held for 15 min. They were then quenched in room-temperature water. Upon examination, neither Class A nor Class B microcracks were found in either of these specimens. Thus, it was evident that no cracking could have occurred at 875° F (at least during the 50-sec exposure). Presumably, the specimens were still susceptible to cracking when removed from the 875° F bath (see Fig. 9) but complete immunization was achieved in the subsequent treatment at 1600° F.

A second group of specimens was treated in a manner designed to test the suspicion that the susceptibility developed in specimens held at 875° F might be especially severe in nature. The three specimens of the group were treated for times ranging from 25 to 90 sec at 875° F. They were then allowed to cool in air after which they were examined for the occurrence of microcracks. All of the specimens were found to contain both Class A and Class B microcracks, the average values for the two types being about 10 and 100, respectively. The discovery of so many cracks in these specimens came as something of a surprise since air cooling allows slow passage through a temperature range in which, according to Fig. 14, one might have expected immunity to be achieved in short order. (As may be seen from Fig. 5, air cooling allows about 13 min to be spent in the range between 750 and 300° F.) Thus the susceptibility acquired at 875° F would seem to be remarkably persistent. The reason for this persistence is not as yet clear. The subject is one which would seem to deserve further investigation.

In summary, it would seem that (*a*) cracking does not occur during

* It has been suggested by several writers that there may be more than one mode of diffusion and that the rate can be expected to depend upon the mode which is operative. In addition to ordinary lattice diffusion, there is the possibility that the existence of rift networks might permit the diffusion of molecular hydrogen.

the 875° F exposure but only upon subsequent cooling; (*b*) the degree of susceptibility developed at 875° F is unusually severe since the subsequent attainment of immunity is sluggish even at lower temperatures.

16. Isothermal Treatments at Temperatures Above A_2

It is to be remembered that the isothermal treatments of Section 6 were conducted at temperatures below A_1. Some additional tests at 1600 and 1700° F are described in this section. The methods employed were generally similar to those used at the lower temperatures.

The results, in terms of microcracking tendency, are shown in Figs. 18 and 19. In each case it will be seen that the behavior is qualitatively similar to that obtained earlier at temperatures below A_1. Susceptibility is unmistakably evident after short periods of treatment. This is followed by the attainment of immunity.

At first glance, it might seem surprising that susceptibility should be shown by the short-time specimens since, as noted earlier, specimens which were quenched to room temperature immediately after welding were nearly immune. In what way could short periods of reheating to austenitic temperatures be harmful? In answer to this question, the following possibilities would seem to deserve consideration.

(*a*) It is known that, at the instant of introduction into an isothermal bath, the temperature of the mid-length portion of the weld is near A_1 and the underlying material is at a somewhat lower temperature. It is conceivable that the internal temperature gradient might cause the temperature of the weld to continue to fall for a brief period even after introduction into the 1700° F bath. If so, this might produce an increase in susceptibility since, as has been seen earlier, short exposures at temperatures just below A_1 seem to be harmful. It is conceivable that specimens quenched in the 1600 and 1700° F baths spend more time in the susceptibility-producing temperature range below A_1 than do specimens quenched in water immediately after welding. No effort has been made, however, to check this possibility by actual temperature measurements.

(*b*) After a specimen has been quenched in the 1600 or 1700° F bath, a certain amount of time elapses before the temperature of the bath is attained and much of this time is spent in the range between A_1 and A_2. During this period there should be a tendency for ferrite to precipitate from low-carbon austenite and for both carbon and hydrogen to concentrate in the remaining austenite. Both tendencies might be expected to make for increasing susceptibility during passage through this temperature range.

The eventual attainment of complete immunity at 1600 and 1700° F is, of course, not surprising. A nearly 100% austenitic condition should be attained ultimately at these temperatures and both carbon and hydrogen should become rather uniformly distributed. Such a condition should be more favorable than that existing immediately after the completion of welding. In addition, there should be a strong tendency for the overall hydrogen content to decrease with time. The latter tendency would be expected to produce an even more favorable condition.

At this point, it is of interest to refer to the behavior of a group of 8 specimens which were subjected to duplex treatments to determine the permanency of the immunity gained by holding at 1600° F. Immediately after welding, the 8 specimens were placed in lead at 1600° F where they were held for periods ranging from 5 min to 1 hr. Upon removal, they were placed in a second bath at 875° F where the holding time was varied between 30 sec and 3 min. The specimens were then quenched in room-temperature water and were examined for microcracks. The complete absence of cracking would seem to indicate that the immunity attained at 1600° F is of a permanent nature.

17. Isothermal Treatment at a Temperature Between A_1 and A_2

Because temperatures between A_1 and A_2 could be expected to produce localized austenite of higher-than-average carbon content, it was considered of interest to explore the effects of isothermal treatment in that temperature range. Accordingly, some specimens were treated at 1400° F. A lead bath was employed and the experimental procedure was in all respects similar to that used at the other temperatures. The results are shown in Fig. 20.

It will be noted once again that specimens which were held for only a short time exhibit a high degree of susceptibility to microcracking. Presumably, the explanation is similar to that suggested in the case of the 1600 and 1700° F tests of the preceding section. (Possibilities "a" and "b" are both pertinent.)

More puzzling, perhaps, is the behavior of the 8 specimens which were held for the longest periods at 1400° F prior to quenching, i.e., for times ranging from 3 to 81 min. The frequency

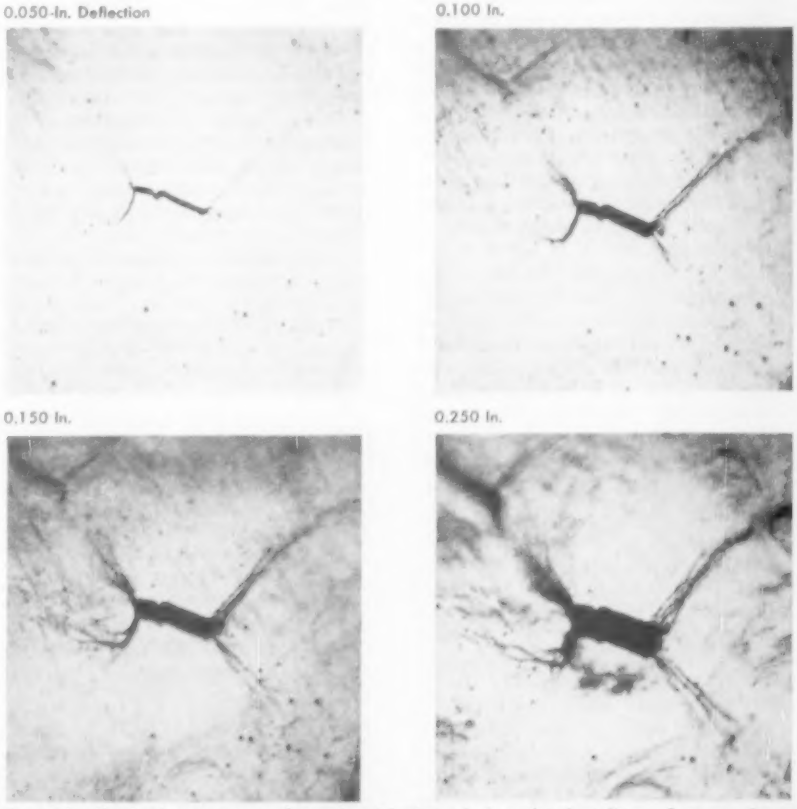

Fig. 22 Typical sequence of crack widening during the bending of a specimen known to contain microcracks. X 500, not etched. (Reduced by 1/2 upon reproduction)

of microcracking is generally low and there is a rather disconcerting degree of scatter, but it seems that at 1400° F, as at 875° F, the attainment of immunity is especially sluggish. The explanation is not clear but one suspects that it may hinge in some manner on the high carbon content of the austenite. Prolonged holding at 1400° F should produce a large reduction in hydrogen content but it is possible that relatively small contents are harmful in high-carbon austenite. Studies on the flaking of plain-carbon steels have shown that susceptibility increases with an increasing carbon content.[21] There have also been indications that, when a steel is cooled from temperatures between A_1 and A_3, the temperature range of martensite formation extends to lower temperatures than when the same steel is cooled from a temperature at which the carbon is more uniformly distributed.[22]

18. Low-Hydrogen Welds

In earlier work, several investigators have found that welds deposited with "low-hydrogen" electrodes have been highly resistant to weld-metal microcracking. It was thought of interest to check this point under the conditions employed in the present study. Accordingly, a group of specimens was prepared in the usual fashion except that the welds were made with E7016 electrodes.

Immediately after welding, these specimens were quenched in a lead bath at 875° F and 30 sec later they were withdrawn and quenched in water at 70° F. The 30-sec treatment at 875° F was selected on the basis of the high degree of susceptibility which it had been found to induce earlier in E6010 welds.

Of the 5 specimens treated in this manner, 4 were found to be entirely free from microcracks. The fifth contained a group of 4 Class A cracks which were concentrated in a single small region. No Class B cracks were found in any of the specimens. Thus, as had been anticipated, the low-hydrogen welds appeared to be especially resistant to cracking.

19. Bend Tests

The reader may wonder if there is any basis for believing that the structural features which have been termed "microcracks" throughout this paper are actually cracks at all. As has been explained earlier, the microscopic examination of an electrolytically polished surface reveals these indications as small dark markings on a white background. In earlier work there has been abundant evidence indicating that similar markings have denoted the presence of fine cracks.[6] In the earlier work, however, the markings were considerably longer than most of those encountered in the present study. For this reason, it was decided to seek additional, direct evidence in the present case. To this end, some auxiliary tests were made patterned after the method of Bland.[1] They were intended to reveal whether or not the widths of the markings would increase in crack-like fashion during plastic deformation.

Small bend-test specimens were cut from welds which had been treated to produce varying degrees of susceptibility to "microcracking." A specimen, 2 in. long, $^1/_4$ in. wide and 0.100 in. deep, was cut from each weld. The location from which the specimen was taken is shown, with reference to the cross section of the weld, in Fig. 21. This location insured that one of the $^1/_4$- × 2-in. faces of the bend specimen would consist entirely of weld metal and that it would represent a region of high microcrack density if cracks were indeed present.

Before bending, the all-weld-metal face of each specimen was ground plane and was given a rough mechanical polish. It was not etched. Electrolytic polishing was not used on these specimens since it was desired to eliminate the possibility that subsequent cracking could be attributed to embrittlement induced by such polishing. In bending, each specimen was simply supported at points $^1/_4$-in. distant from the ends and a concentrated load was applied at mid-span. The all-weld-metal face was located on the tension side of the specimen. Each specimen was subjected to a careful microscopic examination before bending and was re-examined after each of several increments of deflection. Bending was discontinued after attainment of a mid-length deflection of from $^1/_4$ to $^1/_2$ in.

Five groups of specimens were prepared, the treatments being as follows:

Group *a*. Two specimens were quenched in water immediately after welding.

Group *b*. Three specimens were air cooled after welding.

Group *c*. Two specimens were held 10 minutes at 750° F and were then quenched in water.

Group *d*. One specimen was held 30 sec at 750° F and was then quenched in water.

Group *e*. Six specimens were held 30 sec at 875° F and were then quenched in water.

From the earlier work, it was expected that Group *a* would be nearly free from microcracks, that Groups *b* and *c* would be entirely free, and that Groups *d* and *e* would contain large numbers of microcracks. Since mechanical polishing was employed instead of the usual electrolytic polishing, however, it was to be expected that few if any markings would be evident before bending even in the specimens of Groups *d* and *e*. (Mechanical polishing has been observed to obscure small markings which are readily revealed by electrolytic polishing.)

In the case of Group *a*, no crack-like indications were apparent either before bending or after deflection of 0.050 in. A few rather doubtful crack-like markings were seen in both specimens, however, after a deflection of 0.250 in. had been attained.

In the case of Groups *b* and *c*, no crack-like markings were apparent in any of the specimens even after a deflection of 0.500 in.

In the case of Groups *d* and *e*, a few rather doubtful markings were observed in 3 of the 7 specimens before bending. After a deflection of 0.050 in., however, large numbers of unmistakable cracks were apparent in all specimens. With increasing deflection the cracks grew in number and in width but there appeared to be little increase in length. It is noteworthy perhaps that, even after a deflection of 0.500 in. had been reached, only a very few of the cracks were large enough to be detected with the unaided eye. The photomicrographs of Fig. 22 represent a typical sequence of crack development. They depict the behavior of a single crack which was first noticed at a deflection of 0.050 in. in a specimen of Group *e*. Photographs were made at that time and after several subsequent increments of bending.

On the basis of these observations it is concluded either that the markings which throughout this paper have been termed microcracks are indeed small cracks (although difficult to reveal by mechanical polishing) or that they represent regions which are predisposed to cracking during plastic deformation. In either case, it would seem that such markings must be regarded as representing an undesirable condition in structural welds.

20. Remarks on the Sizes of Microcracks

In the preceding figures and tables, the frequencies of cracking have been described for both Class A and Class B microcracks. In many cases the two classes of cracks have tended to occur under identical conditions and the behavior with respect to one class has paralleled that with respect to the other. In the case of some treatments, however, only one class of crack was encountered. This section summarizes such exceptional cases and offers a few additional comments on the sizes of microcracks.

The following three points would appear to deserve mention:

(*a*) After certain treatments Class A cracks were ordinarily the only type

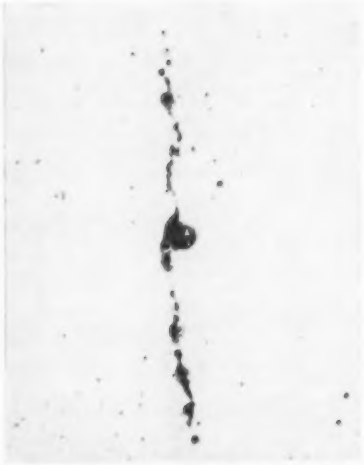

Fig. 23 A microcrack typical of the size found in specimen treated at 450° F. X 200, not etched

found. These cases included the specimens which were quenched directly after welding and those which were quenched after isothermal treatments at 212, 450 and 750° F, the three lowest temperatures employed.

(*b*) In some of the cases mentioned in item "a" above the cracks were especially large. These cases included the directly quenched welds and those treated isothermally at 212 and 450° F. (Fig. 23 illustrates the size of a typical crack found in a 450° F specimen. It should be compared with Figs. 3 and 4 which indicate the sizes of typical microcracks found in specimens treated at the higher temperatures.) After treatment at 750° F only Class A microcracks were encountered but they did not appear to be especially large.

(*c*) In the case of isothermal treatments at 810° F and all higher temperatures, both Class A cracks and Class B cracks were encountered and the cracks of Class A tended to be rather small.

A completely satisfactory explanation of the mechanism of weld-metal microcracking would, of course, be able to account for these observations on crack size. The authors, however, are unable to furnish such an explanation at this time. The hydrogen-retained austenite hypothesis, as it has been stated in this paper, would appear to be non-committal on the subject. Further elaboration of the hypothesis would seem to be required before it can be used as a basis for predicting crack size.

In connection with the Class B microcracks encountered in the present investigation, it is of interest to note that small and, perhaps, related markings have been reported by others engaged in research on weld-metal microcracking and flaking. Recently Warren and Vaughan,[9] working with weld metal, observed crack-like markings which were so small as to escape detection at ×120 although they were visible at ×480. In earlier work on flaking, Andrew, *et al.*,[18] noted that some of their specimens exhibited what they termed "dots," markings which were a good deal smaller than the usual cracks. The distribution of these markings was such as to suggest that they were similar to cracks in origin. In another paper on flaking, Andrew, *et al.*,[20] report that some of their specimens exhibited, in addition to the usual cracks, a number of small "pits" some of which could be identified as very short cracks. It is perhaps of interest to note their belief that these pits tended to form at higher temperatures than did the usual cracks.

21. Summary and Conclusions

This investigation was intended to determine, for the case of a particular type of weld, the temperature-dependence of the time required to achieve isothermal immunization against weld-metal microcracking. It was hoped also that the data could be used to test the reasonableness of the hydrogen-retained austenite hypothesis as an explanation of the phenomenon of microcracking.

Bead-on-plate welds were deposited with AWS-ASTM E6010 electrodes on small pieces of ASTM A285-C plate. About $1^1/_2$ sec after the completion of welding (at which time the temperature was in the vicinity of A_1), the welds were placed in constant-temperature baths which were maintained at a number of temperatures ranging from 1700 to 212° F. After various periods in the baths, they were removed and were quenched in room-temperature water in an attempt to induce microcracking. Subsequently, the specimens were examined for the occurrence of microcracks and in some cases hardness tests were made. In a strict sense, the treatments were not entirely isothermal for, although the specimens were small, an appreciable time was required for their approach to the temperatures of the baths.

The principal results and conclusions may be summarized as follows:

(*a*) During "isothermal" treatment at most temperatures there occurred a brief initial period in which increasing susceptibility, rather than immunization, was fostered. This behavior was completely unexpected. During this period, a maximum degree of susceptibility was developed within the first minute. This was followed by a period of increasing immunization. At most (but not all) temperatures it appeared that complete immunity was accomplished.

(*b*) The time required for attainment of immunity was found to have a maximum value in the case of treatment at 875° F where even 18 hr proved insufficient. At both higher and lower temperatures the required times were shorter.

(*c*) Immunization was found to be especially rapid at the lower temperatures of treatment. In the range from 750 to 212° F, the required time amounted to only a few minutes and appeared to be nearly independent of temperature.

(*d*) Surprisingly enough, only a few cracks were found in welds which were quenched to room temperature directly after the completion of welding, i.e., without intervening isothermal treatment.

(*e*) In general, there appeared to be no correlation between weld-metal hardness and the incidence of microcracking. Indeed, the hardness of the weld metal was found to be nearly independent of the treatment employed. This, presumably, was due to the thermal lag which attended quenching. In all cases it may have caused the bulk of the austenite transformation to occur at temperatures not far below A_1.

(*f*) The rapidity of immunization in the 750–212° F range appears to be consistent with numerous indications that, under practical welding conditions, it is the cooling rate in the low-temperature range which is ordinarily decisive in determining whether or not microcracking will occur. On the basis of the immunization times which were measured, it seems unlikely that a cooling weld would traverse the higher temperatures slowly enough to permit immunization during passage through these temperatures. At the lower temperatures, however, cooling is slower and the required immunization times are sufficiently short to make immunization feasible.

(*g*) Observations *a* and *d* above suggest that the weld metal was nearly immune to microcracking immediately following deposition and that susceptibility developed only during some stage of subsequent cooling. It is suggested that it developed in a range of temperatures not far below A_1. Presumably, the directly quenched welds traversed this range too rapidly to permit the development of susceptibility while the isothermally treated welds traversed the same range sufficiently slowly.

(*h*) The hydrogen-retained austenite hypothesis would appear to be qualitatively consistent with the various experimental findings. The apparent immunity immediately after solidification can be explained by supposing that at this stage the hydrogen was rather uniformly distributed so that dangerous concentrations did not prevail. The period of increasing susceptibility can be explained by supposing that the nearly complete decomposition of austen-

ite at the higher temperatures was attended by a dangerous increase in the hydrogen content of the last vestiges of untransformed austenite. The eventual attainment of immunity can be explained in a variety of ways. These matters are discussed in detail in Sections 11 through 14. Unfortunately, it would appear difficult as yet to use the experimental data to test the hypothesis in a quantitative manner. Thus it must be concluded that, while the hypothesis is not contradicted by the data, its validity has by no means been established. There remains the possibility that other explanations may eventually prove superior.

(*i*) To one who is interested in the mechanism of weld-metal microcracking, perhaps the most interesting observations are those concerned with the existence of an initial period of increasing susceptibility. It would seem necessary to take this evidence into account in attempts to explain the mechanism of microcracking. One wonders if the implications may not prove eventually to apply to the general problem of flaking as well.

References

1. Bland, J., "Effect of 'Quench Time' on Weld Metal," The Welding Journal, **28** (5), Research Suppl., 216-s to 226-s (1949).
2. Flanigan, A. E., "An Investigation of the Influence of Hydrogen on the Ductility of Arc Welds in Mild Steel," *Ibid.*, **26** (4), Research Suppl., 193-s to 214-s (1947).
3. Rollason, E. C., and Roberts, R. R., "Effects of Cooling Rate and Composition on the Embrittlement of Weld Metal," *Jnl. Iron Steel Inst. (London)* **166** (II), 105–112 (Oct. 1950).
4. Flanigan, A. E., Bocarsky, S. I., and McGuire, G. B., "Effects of Low-Temperature Cooling Rate on the Ductility of Arc Welds in Mild Steel," The Welding Journal, **29** (9), 459-s to 466-s (1950).
5. Steinberger, A. W., DeSimone, B. J., and Stoop, J., "Crack Sensitivity of Aircraft Steels," *Ibid.*, **29** (9), 752–764 (1950).
6. Flanigan, A. E., and Kaufman, M., "Microcracks and the Low-Temperature Cooling Rate Embrittlement of Welds," *Ibid.*, **30** (12), Research Suppl., 613-s to 622-s (1951).
7. Steinberger, A. W., and Stoop, J., "Studies of the Crack Sensitivity of Aircraft Steels," *Ibid.*, **31** (11), Research Suppl., 527-s to 542-s (1952).
8. Flanigan, A. E., and Micleu, T., "Relation of Preheating to Embrittlement and Microcracking in Mild Steel Welds," *Ibid.*, **32** (2), Research Suppl., 99-s to 106-s (1953).
9. Warren, W. G., and Vaughan, H. G., "The Initiation of Brittle Fracture at Welded Joints in Steel Structures," *Trans. Inst. of Welding (London)*, **16**, 127–135 (1953).
10. Harris, L. A., Matthiesen, R. B., and Newmark, N. M., "Low-Temperature Bend Test Properties of Bead-on-Plate Welds," *Ibid.*, **32** (12), Research Suppl., 585-s to 599-s (1953).
11. Christensen, N., and Rose, R., "Hydrogen in Mild Steel Weld Deposits," *British Welding Jnl.*, **2** (12), 550–558 (1955).
12. Roberts, R. R., "Welding Heavy Sections of Mild Steel," *Welding and Metal Fabrication*, **21** (12) 63–68 (February 1953).
13. Van der Willigen, P. C., "Microcracks in Weld Metal," *Journal of Scientific and Industrial Research (New Delhi)*, **13A** (1), 26–30 (1954).
14. Cottrell, C. L. M., "Hydrogen-Barrier to Welding Progress," *British Welding Jnl.*, **1** (4), 167–176 (1954).
15. Wooding, W. H., "Welding Air-Hardening Steels," The Welding Journal, **29** (11), Research Suppl., 552-s to 564-s (1950).
16. Dana, A. W., Shortsleeve, F. J., and Troiano, A. R., "Relation of Flake Formation in Steel to Hydrogen, Microstructure, and Stress," *AIME Jnl. Metals*, **7** (8) 895–905 (August 1955).
17. Lefevre, M., "Flakes in Welds," The Welding Journal, **26** (1), Research Suppl., 57-s to 64-s (1947).
18. Andrew, J. H., Lee, J., Mallik, A. K., and Quarrell, A. G., "The Removal of Hydrogen from Steel," *Jnl. Iron and Steel Inst. (London)*, **153** (1), 67P to 113P (1946).
19. Bennek, H., Schenk, H., and Muller, H., "Die Entstehungsursache der Flocken im Stahl," *Stahl. u. Eisen* (Mar. 21, 1935). (Cited in Reference 17.)
20. Andrew, J. H., Lee, H., Lloyd, H. K., and Stevenson, N., "Hydrogen and Transformation Characteristics in Steel," *Jnl. Iron and Steel Inst. (London)*, **156**, 208–253 (1947).
21. Dubovoi, V. Ya., *Flakes in Steel*, Metallurgizdat, Moscow (1950).
22. Sims, C. E., "The Behavior of Gases in Solid Iron and Steel," *Gases in Metals*, Am. Soc. for Metals (1953).
23. Nosyrieva, S. S., "Mechanism of Formation of Flakes in Steel," *Stal*, **7** (1), 49–52 (1947).
24. Cottrell, C. L. M., "Effect of Hydrogen on the Continuous Cooling Transformation Diagram for a Mn-Mo Steel," *Jnl. Iron and Steel Inst. (London)*, **176** (3), 273–282 (1954).
25. Cottrell, C. L. M., "Weldability of a Boron-Molybdenum Steel Related to Properties of the Heat-Affected Zone," *British Welding Jnl* **1** (7), 315–321 (1954).
26. Houdremont, E., and Heller, P. A., "Hydrogen as an Alloying Element in Steel and Cast Iron," *Stahl u. Eisen*, **61**, 756–760 (1941).
27. Aplett, W. R., Poole, L. K., and Pellini, W. S., "The Continuous Cooling Transformation of Weld Heat-Affected Zones," The Welding Journal, **31** (9), Research Suppl., 421-s to 430-s (1952).

FACTS ABOUT THE WELDING RESEARCH COUNCIL

• The Council operates on annual subscriptions, has no capital and makes no profit.

• More than 600 leading scientists and engineers are affiliated with the work of the Council.

• Some 30 laboratories in this country and Canada participate in the research programs.

• Total value of the work cleared through the various publications of the Council amounts to more than one and a half million dollars a year.

• Total cash budget of the Council is well over $500,000.

• Exchanges reports with the British Welding Research Association.

* * * * *

The regular publications of the WRC are as follows:

• *Welding Research.* This publication is printed monthly and includes practically all the completed reports of the various project committees of the Council and affiliated research work.

• *Reports of Progress.* A photo-offset Progress Reports Series issued monthly contains reports of progress on uncompleted researches, proposed programs of research, translations of important articles, and other pertinent information helpful to research worker and subscriber.

• *Welding Research News.* This is a bi-monthly printed four-page news letter containing condensed interpretive summations of results of completed researches.

• *Bulletins.* These Bulletins are published at irregular intervals and contain important papers presented before engineering societies, and other important papers which are not published in Welding Research.

• *Welding Research Abroad.* A quarterly publication aimed at keeping Americans informed of the latest research developments abroad and the activities of the International Institute of Welding.

* * * * *

For further information address: W. Spraragen, Director, Welding Research Council, 29 W. 39th St., New York 18, N. Y.

EFFECT OF TEMPERATURE ON THE FRACTURING BEHAVIOR OF MILD STEEL

Strength, energy-absorbing capacity, ductility, and amount of gradual tearing preceding brittle crack propagation by cleavage are among the fracture properties observed at various temperatures

BY J. D. LUBAHN

ABSTRACT. Four-in. SAE 1020 steel plate was tested in various ways and various fracture properties were observed: strength, energy-absorbing capacity, ductility (local plastic strain preceding crack initiation), and amount of gradual tearing preceding brittle crack propagation by cleavage. Each property was measured for various temperatures, loading rates, and biaxialities for both notched and unnotched specimens cut in both the rolling and thickness directions of the plate.

At temperatures above +150° C the ductility, strength, and energy-absorbing capacity are large and the crack propagates entirely by gradual tearing (fibrous). As the temperature is lowered, sudden crack propagation by cleavage appears and the energy-absorbing capacity begins to fall. At +30 to −40° C, depending on the loading rate, fibrous fracture has disappeared and the energy values are quite low, but the strength is still good and the ductility is still 50%, even in notched specimens. The ductility becomes very small at −100 to −180° C, depending on strain rate, biaxiality and presence of a notch (triaxiality). The slow notch bend strength, based on crack initiation, rises continuously with decreasing temperature to −150° C and then drops off slightly. At temperatures below −80° C, complete separation occurs when the first crack appears. At all higher temperatures, the bending load rises while the crack gradually tears open, resulting in a fictitious "strength" value if one bases strength on maximum load. Maximum load is 50% higher than the load for crack initiation for temperatures above about −20° C.

The notch bend ductility is the same as the biaxial unnotch bend ductility in the neighborhood of room temperature, but much less at −60 to −120° C. This result is discussed in terms of triaxiality (tension in all three principal directions) and the location of crack initiation.

The ductility in the normal direction is much lower and more erratic than in the rolling direction, but the strengths in the two directions are essentially the same except below −150° C.

The results show that "transition temperature" in a Charpy impact test is related to the temperature range where the metal is losing its ability to gradually tear (without cleavage), while "transition temperature" in an unnotched impact bend test is related to the temperature range where the metal is losing its ductility. The latter temperature is about 100° C lower than the former one.

There is nothing about these particular test results to indicate that mild steel would be either weak or brittle at temperatures above −50° C, that is, under normal conditions of service. Catastrophic service failures are discussed in terms of other factors not present in these tests, such as size, notch sharpness and secondary loads.

J. D. Lubahn, is associated with General Engineering Laboratory, General Electric Co., Schenectady, N. Y.

Introduction

The fracturing behavior of metals may be considered as having two aspects—crack initiation and crack propagation. Crack initiation behavior is expressed in terms of "ductility," or the plastic strain preceding the appearance of the first crack. In the following, ductility values will be expressed as the conventional strain (change in gage length/initial gage length) in the direction of the largest principal stress. The crack propagation behavior has often been expressed in terms of energy absorption or appearance (texture) of the fracture surface—thus, in the case of mild steel, the relative amounts of "cleavage" and "fibrous" fracture. In this report the crack propagation behavior will be described in terms of the distance to which gradual tearing proceeds before sudden crack propagation by cleavage sets in. Both ductility and crack-propagation behavior are affected by a number of variables, including temperature, strain rate and stress state (relative magnitude of the three principal stresses).

The primary objective of this investigation was to observe ductility and mode of crack propagation as a function of temperature for several kinds of tests which subject the metal to different combinations of the above variables. A secondary objective was to obtain a better understanding of the nature and significance of the notched bar impact test. It should be possible to describe the behavior of metal in an impact test in terms of the effects of stress state and strain rate on the fracturing behavior, because the impact test differs from the tensile test primarily in terms of these two factors.[1]

Some of the literature is concerned with the initiation of the crack, some with the propagation of the crack and some with the general behavior of metals in impact tests. McGregor and Grossman[2] were primarily concerned with the circumstances which would cause the crack to begin with practically no prior plastic deformation. Pellini[3, 4] has shown that the mode of crack propagation is similar in different kinds of tests for a given temperature. Typical of papers concerned with the general behavior of metals in a notched bar impact test is the one by Low and Zeno.[5] This investigation shows that the temperature at which the energy drops off is lowest for square unnotched specimens, slightly higher for a double width (biaxial) specimen, and considerably higher for specimens notched in various ways. The conclusion from these experiments was that the metal becomes "brittle" at a slightly higher temperature if the stress is biaxial, and at a *much* higher temperature if the stress is triaxial (that is, if the specimen contains a notch or a crack).

Kahn and Imbembo[6] concluded that the sudden decrease in energy with temperature was due entirely to the appearance of cleavage fracture, since the energy associated with the beginning of the crack was practically independent of temperature in the range of temperatures where the total energy dropped off suddenly. They found that the energy to propagate the crack may be as large as that to initiate the crack, and other tests[7] show that the crack-propagation energy may be several times as large as the crack-initiation energy.

Material

The material used was hot-rolled SAE 1020 steel plate 4 in. thick (0.22% C). From a superficial inspection of the square piece of plate, it was not obvious which was the rolling direction. Consequently, metallographic sections were cut perpendicular to the surface of the plate and parallel to the two edges. There were no differences except for the nonmetallic inclusions. The smaller inclusions were round in both sections. Of the larger inclusions, there were many more elongated ones in one section than in the other, and so this section was assumed to be in the rolling direction. The shape distributions for the two sections were as follows:

Approximate ratio of maximum to minimum dimension	—*Number of inclusions*— *Section parallel to rolling direction*	*Section parallel to transverse direction*
1	33	64
1 1/2	26	21
2	14	14
3	13	3
4	8	0
5	5	1
10	4	0
	103	103

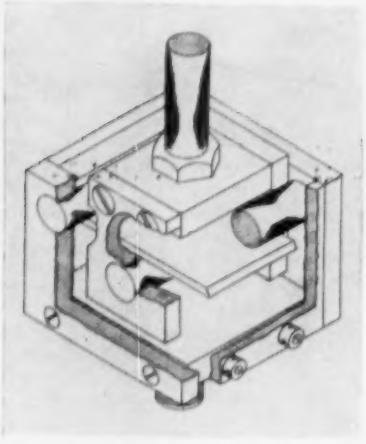

Fig. 1 Unnotch bend test fixtures for use in a furnace or liquid bath

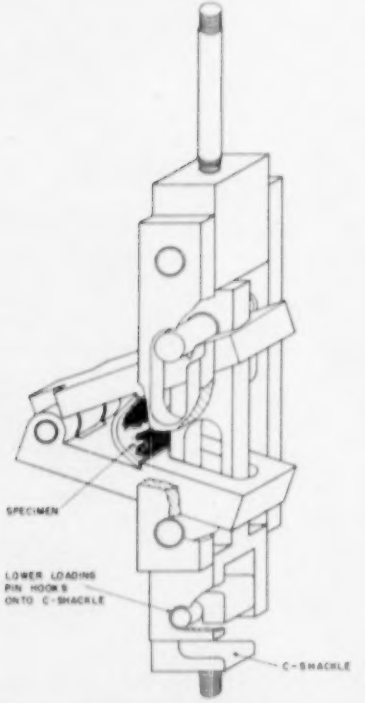

Fig. 2 Unnotch bend fixture for large strain

Rough preliminary tests (8) at room temperature on wide, unnotched bend specimens cut in various directions showed that the ductility in the normal direction is considerably less than the ductility in either direction parallel to the plate surface and that the ductility in the rolling direction was slightly larger than in the transverse direction.

Previously[7] it was found that the crack might begin high up on the root radius, instead of at the very bottom of the notch, if the ductility in the thickness direction of the notched beam was small compared to the ductility in the long direction of the beam. To avoid this difficulty in the rolling direction specimens, the notch was cut so that its long direction was in the normal direction of the plate, rather than in the transverse direction. The normal direction specimens had the long direction of the notch in the rolling direction.

Test Procedure

Six kinds of tests were made as a function of temperature. Details of the equipment and testing techniques are described elsewhere.[8]

1. Tensile tests were made on 1/4-in. threaded-end specimens. A 1-in. fillet radius insured that fracture would occur in the cylindrical portion, even where the ductility was very small. For specimens with large ductility, the diameter change after fracture was converted to axial strain by using the constant volume condition. For brittle specimen, the ductility was taken as the offset from an extension of the linear portion of the stress-strain curve.

2. Unnotched bend specimens 3/16 in. thick by 2 in. wide were used to determine ductility under conditions of plane strain (zero strain in the axial direction). These dimensions yield a biaxiality equal to Poisson's ratio in the elastic region and a biaxiality of essentially 0.5 in the plastic region according to data of Sachs, *et al.*, on bend tests of aluminum alloys.[9] The tests were made in special fixtures, shown in Figs. 1 and 2, which permitted the entire assembly to be lowered into a furnace or liquid bath and supplied a suitable means of applying the load. At the higher temperatures, the test was interrupted from time to time to examine the surface of the specimen for cracks and to measure the curvature. The curvature gage is described in Reference 19. The gage measures the distance between the arc of a circle and a chord over a chord length of 0.15 in. Reference 8 shows that this chord length was short enough to insure reliable values of curvature. Curvature was converted to strain using the bending analysis of Lubahn and Sachs.[10] Ductility was taken as the strain at which the "first crack" appeared.

At temperatures above approximately −75° C, the crack begins to open up in a very gradual and unobstrusive fashion (see also Reference 11). Consequently, for purposes of stating a ductility value, it was necessary to come to an arbitrary decision as to the point where "the crack begins." Part of the difficulty of determining when a crack begins is due to the orange-peeled surface which develops in the early stages of bending (Fig. 3). The first markings to disturb the orange-peeled surface are about as long as the grain size. They resemble cracks, but usually do not have any appearance of depth. As the deformation proceeds, they do not continue to get deeper, but rather, spread out into broader and broader "troughs" or

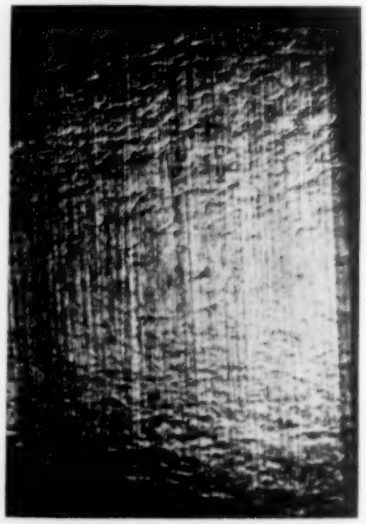

Fig. 3 Photograph of tension surface of unnotch bend specimen after considerable plastic flow, showing "orange peel"

"furrows." Eventually, short troughs begin to join together into longer ones, and at about the same time, an appreciable appearance of depth may develop, as judged by the blackness. The first shallow grooves may be merely the splitting of the hard skin due to machining.[7] Consequently, ductility was taken to be the strain at which the crack began to have an appearance of significant depth. Such a ductility value is not only arbitrary, but also uncertain. A typical degree of uncertainty might be: 25% ± 15%. Thus, if one decided arbitrarily that the ductility figure should be given as 25%, one should also admit that this ductility value might conceivably be as little as 10% or as large as 40%. In this particular example, if one had examined the surface at 10% strain, it would be highly unlikely that anything remotely resembling the beginning of a crack could be found. At the other extreme, if one examined the specimen at a "strain" of 40%, one would find at least one very obvious, deep, gaping crack. By this time, of course, one cannot properly speak of strain at all, because the extension between gage marks is partly due to the gaping open of cracks.

At temperatures above −75° C, the occurrence of these gradually tearing cracks could also cause the apparent ductility in tensile tests to be too high, because of additional contraction of diameter while the crack gradually opens up on the axis. This phenomenon has been called the "rim" effect[21] and has been shown to cause considerable error in ductility[19] in certain cases. Reference 8 shows, however, that the rim effect is not a source of error for the conditions of this investigation.

At temperatures below −75° C, no gradual tearing was observed prior to complete, sudden rupture by cleavage. At these temperatures, the ductility value was not subject to the above uncertainties. It was determined by measuring curvature over a 0.15-in. chord length adjoining the fracture on each side, and averaging the two corresponding values of strain. Reference 8 shows that there is a negligible error due to measuring average strain over two adjacent, finite gage lengths instead of the zero-gage-length strain at the fracture location.

For ductility values less than 1%, the curvature gage is not sensitive enough to give a satisfactory value. In this case, an attempt was made to estimate the ductility by using the breaking load and the stress-strain curve from the tensile test.[8] Ductility values so obtained are open to question because the analysis assumes uniform flow proceeding inward from the tension surface, whereas actually the deformation of mild steel proceeds by the propagation of wedge-shaped Lüder's bands with elastic material between.

In a few cases, fracture did not occur at the location of maximum strain (Fig. 7). In this case, two ductility values were reported for the test: (*a*) the ductility at the fracture site, and (*b*) "greater than" the maximum strain in the specimen. The latter values are shown in the graphs as data points with arrows pointing upwards.

3. Square, unnotched slow bend tests were made to determine the ductility under uniaxial tension, for comparison with the value obtained from a tensile test. According to Sach's data on aluminum alloys,[9] the biaxiality at mid-width of a square bend test is much smaller (0.2) than in wide bend tests (0.5). Actually, the square bend test is in uniaxial test since the fracture begins at the corners (see Appendix). These narrow specimens were bent, measured, and analyzed in the same fashion as the wide ones except for a slight modification of the fixtures.[8]

4. A few narrow bend specimens were broken in the impact machine in order to estimate the effect of loading velocity on the uniaxial ductility. Ductility was measured after fracture using the curvature gage in the same manner as in the slow bend tests. The striking velocity for a Charpy impact machine is 17.4 fps; this is about 250,000 times the characteristic crosshead speed in slow notched bend tests.

5. Slow notched bend tests on standard V-notch Charpy impact specimens were performed in special fixtures similar to those for unnotched bending.[8] The notched bend tests were performed sometimes continuously and sometimes with interruptions to measure strain and examine the bottom of the notch for cracks.

At temperatures below −75° C, ductility was determined by measuring the local strain at the bottom of the notch from time to time, plotting against load, and extrapolating to the breaking load (Fig. 4). The local strain at the bottom of the notch was determined from the measured bend angle as described in a previous paper.[12] In the few cases where fracture occurred at a load lower than the highest preceding load (as much as 5% less), the ductility was taken as that measured after the previous loading.

At temperatures above approximately −75° C, an uncertainty existed regarding the beginning of cracking, similar to that encountered with un-

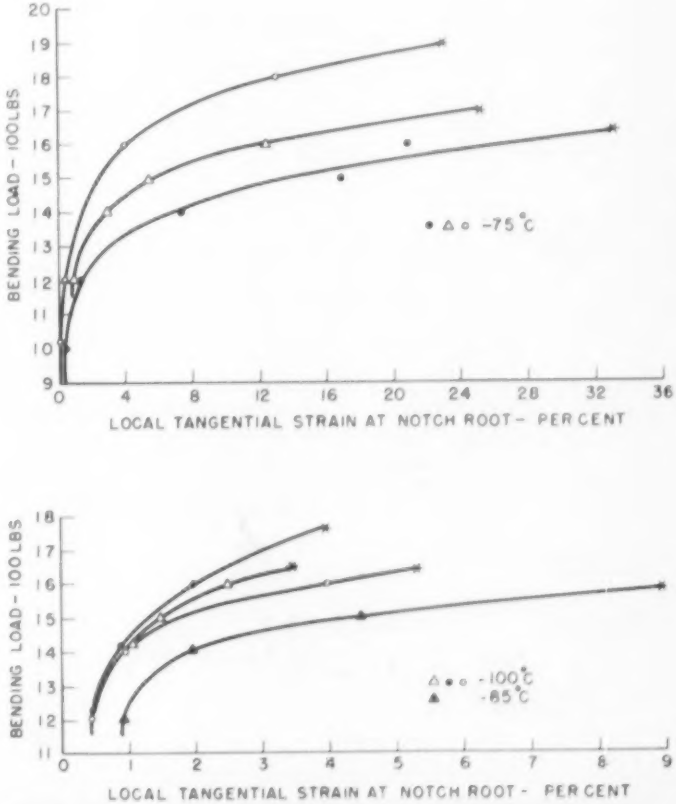

Fig. 4 Examples of curves of load vs. notch strain, showing extrapolation to failure

Fig. 5 Microsection of notch bend specimen showing crack at notch root. X 100. (Reduced by $^2/_3$ upon reproduction)

notched specimens. However, certain differences are worth noting. In the notched specimens, the cracks sometimes had the appearance of beginning below the surface, or at least having a wider opening at a point below the surface than at the surface (see Fig. 5 and Reference 8). Also, the notched specimens sometimes developed cracks with considerable depth at a time when the cracks were only one grain long, whereas in the unnotched specimens, the cracks generally did not exhibit appreciable depth until several smaller cracks had joined together.

In some tests, load and deflection measurements were made continuously (without interruption for strain measurements) and total energy was obtained by integration, thus making possible a comparison with the Charpy V-notch impact energy.

6. Standard V-notch Charpy impact specimens were broken in an impact tester. These specimens were brought to a temperature slightly farther from room temperature than the desired test temperature, in order to allow for the change in temperature while transferring the specimen from the bath or furnace to the impact machine. The temperature change following removal from the bath or furnace was found to be $^1/_4$° F/sec/100° F temperature difference from room temperature. The methods of obtaining the various temperatures are described in Reference 8.

Results

Figure 6 summarizes the ductility values from the tensile tests and the narrow

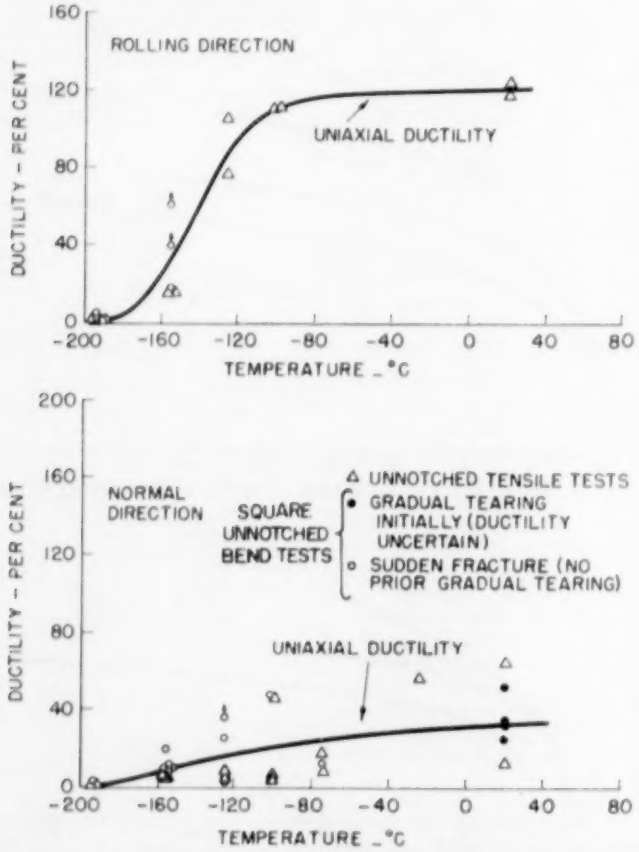

Fig. 6 Effect of temperature on the uniaxial ductility of mild steel. Ductility in a tensile test is local axial strain; in a bend test, ductility is local tangential strain

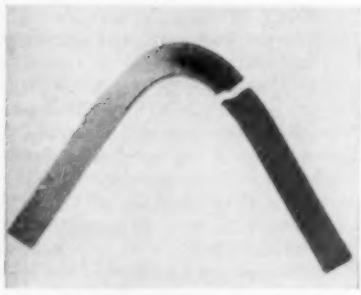

Fig. 7 Fractured unnotched $^3/_{16}$ in. square bend specimens tested at −125° C. Normal direction

unnotched slow bend tests. For specimens in either the rolling or the normal direction, the ductility changes but little as the temperature is lowered from room temperature to about −100° C. Below this point, the ductility drops rapidly with temperature until it reaches zero rather abruptly at approximately −180° C. This temperature will be called the "brittle temperature." (For uniaxial tests it is difficult to estimate exactly the brittle temperature because temperatures between −155 and −195° C were not obtainable with the procedure used.) This general variation of uniaxial ductility with temperature has been observed previously by Eldin and Collins.[13]

The variation of ductility with temperature is qualitatively the same for both the rolling and the normal directions, but the level of ductility for the normal direction is consistently smaller by a factor of 3 or 4, and also the scattering is much greater for the normal direction. In the rolling direction, the scattering may be a factor of 2 or 3, particularly at temperatures where the ductility is changing rapidly. For the normal direction the scattering is so large (sometimes as much as a factor of 20) as to make the drawing of a trend curve almost unjustified. The great degree of scattering is illustrated by the test of Fig. 7. In this single specimen, the ductility at the maximum curvature must be greater than the measured strain of 37%, while the ductility at fracture was only 2%.

Although the amount of scattering makes the conclusion somewhat uncertain, it appears that the ductility in tensile tests is the same as that in square, unnotched bend specimens, for temperatures above −195° C. This result is expected, since both types of tests represent uniaxial tension. The agreement between ductility values in these two types of tests has also been noticed by Barlow.[14]

At the two lowest test temperatures, where the ductility is becoming quite small, there is a tendency for the uniaxial ductility in the narrow bend test

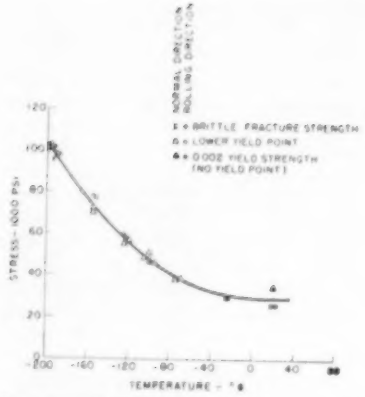
NORMAL DIRECTION
ROLLING DIRECTION
● = BRITTLE FRACTURE STRENGTH
Δ = LOWER YIELD POINT
▲ = 0.002 YIELD STRENGTH (NO YIELD POINT)
STRESS - 1000 PSI
TEMPERATURE - °F

Fig. 8 Effect of temperature on the deformation resistance of mild steel

Table 2—Ductility Values at Low Temperatures, %

Rolling direction, ° C	*Slow tensile test*	*Fast narrow bend test*	*Slow narrow bend test*	*Slow wide bend test*
−155	14	1.0	>21	3.0
	15	1.0	25*	
			>62	
			17*	
			>39	
−195	0.2		1.0	0.3(0.14†)
	0		2.0	0.3(0.16†)
	2.0			
	0.4			
Normal direction, ° C				
−155	7	0.3	7	1.3
	3	1.0‡	9	2.0
	6	1.3‡	9	1.3
	3		10	
			20	
−195	0		1.0	0(0.13†)
	0			0.3

* From the same specimen.
† Calculated from load and stress-strain curve.
‡ Four-tenths in. square instead of 3/16.

to be larger than that in the tensile test (Table 2). At −195° C, for example, the ductility in the narrow bend test was consistently 1% or more for both the rolling and the normal directions whereas in the tensile tests, the ductility was only a small fraction of a percent or zero, except for one test.

Apparently, at −195° C tensile specimens behave in either of two distinctly different ways: (*a*) the specimen breaks almost simultaneously with appearance of the first strain; or (*b*) the behavior is characterized by the usual stress-strain curve having a yield point, with fracturing occurring at just about the instant that one would expect the stress-strain curve to begin rising again. In other words, the ductility is either zero or equal to the yield point elongation (see also Reference 15).

At the low temperatures shown in Table 2, the uniaxial ductility continues

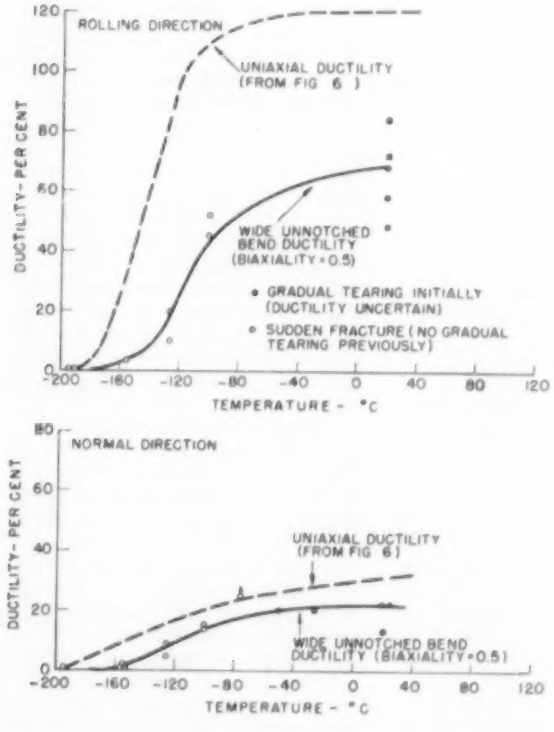
ROLLING DIRECTION
UNIAXIAL DUCTILITY (FROM FIG 6)
WIDE UNNOTCHED BEND DUCTILITY (BIAXIALITY = 0.5)
● GRADUAL TEARING INITIALLY (DUCTILITY UNCERTAIN)
○ SUDDEN FRACTURE (NO GRADUAL TEARING PREVIOUSLY)
DUCTILITY - PER CENT
TEMPERATURE - °C
NORMAL DIRECTION
UNIAXIAL DUCTILITY (FROM FIG 6)
WIDE UNNOTCHED BEND DUCTILITY (BIAXIALITY = 0.5)
DUCTILITY - PER CENT
TEMPERATURE - °C

Fig. 9 Comparison of uniaxial and biaxial ductility for mild steel at low temperatures. Biaxial bend specimens are 2 in. wide x 3/16 in. deep

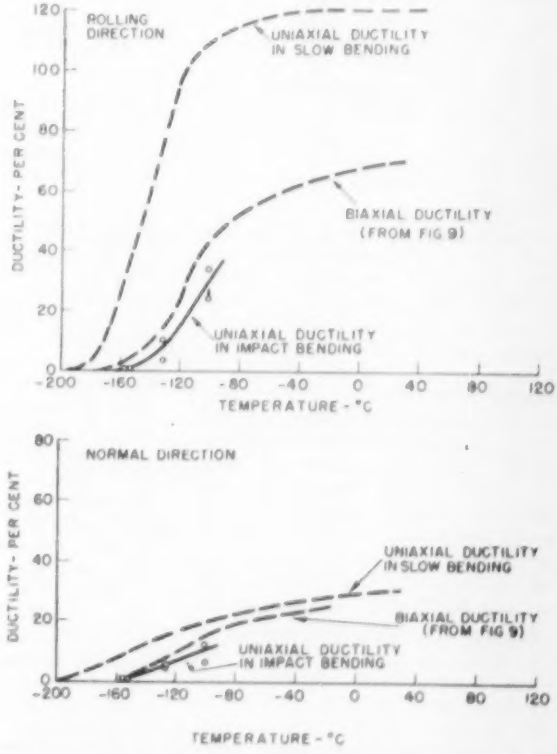
ROLLING DIRECTION
UNIAXIAL DUCTILITY IN SLOW BENDING
BIAXIAL DUCTILITY (FROM FIG 9)
UNIAXIAL DUCTILITY IN IMPACT BENDING
DUCTILITY - PER CENT
TEMPERATURE - °C
NORMAL DIRECTION
UNIAXIAL DUCTILITY IN SLOW BENDING
BIAXIAL DUCTILITY (FROM FIG 9)
UNIAXIAL DUCTILITY IN IMPACT BENDING
DUCTILITY - PER CENT
TEMPERATURE - °C

Fig. 10 Uniaxial ductility of mild steel in unnotched impact bending at low temperatures as compared with slow bending. Three-sixteenths in. square unnotch bend specimens tested in Charpy impact machine

to be considerably different for the rolling and normal directions, but the difference is somewhat smaller than at higher temperatures. The rolling direction has about three times as much ductility as the normal direction at −155° C for either tensile tests or narrow bend tests. At −195° C, the normal ductility is not much lower than the rolling ductility for the narrow bend test; and in tensile tests both directions may show complete brittleness, but the normal direction seems to be more consistently brittle.

Figure 8 summarizes the yield strength values from tensile tests. One of two distinctly different behaviors was observed at the onset of yielding: either a pronounced yield point was observed, or there was no evidence of a yield point at all.* Only 4 out of 22 tensile tests failed to exhibit a definite yield point, and in these cases the strength plotted in Fig. 18 is the stress at 0.2% plastic strain. In 3 tensile tests at liquid nitrogen temperature where there was no measurable ductility, the brittle fracture strength was the same as the yield strength for those specimens which showed some slight ductility. Thus, it appears that brittle fracture occurs when the first plastic flow begins (see also Reference 16). Although there is a pronounced difference in the fracturing characteristics for the rolling direction and the normal direction, Fig. 8 shows that the deformation resistance is essentially the same for these two directions. The yield strength increases tremendously as the temperature is lowered from room temperature to −195° C, by a factor of more than 3 (see also Reference 13).

Figure 9 shows the results of slow bend tests on wide unnotched specimens. The ductility is considerably smaller under this biaxial stress state than under uniaxial tension, particularly for the rolling direction (see also References 9 and 14). The two-to-one loss of ductility with biaxiality at room temperature is about the same as that noted previously by Barlow[14] and by Sachs.[9] As the temperature is lowered, the biaxial ductility diminishes sooner than the uniaxial ductility, so that in the range from −125 to −195° C the biaxial ductility is somewhere between 5 and 10 times smaller than the uniaxial ductility (see also Table 2).

In both the rolling and the normal directions and for both uniaxial and biaxial bend tests, the ductility drops off rather rapidly with temperature to 1% or less. Although the ductility for a given biaxiality is considerably different for the rolling and normal directions at the higher temperatures,

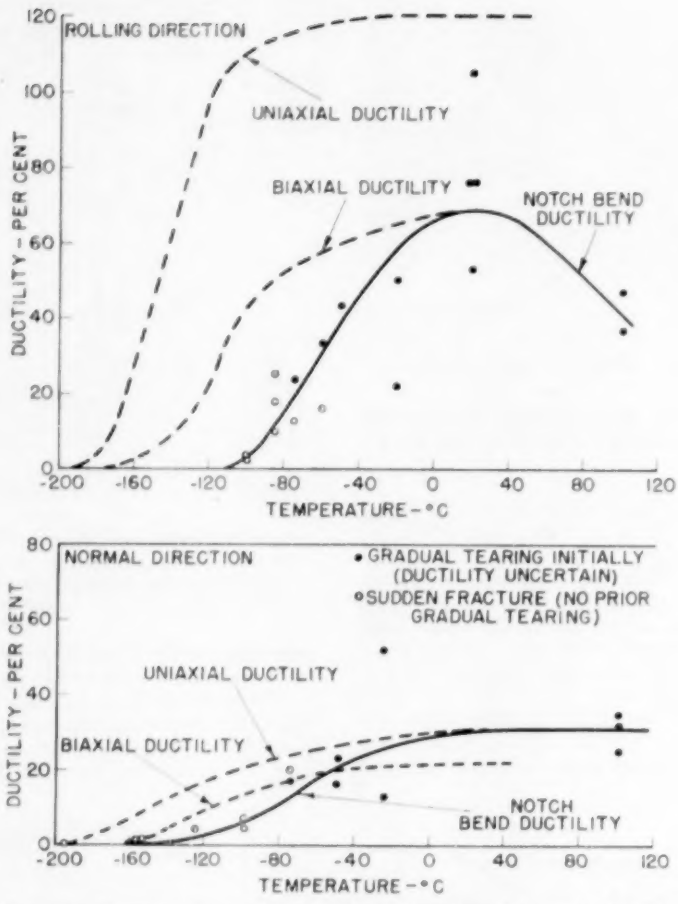

Fig. 11 Comparison of uniaxial, biaxial and notch bend ductility values for mild steel at various temperatures. Notch bend specimens are standard V-notch Charpy impact specimens

the temperature at which the ductility becomes very small (the brittle temperature) is approximately the same for both directions, namely about −155° C for biaxial conditions and −195° C for uniaxial conditions. Thus, for either the rolling or the normal direction, as the biaxiality changes from 0 to 0.5, there is an upward shift of about 40° C in the brittle temperature. MacGregor and Grossman[2] observed about a 30° C rise in the brittle temperature of annealed tool steel as the biaxiality was increased from 0.48 to 1.00. Surprisingly, the brittle temperature in their tests on an annealed tool steel (−195 to −165° C) was essentially the same as for mild steel (−195 to −155° C). Low and Zeno[5] did not measure ductility directly, but if the energy values which they did measure are related to ductility, there appears to be an upward shift of about 25° C in the brittle temperature for the increase of biaxiality which they considered (double-width specimens as compared with square specimens). Sachs' data on duralumin[9] indicates that a change in breadth-to-highth ratio from 1 to 2 corresponds to a change in biaxiality from 0 to 0.25. Thus, Low and Zeno observed about the same shift in brittle temperature per unit biaxiality change as that shown in Fig. 9. MacGregor and Grossman's data on tool steel[2] indicates less temperature shift per unit biaxiality change.

Impact bend tests on square, unnotched bend specimens (Fig. 10) show that there is about as much loss of uniaxial ductility due to a 250,000-times-faster deflection rate as the loss of ductility in slow bend tests due to introducing a biaxiality of one-half. At a given temperature, the unnotched impact bend ductility is greater for the rolling direction (30% at −100° C) than for the normal direction (10% at −100% C). Fig. 10 and Table 2 show that the ductility diminishes to approximately 1% at a temperature of −155° C for both the rolling and normal directions. This temperature is about 40° C higher than the brittle temperature in a slow bend test. Mac-

* Reference 8 gives details of yield point behavior.

Gregor and Grossman[3] also noticed that the brittle temperature for annealed tool steel was considerably higher for a faster deflection rate. However, they observed a considerably larger effect: a 60° C shift of temperature for 3000 to 1 in. rate for tool steel as compared with a 40° C shift in temperature for 250,000-to-1 in. rate for mild steel (Fig. 10).

Figure 11 shows the ductility values obtained from slow notched bend tests. At room temperature, the slow bend ductility in a notched test is not significantly different from that in a wide unnotched test. This behavior is to be expected, since for both specimens the surface biaxiality is one-half and fracture begins at the surface. As the temperature is lowered below room temperature, the notched bend ductility decreases faster than the ductility in the wide, unnotched bend test; for the rolling direction, the notched bend ductility has decreased to a few percent at −100° C, whereas the ductility in the wide, unnotched bend test is still approximately 40%.

Presumably, the reason why the notched bend ductility and the wide, unnotched bend ductility are the same at room temperature but are different at lower temperatures is that the metal becomes more sensitive to triaxial stress as the temperature is lowered. The schematic diagram of Fig. 12 suggests how the sensitivity to triaxiality may influence the relative ductility in notched and unnotched bend specimens. Here triaxiality is defined as the ratio (S_3/S_1) of the smallest principal stress to the largest one. The upper diagram shows hypothetical curves of ductility against triaxiality, where the ductility diminishes almost to zero for a triaxiality of 0.2 if the temperature is low, but it decreases only by 30% if the temperature is high. The two lower diagrams illustrate schematically the behaviors at room temperature and low temperature. The distributions of strain and triaxiality are similar for the two temperatures, but the corresponding ductility distributions, converted from triaxiality by means of the upper diagram, are greatly different, depending upon the shape of the curve in the upper diagram. At room temperature, there is a very slight dip in the ductility corresponding to the given triaxiality peak, while at low temperature there is a very deep ductility dip corresponding to the same triaxiality peak. Any point on these ductility distribution curves represents the limiting strain, or the strain at which fracture would occur, if the actual strain did reach this value. The concept that such a curve exists is illustrated by some unnotched bending data in the Appendix. The lower left diagram for room temperature and low triaxiality sensitivity, shows that the actual strain (E_1) reaches the limiting strain first at the bottom of the notch, while the lower right hand diagram, for low temperature and high triaxiality sensitivity, shows that the actual strain reaches the limiting strain or ductility near the place where the ductility has a minimum. Thus, for a sufficiently high triaxiality sensitivity, fracture begins below the surface, and the surface strain at the instant of fracture is smaller than the (biaxial) ductility at the bottom of the notch.

The existence of a triaxiality peak in notched bend specimens, as shown in Fig. 12, can also be inferred from other investigations. It is known from photoelastic measurements[32] that such a triaxiality peak exists in the elastic region, and it is reasonable to suppose that the restraint which causes this triaxiality also persists in the plastic region and causes similar triaxiality. Soete[17] and Matton-Sjoberg[18] have shown that subsurface cracks start in a plane parallel to the tension surface. Such cracks presumably would occur only if there were tensile stress in the thickness direction of the specimen (triaxiality).

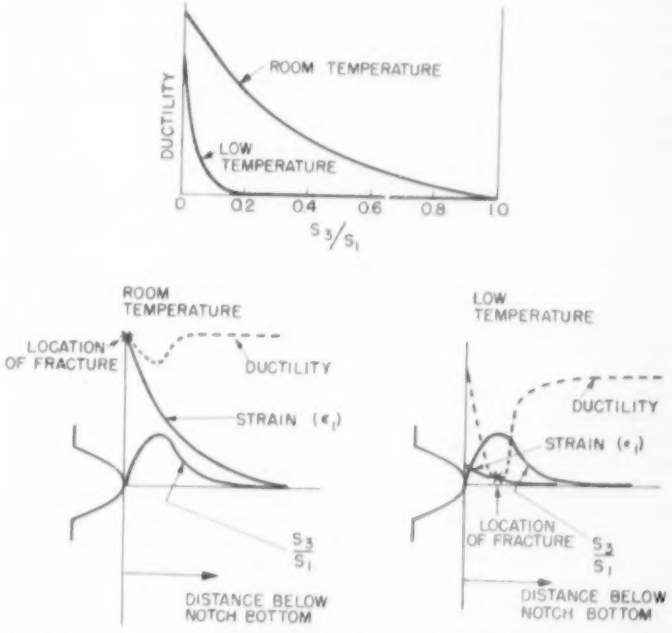

Fig. 12 Schematic diagram illustrating possible differences in stress, strain and ductility distributions in notch bending for high and low temperatures, respectively

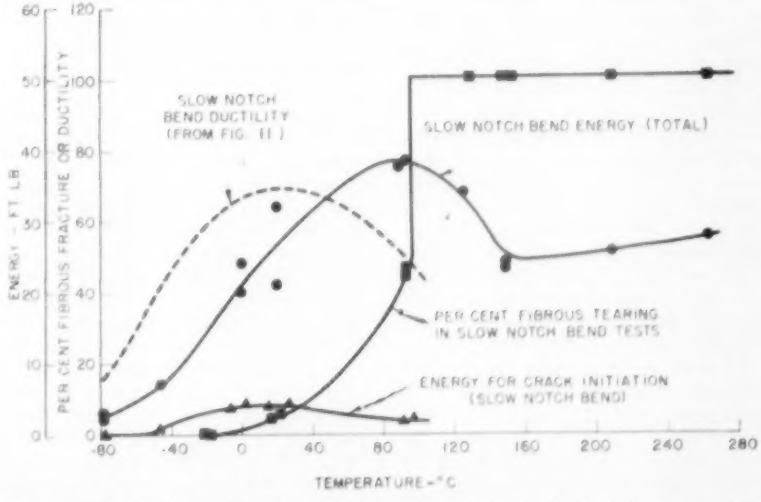

Fig. 13 Comparison of various fracture characteristics derived from the slow notch bend test. Rolling direction

The fact that notched bend ductility may be equal to the wide, unnotched bend ductility under one set of circumstances and greatly different under other circumstances has been observed previously[19] for an alloy steel heat treated to produce two slightly different values of hardness. For both hardnesses, the unnotched bend ductility was greater than 120% for biaxial conditions and the tensile ductility was about 300%. By contrast, the notched bend ductility was only 5% for the somewhat harder condition, and 170% for the softer one.

At −100° C, for the rolling direction, there is a ratio of ductilities for notched and unnotched specimens of more than 10 to 1 (Fig. 11). This is a significantly larger effect of triaxiality than found by Sachs[20] for duralumin. On the other hand, the triaxiality values reached in Sachs' notched tensile tests are not much greater than 0.4, whereas the triaxiality might be as high as 0.6, or even 0.7 in the notched bend test, judging by Brown's photoelastic data.[22] There is also the possibility that mild steel tested at −100° C is simply more sensitive to triaxiality than is duralumin at room temperature.

Figure 13 shows that the energy absorbed in slow notched bend tests gradually decreases with temperature in the temperature range between −80 and +100° C, as commonly observed in notched bar impact bend tests. At temperatures above 100° C, the energy decreases as the temperature is raised. This behavior is not characteristic of typical impact energy curves, and will be discussed presently.

The notch ductility curve has been reproduced in Fig. 13 for comparison with the energy curve. We find that the ductility is not changing very fast in the region of temperature where energy is diminishing rapidly with temperature. In fact, the ductility is decreasing with temperature in a temperature range where the energy is increasing (between 20 and 100° C).

To understand better how ductility is related to energy, the total energy was divided into two parts: that associated with the initiation of the crack and that associated with the propagation of the crack.* Figure 13 shows that energy for crack initiation roughly parallels the ductility. This is not surprising, since energy is roughly proportional to the product of ductility and strength (deformation resistance), and the ductility is much more affected by temperature than is the strength in the temperature range considered. Figure 13 also shows that the energy for crack initiation is only a small part of the total energy and that the energy for crack initiation is not changing much in the range of temperatures where the total energy is falling rapidly. These trends have been noted earlier by Lubahn[7] and by Kahn and Imbembo.[6] Obviously, total energy is not governed primarily by ductility, but rather by the mode of crack propagation. Figure 13 also shows that the depth of fibrous tearing prior to sudden cleavage increases with temperature in a manner very similar to that in which total energy increases. Again we see that the total energy is primarily governed by the mode of crack propagation in the temperature range from −80 to 100° C.

* Reference 8 gives the details of the analysis.

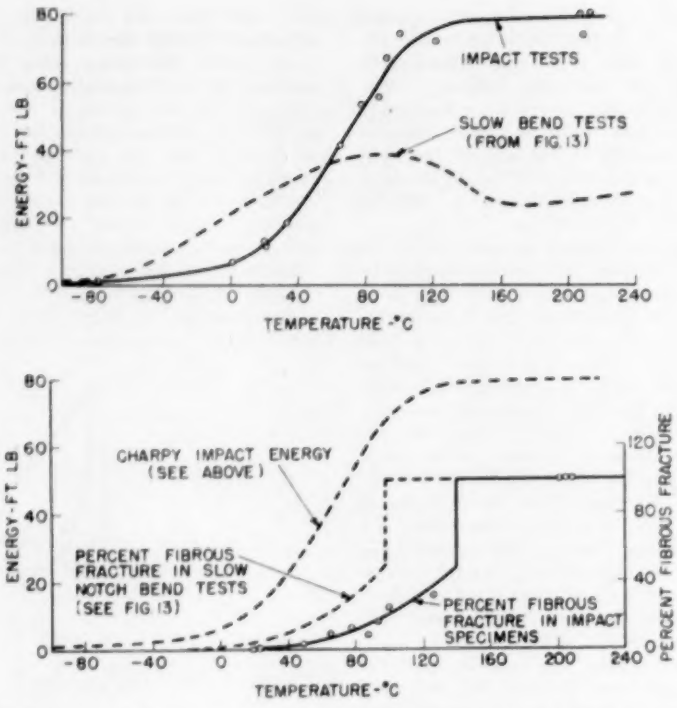

Fig. 14 Comparison of V-notch Charpy impact characteristics with slow notch bend test results

In various investigations described in the literature, it has usually been concluded that fibrous tearing is not existent at a temperature slightly below the so-called "transition temperature," or the temperature at which the energy "diminishes abruptly to a small value." This conclusion is usually based on the appearance of the fracture, which is apparently free of fibrous fracture at temperatures low enough so that the impact energy is small. In this investigation it was likewise observed that there was "100% cleavage" at a temperature (−25° C) where the energy had dropped to only 10 ft-lb (Fig. 13), but it is important to note that there was slight ductile tearing even at temperatures as low as −125° C. This ductile tearing cannot be observed by examining the fracture surface after complete separation, but must be observed with a microscope as small cracks forming at the notch bottom.

Figure 14 shows the results of standard V-notch Charpy impact tests. Between −50° C and room temperature the energy curve for the slow tests is parallel to that for the impact tests and is displaced downward in temperature by about 50° C. This displacement is about the same as for narrow unnotched bend tests (Fig. 10). At temperatures above 50° C, the energy in the slow notched bend test fails to rise with temperature as rapidly as the energy in the impact test. Above 100° C the energy in the slow notched bend test decreases with temperature until finally it is only a third as large as that for the impact notched bend test at 200° C. This difference probably arises because the rate sensitivity increases with temperature until a considerable difference in deformation resistance can occur between fast and slow tests, resulting in a lower load-deflection curve for the slow test and lower energy (the area under the load deflection curve). Data taken by MacGregor and Fisher[21] on mild steel, which has been reduced to rate sensitivity by Lubahn[23], indicates that the probable

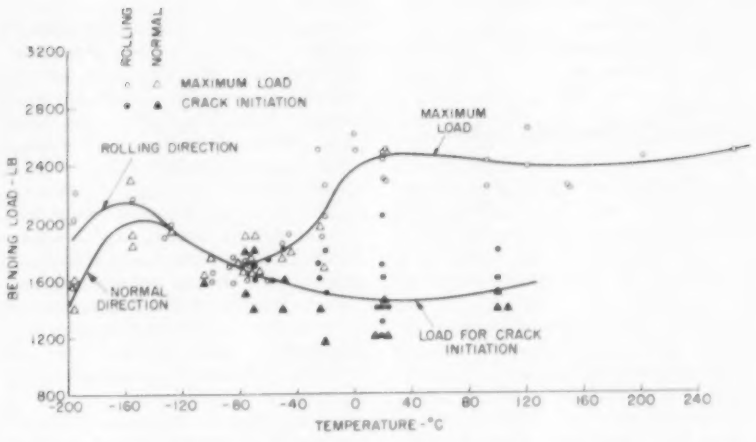

Fig. 15 Bending strength of standard V-notch Charpy impact specimens tested slowly on a 1.575-in. span. Mild steel

rate sensitivity (disregarding the minimum due to strain aging) is 0.07 at 200° C. Using this rate sensitivity, it can be shown[8] that the strength ratio should be 2.4 for the 250,000-to-one difference in rate between the slow notch bend test and the impact notch bend test. This ratio is approximately the same as the energy ratio for the fast and slow tests in Fig. 14.

The lower diagram of Fig. 14 shows that most of the large drop in energy occurs in the same temperature range as that where the mode of crack propagation is changing from fibrous to cleavage. This correlation between the amount of fibrous fracture and the impact energy has been noted repeatedly throughout the literature. In such comparisons, however, it is customary to plot the percentage of fibrous fracture over the entire cross section, rather than the percentage of depth to which fibrous fracture has progressed without cleavage, as in Fig. 14. Figure 14 emphasizes the fact that cleavage fracture *begins* earlier and earlier as the temperature is lowered. The distance to which fibrous tearing can proceed without cleavage may be the criterion for the suitability of the metal in various applications. It seems reasonable to suppose that some additional fibrous tearing at the end of the test, after cleavage has occurred, may be of little benefit if the service application involves some slightly different conditions which would cause the cleavage to result in complete separation of the part.

Figure 15 shows fracture load for the notched bend tests. There are two general kinds of behavior, depending upon the temperature. Above −80° C, the load increases after the crack begins, because of the large amount of strain hardening accompanying the fibrous tearing. The amount by which the load rises after the crack begins becomes larger and larger as the temperature is raised from −80° C to about room temperature, where the maximum load is about 50% higher than the load at which ductile tearing began. Below −80° C, the load for crack initiation equals the maximum load; in other words, the specimen breaks almost immediately as soon as the first crack appears.

It should be clear from Fig. 15 that maximum load is a fictitious and meaningless strength value, and it shouldn't be used as a criterion of fracturing behavior unless the temperature is below about −80° C. Fracture has begun long before, and a deep crack is already present at maximum load. If one considers only crack initiation as the criterion of strength, then it can be seen that the bending strength rises continuously with decreasing temperature in the range where maximum load is decreasing. This increase in strength (for crack initiation) is not nearly so large, however, as the increase in deformation resistance, (Fig. 8), because of the diminishing ductility; as the temperature is lowered from room temperature to −125° C, the yield strength doubles while the load for crack initiation increases by only 30%.

For specimens in both directions, there was loss of strength (for crack initiation) with decreasing temperature only at the lowest temperature investigated.

Only at the very lowest temperatures was there any tendency for the load carrying capacity to be smaller in the normal direction than in the rolling direction. Apparently, the ductility level must be exceedingly low before the ductility differences between the normal and rolling directions (Fig. 11) are reflected in strength differences of any significance.

The strength of notched and unnotched specimens can be compared by converting the bending load to "nominal bending strength" (sometimes also called the "modulus of rupture"). In general, nominal stress is the largest tensile stress which would exist if the specimen were elastic and if no stress raiser were present, and specifically for bending, it is the moment divided by the section modulus under the notch. For unnotched specimens, a value of bending moment can be obtained from the bending load at fracture only if the ductility is sufficiently small that fracture occurs before the specimen pulls through the three-point bending fixture. This was true only for temperatures below −100° C.

The values of nominal bending strength are summarized in Table 3 for the notched bend specimens and the wide, unnotched bend specimens (biaxiality of 0.5 in both types of tests). All the temperatures considered are low enough that separation occurs as soon as the first crack appears. Consequently, the strength values correspond both to maximum load and to crack initiation.

Table 3 shows that the notch bend strength is considerably less than the unnotched bend strength at −195° C, that it is essentially equal to the unnotched strength at −155° C, and that

Table 3—Nominal Bending Strength at Low Temperatures for Notched and Wide, Unnotched Bend Tests

	Rolling direction			*Normal direction*		
Temperature	*Notched*	*Unnotched*	R_n	*Notched*	*Unnotched*	*Yield strength**
−100° C	97,000		0.68	99,000	151,000	48,000
	100,000			106,000	152,000	
−125° C	117,000†	152,000	0.82	118,000	139,000	58,000
		140,000			148,000	
−155° C	130,000†	143,000	1.02	112,000	120,000	72,000
				117,000	121,000	
				139,000	123,000	
−195° C	123,000	142,000	0.58	85,000	140,000	102,000
	133,000	144,000		86,000	153,000	

* Averaged from the data of Fig. 8.
† From the trend curve of Fig. 15.

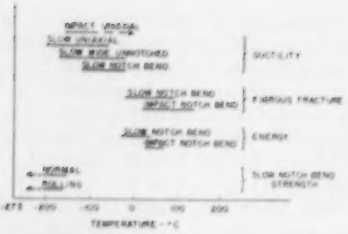

Fig. 16 Range of temperature in which various fracture characteristics decrease from a high value to a low value with decreasing temperature. "Low" means less than 1% ductility, less than 1% fibrous tearing preceding cleavage, and less than 20% of the maximum energy

it is again less than the unnotched bend strength at −100 and −125° C. This behavior is contrary to notch tensile testing experience,[23] which shows that as the ductility increases, the ratio of notched to smooth strength increases continuously from less than unity to greater than unity. By contrast, Table 3 shows that for the normal direction, this ratio (R_n) changes from 0.58 to 1.02 to 0.68 as the temperature and ductility increases.

The above discussion is concerned with the relative strengths of smooth and notched specimens. It is also valuable to consider the notch strength values in relation to the yield strength. If the metal were completely brittle, the unnotched nominal bending strength should be equal to the yield strength and the nominal notch bending strength would be about one-quarter as large as the yield strength, since the stress concentration factor is 4.2 for the specimens being considered here.[24] For the lowest temperature, where the ductility is lowest, the unnotched bending strength is almost 50% higher than the yield strength, and the notch strength is in the neighborhood of the yield strength (somewhat less for the normal direction and somewhat more for the rolling direction). These results indicate that ductility values of 0.1 to 0.3% for unnotched specimens (Table 2), and probable values considerably smaller than these for notched specimens (see Fig. 11) are large enough to permit strength values which are several times the expected strength for complete brittleness.

At −100° C, where the notch bend ductility is in the neighborhood of 5% (Fig. 11), and the unnotched bend ductility is 15–50%, depending on the orientation (Fig. 9), the notch bend strength is twice the yield strength and the unnotched bend strength is three times the yield strength (Table 3). The values can be so high partly because of strain hardening, partly because of the beneficial effect of large plastic deformation on stress raisers, and partly because of the fictitious nature of nominal stress.

Summary: Discussion of Unsolved Problems

The quantities which appear at the moment to best describe the fracturing characteristics are: (1) ductility, (2) depth of initial tearing (prior to cleavage), (3) energy-absorbing ability, and (4) strength, or load-carrying capacity. As the temperature is lowered, all four quantities either remain constant or increase slightly over a certain range of temperature and then drop off rather rapidly to comparatively small values. The temperature at which ductility, energy, etc., begins to fall off with decreasing temperature can be stated with a fair degree of certainty, and if arbitrary definitions are taken of "a very low value characteristic of lower temperatures," then definite values can be assigned to the temperature ranges within which these various quantities decrease markedly. A "low" value will be defined in the following arbitrary way: less than 1% strain to fracture in the case of ductility; less than 1% fibrous tearing before cleavage sets in, in the case of crack propagation. Energy will be considered to be "diminishing rapidly" if the energy is more than 20% away from either the highest or lowest value.

Figure 16 shows that the metal is losing its capacity to absorb energy as the temperature is lowered through a range near room temperature, and that its ability to tear gradually without the appearance of cleavage is disappearing rapidly in about the same temperature region. The metal loses its ductility rapidly in a range of temperature near −100° C., more or less, depending upon the conditions of biaxiality and strain rate. The metal does not even begin to lose its strength until temperatures less than −150° C are reached, even for notched specimens.

The variation of impact energy with temperature is usually used to determine a "transition temperature" according to one of several arbitrary definitions. Most writers presume that "transition temperature" indicates the onset of "brittleness," but they fail to differentiate between the kind of brittleness which means absence of ductility (absence of plastic flow preceding crack initiation) and the kind of brittleness which means sudden crack propagation by cleavage, where no visible plastic flow accompanies the propagation of the crack. It should be clear from Fig. 16 that "transition temperature" defined in terms of energy, is related to crack propagation by cleavage, and is *not* related to the temperature at which the metal fails to show any plastic flow prior to crack initiation. Absence of plastic flow prior to crack initiation is considered by the writer to be true brittleness, in contrast to "brittle crack propagation." Figure 16 shows that brittle crack propagation sets in at temperatures near room temperature, while true brittleness only occurs at temperatures below about −100° C, depending on the strain rate and stress state.

It should now be clear that the term "transition temperature" has different meanings in different technical papers.

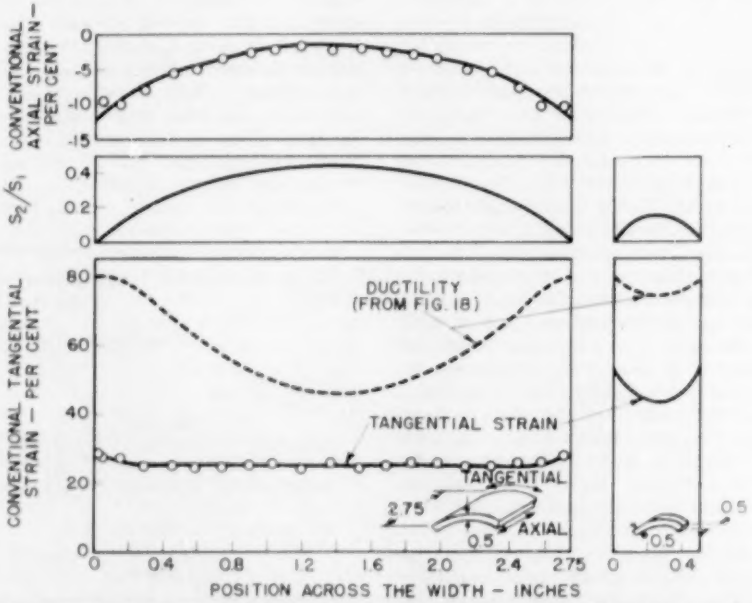

Fig. 17 Conditions of strain and biaxiality and limiting strain for fracture on the tension surface of two bend specimens of $^1/_2$-in. 24SO plate. From Sachs, *et al.*[22]

For unnotched specimens it is related to true brittleness,[2] and in this usage is synonymous with the term "brittle temperature" used above. On the other hand, the term "transition temperature," when applied to the energy absorbed by notched specimens, is usually related to an entirely separate and distinct phenomenon—brittle crack propagation. The "shift of transition temperature" from −130 to +40° C obtained by Low and Zeno[5] by putting a notch in the specimen is not entirely due to the triaxial stress state of the notched specimens, but is primarily caused by a shift in the phenomenon being considered. There *is* a shift in the brittle temperature due to triaxial stress, but the shift is much smaller and in an entirely different range of temperatures than that observed by Low and Zeno. Figure 11 shows that the brittle temperature shifts from −180° C for uniaxial stress to −100° C for the triaxial state of stress occurring in a notched specimen. On the other hand, Fig. 13 shows that a "transition temperature" near room temperature arises from a change in the mode of crack propagation from fibrous to cleavage. Figure 16 indicates that notched mild steel will absorb energy satisfactorily down to temperatures of +100° C, can be plastically deformed satisfactorily down to −40° C, and will carry load satisfactorily down to −160° C. In contrast, many welded mild-steel structures, and even some that did not involve welding, have exhibited distressingly small static load carrying capacities in service at room temperature or slightly below. For example, the S.S. *Schenectady*, which broke in two in quiet water, had only 9000-psi nominal stress in the deck at the time of fracture, and oil well piping of 90,000-psi yield strength minimum has failed at nominal stresses as low as 20,000 psi.[25] Similarly, various other kinds of structures, notably large gas pipes, storage tanks and bridges, have failed under static loading at low nominal stresses. These service failures seem to be incompatible with the test results of Fig. 16. Of course, the test results of Fig. 16 do not involve such factors as large size and welding (with attendant residual stress, etc.); but on the other hand, Wells[26] points out that laboratory tests on various large welded structures have similarly failed to exhibit load-carrying capacities less than 0.78 of the yield strength. In short, neither the static tests of this investigation nor of any other investigation yielded a nominal strength very much lower than the yield strength, while static failures in service have occurred at nominal strengths *much* lower than the yield strength. The only test which has yielded a low nominal strength is the SOD (Standard Oil Development) test.[27] where a secondary impact wedge loading is applied to a notch at the edge of the plate, in addition to the primary static load.

The above considerations raise the question as to what circumstances resulting in low values of nominal strength are present in service but are not present in laboratory tests. One possibility, suggested by the results of the SOD test, is that the service failures were caused by a secondary local impact loading superimposed upon the primary static loading. On the other hand, it is hard to imagine local conditions in large welded mild-steel structures that would be comparable to the conditions in an SOD test at the edge of the plate. A second possibility has to do with the relative size of the whole structure and the local, highly stressed region in which the cleavage crack gets its start. The work of Feeley[27] and Robertson[28, 29] indicates that, once started, crack propagation by cleavage may continue under a comparatively small nominal stress. Investigations of the size effect in mild steel (see References 7 and 30) have indicated that a large region of highly stressed metal is necessary in order to launch a self-sustaining cleavage crack. It is conceivable that a combination of *two* circumstances is the cause of cleavage fracture under low nominal stress: (1) the existence of a highly stressed region which is of sufficient absolute size to generate a cleavage crack capable of proceeding under a low value of nominal stress; and (2) the existence of an amount of material which is large in comparison with the local highly stressed region, and which has a sufficiently low stress that the average stress (or nominal stress) for the entire specimen or structure is much smaller than the yield strength.

In terms of the above concepts, one would envision that laboratory tests of large welded specimens have failed to exhibit low values of nominal strength because the region of high, critical stress was either too large or too small. If the critically stressed region is too small, it will not generate a self-propagating cleavage crack, and if it is too large compared with the whole specimen, the average stress for the whole specimen will not be significantly less than the yield strength.

Either of the two possibilities described above may account for the failure of laboratory tests to simulate the conditions of service that result in low nominal strengths: (1) the necessity for a secondary impact load in addition to the primary static load, or (2) the necessity for having a critically stressed region of optimum size. On the other hand, it is equally probable that neither of these possibilities is the correct one, and that the real conditions leading to low nominal strength in service have yet to be discovered. What these conditions are is the all-important question to be answered today regarding the behavior of mild steel. Although the test results presented in this report have served to clarify several previous misconceptions, they still fail to answer this all-important question.

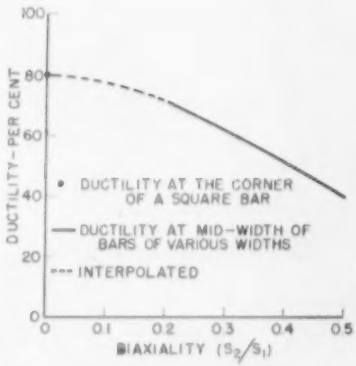

Fig. 18 Effect of biaxiality on the ductility of $^1/_2$-in. 24SO plate. From Sachs, *et al.*[33]

APPENDIX

Strain Analysis of Unnotched Bending Specimens

The following data illustrate the usefulness of the concept that fracture occurs where the actual strain first reaches the limiting strain for fracture, or where the metal first "runs out of ductility." This limiting strain depends on the local conditions of strain rate, stress state, etc., and is not affected by the strain or conditions elsewhere.

Figure 17 shows strain analyses for two unnotched bend specimens—one square ($w/h = 1.0$) and the other side compared to the thickness ($w/h = 5.5$). From the measured axial and tangential strains, the biaxiality (axial stress divided by tangential stress) can be found from the Von Mises condition:

$$\frac{S_a}{S_t} = \frac{2(\epsilon_a/\epsilon_t) + 1}{2 + (\epsilon_a/\epsilon_t)}$$

where ϵ is logarithmic, or natural, strain. Figure 17 shows that the biaxiality reaches almost 0.5 at mid-width for $w/h = 5.5$, while the maximum biaxiality in the square bar is comparatively small.

For each value of biaxiality across the width of the specimen there will be a corresponding ductility, or limiting strain that will cause fracture. Figure 18 shows such ductility values, as derived from bend test results.[9, 33] Using Fig. 18, the biaxiality distributions of Fig. 17 can be converted to ductility distributions, shown dashed. Both specimens have zero biaxiality at the corners, and therefore the same duc-

tility. The narrow specimen has only a small biaxiality at the center, and therefore, only a slight loss of ductility; the wide specimen attains a biaxiality of almost 0.5 at mid-width, where the ductility is not much over half that at the edges.

If the tangential strain were uniformly distributed across the width, failure at mid-width would be expected, because the ductility is least at that point. The tangential strain is not uniformly distributed, however. The tangential stretching on the tension side causes a tendency for axial contraction, and the tangential contraction on the compression side causes a tendency for axial spreading. These tendencies, if unrestrained, would cause transverse bending opposite to the primary tangential bending, resulting in a saddle-shaped tension surface. In the wide specimen, the inherent stiffness of a curved plate prevents this transverse bending, except at the unrestrained edges, where a slight "curling" occurs. Because of this curling up, the metal at the edges is stretched around a slightly larger circle, and therefore has more strain (Fig. 17). The square bar is not restrained against this transverse bending. It develops considerable curvature in the axial direction, with the result that the tangential strains are considerable higher at the edges than at the center.

Summarizing: if the tangential strains were uniform across the width, fracture would occur at mid-width because of the higher biaxiality; and if the biaxiality were uniform across the width, fracture would occur at the edges because of the higher tangential strain. What actually happens depends on the relative magnitude of these two effects. Figure 17 shows that the biaxiality effects predominate in the wide specimen, so that the metal first runs out of ductility at mid-width; while the nonuniformity of tangential strain is the predominating feature in the square specimen, with the result that the metal first runs out of ductility at the edges. Consequently, one would expect the first cracks to occur near mid-width of the wide specimen and at the corners of the square bar. The observations[33] confirmed this expectation.

References

1. Hollomon, J. H., "The Notched-Bar Impact Test," *Trans. AIME*, **158**, 298 (1944). Also *Welding Research Supplement* (April 1945).
2. MacGregor, C. W., and N. Grossman, "Dimensional Effects in Fracture," *Welding Research Supplement*, **42** (1) 20 (January 1952).
3. Pellini, W. S., and Hartbower, C. E., "Explosion Bulge Test Studies of the Deformation of Weldments," THE WELDING JOURNAL, **30**, (6) Research Suppl., 307-s (1951).
4. Pellini, W. S., "Evaluation of the Significance of Charpy Tests," ASTM Symposium on Effect of Temperature on the Brittle Behavior of Metals, with Particular Reference to Low Temperatures, ASTM Special Tech. Pub. No. 158 (1954), p. 216.
5. Low, J. R., and R. S. Zeno, "The Effect of Variation in Notch Severity on the Transition Temperature of Ship Plate Steel in the Notched Bar Impact Test," *Welding Research Supplement* (March 1948).
6. Kahn, N.A., and E.A. Imbembo, "Notch-Sensitivity of Ship Plate—Correlation of Laboratory-Scale Tests with Large-Scale Plate Tests," Symposium on Deformation of Metals as Related to Forming and Service, ASTM (1948).
7. Lubahn, J. D., "Room Temperature Crack Propagation and Size Effect in Mild Steel," THE WELDING JOURNAL, **34** (10), Research Suppl., 518-s to 528-s (October 1955).
8. Lubahn, J. D., "The Effect of Temperature on the Fracturing Behavior of Mild Steel," General Electric Company Research Lab. Report No. 56-RL-1508 (April 1956).
9. Sachs, G., Sangdahl, G. S., Jr., and Aul, E. L., "An Investigation of the Stress and Strain States in Bending Rectangular Bars," *Proc. Soc. Exptl. Stress Anal.*, **6** (1), 1 (1948).
10. Lubahn, J. D., and Sachs, G., "Bending of an Ideal Plastic Metal," *Trans. ASME*, 201 (February 1950).
11. Friedman, Ya. B., and Zilova, T. K., "Process of Fracture of Plastic Metals," *Doklady Akad. Nauk SSR*, **73**, 697–700 (1950).
12. Lubahn, J. D., and Lequear, H. A., "Root Conditions in a V-Notch Charpy Impact Specimen," *Welding Research Supplement*, **XXI**, 585-s (1954).
13. Eldin, A. S., and Collins, S. C., "Fracture and Yield Stress of 1020 Steel at Low Temperatures," *J. Appl. Phys.*, **22**, 1296 (1951).
14. Barlow, D. A., (Aluminum Laboratories Limited) "Yield Criteria and the Bending of Wide Beams," *J. Mech. and Phys. of Solids*, **2**, 259–264 (1954).
15. Hollomon, J. H., and Zener, C., "Problems in Fracture of Metals," *J. Appl. Phys.*, **17**, 82 (1946).
16. Zener, C., "The Micro-Mechanism of Fracture," Fracturing of Metals, ASM, Cleveland (1948), p. 3.
17. Soete, W., "Transverse Strength and Brittle Fracture," Conference on Brittle Fracture in Steel, West Scot. Iron Steel Inst., Glasgow, paper No. 457, May 1953.
18. Matton-Sjöberg, P., "The Mechanism of Fracture in Impact Tests," Conference on Brittle Fracture in Steel, May 15, 1953, published by West Scot. Iron Steel Inst., 39 Elmbank Crescent, Glasgow. Also *J. West Scot. Iron Steel Inst.*, **60**, 39 (1952–53).
19. Lape, E. M., and Lubahn, J. D., "On the Relations Between Various Laboratory Fracture Tests," *Trans. ASME*, 823 (May, 1956).
20. Sachs, G., Dana, A. W., and Aul, E. L., "The Tension Properties of Aluminum Alloys in the Presence of Stress Raisers—Part I. The Effects of Triaxial Stress States on the Fracturing Characteristics of 24ST," Final Report to the NACA (May 1947).
21. MacGregor, C. W., and Fisher, J. C., "Tension Tests at Constant True Strain Rates," *J. Appl. Mech.*, **12**, A217–A227 (1945).
22. Lubahn, J. D., "Strain Aging Effects," *Trans. ASM*, **44**, 643–666 (1952).
23. Sachs, G., and Lubahn, J. D., "Notched Bar Tensile Tests on Heat Treated Low Alloy Steels," *Trans. ASM*, **31**, 125–160 (1943).
24. Neuber, H., "Theory of Notch Stresses: Principles for Exact Stress Calculation," Julius Springer, Berlin, 1937. Translated by F. A. Raven, David Taylor Model Basin, Washington D. C.
25. Prange, F. A., and Hebard, G. G., "The Role of Ductility in Oil-Well Tubing and Casing," American Petroleum Institute Preprint No. 851-29-D (1955).
26. Wells, A. A., "The Mechanics of Notch Brittle Fracture," Welding Research (British) April 1953.
27. Feely, S. J., Jr., Hrtko, D., Kleppe, S. R., and Northrup, M. S., "Report on Brittle Studies," THE WELDING JOURNAL, **33**, (2) Research Suppl., 98-s (1954).
28. Robertson, T. S., "Brittle Fracture of Mild Steel," *Engineering*, **172**, 445 (1951).
29. Robertson, T. S., and Hunt, D. le M., "The Propagation of Brittle Fracture," Conference on Brittle Fracture in Steel, May 15, 1953, published by West Scot. Iron Steel Inst., 39 Elmbank Crescent, Glasgow. Also *J. West Scot. Iron Steel Inst.*, **60** (1952–53).
30. Docherty, J. G., "Slow Bending Tests on Large Notched Bars," *Engineering*, **139**, 211 (1935).
31. McAdam, D. J., and Mebs, R. W., "An Investigation of the Technical Cohesive Strength of Metals," AIME Technical Paper No. 1615 (1943).
32. Brown, A.F.C., "Triaxial Stresses Caused by Notches," *Brit. J. of Appl. Phys.*, **5**, 280 (1954).
33. Sachs, G., Lubahn, J. D., and Schmitt, J. E., "Correlation of Information Available on the Fabrication of Aluminum Alloys (NA-126): Section V—Formability of Aluminum Alloys for Use in Military Aircraft; Part VII—Experimental Strain Analysis of Bent Rectangular Shapes," War Metallurgy Division of NDRC, Office of Scientific Research and Development, OSRD No. 6205 (Oct. 23, 1945).

Welding Research Council Bulletin No. 30

Oxidation-Resistant Brazing Alloys

by George H. Sistare, Jr., and Allen S. McDonald, Handy & Harman Research Laboratory

This bulletin covers investigation undertaken for the Wright Air Development Center with the objective of developing brazing alloys for use in joining conductive service at the highest temperature at which the fin materials can be used.

Price one dollar a copy. Copies may be ordered through the AMERICAN WELDING SOCIETY, 33 W. 39th St., New York 18, N.Y.